FILTRATION OF PERCHLORATE FROM WATER USING HEXADECYLTRIMETHYLAMMONIUM (HDTMA)-MODIFIED MONTMORILLONITE

by

MARY ELIZABETH PURVIS CARY

(Under the Direction of Valentine A. Nzengung)

ABSTRACT

Perchlorate (ClO_4^-) has been detected in the drinking water supplies of millions of people and is potentially hazardous to humans due to its passive interference with iodide uptake by the thyroid gland. Surfactant-modified montmorillonite (SMM) was evaluated as a cost-effective filtration media to treat perchlorate-contaminated waters. SMM has a high perchlorate sorption capacity and remains selective for perchlorate, even when applied to filter perchlorate from brines produced during the regeneration of ion-exchange resin. In parallel tests performed with surfactant-modified zeolite (SMZ), the SMM had a relatively higher perchlorate sorption capacity.

The physical characteristics of SMM and SMZ determine their effectiveness as filtration media for perchlorate. The low hydraulic conductivity of SMM makes it best suited for use as a landfill liner or as filtration media in fluidized-bed reactors. SMZ is suitable for use in packed-bed reactors and permeable sorption barriers. Perchlorate transport was modeled through a 100cm long column with an inner diameter of 50cm. In a packed column filled with SMZ, with an average solution velocity of 10cm/hr and with a dispersion of 500cm^2/hr, breakthrough would occur after 2.5yrs, and 4,388 pore volumes

(431m^3) of perchlorate-contaminated water would be treated. Meanwhile, in a column filled with SMM, with an average solution velocity of 1.008cm/d, and with a dispersion of 84cm^2/d, perchlorate breakthrough would occur after 712yrs. Prior to breakthrough, 5,697 pore volumes (514m^3) of solution would be treated.

While filtration is widely accepted as a means to remove contaminants from water, this process merely transfers the contaminant from the solution to the solid phase. Unless treated, spent filtration media requires disposal as a hazardous waste. Biodegradation was successful at degrading perchlorate bound to the spent SMM. When water was added to the spent SMM containing 21,500mg ClO_4^-/kg, the resulting solution contained 12mg ClO_4^-/L. Throughout the treatment, SMM provided a constant source of perchlorate, due to continuous desorption. After 120 days of treatment, the solution concentration was <1.1mg ClO_4^-/L, a 94% reduction. The results of this study provide a cost-effective process for filtration of perchlorate from water and treatment of the spent SMM using biodegradation. Enhancement of the process is needed for pilot scale testing.

INDEX WORDS: montmorillonite, surfactant-modified montmorillonite, perchlorate, hexadecyltrimethylammonium, HDTMA, cetyltrimethylammonium, sorption, filtration, Langmuir, Freundlich, isotherm, biodegradation, clay, organoclay, surfactant, perchlorate reducing bacteria, chemical oxidation, advection, dispersion, column tests, kinetic, zeolite, surfactant-modified zeolite, Hofmeister, hydration energy

FILTRATION OF PERCHLORATE FROM WATER USING HEXADECYLTRIMETHYLAMMONIUM (HDTMA)-MODIFIED MONTMORILLONITE

by

MARY ELIZABETH PURVIS CARY

B.S. The University of Georgia, 2003

A Dissertation Submitted to the Graduate Faculty of the University of Georgia in Partial Fulfillment of the Requirements for the Degree

DOCTOR OF PHILOSOPHY

ATHENS, GEORGIA

2012

FILTRATION OF PERCHLORATE FROM WATER USING HEXADECYLTRIMETHYLAMMONIUM (HDTMA)-EXCHANGED MONTMORILLONITE

by

MARY ELIZABETH PURVIS CARY

Major Professor: Valentine Nzengung

Committee: John Dowd
Paul Schroeder
David Wenner

Electronic Version Approved:

Maureen Grasso
Dean of the Graduate School
The University of Georgia
December 2012

ACKNOWLEDGEMENTS

I want to give a special thank you to my advisor, Valentine Nzengung. This dissertation would not have been possible without his guidance and support. I have been fortunate to have an amazingly supportive committee. Thanks to Paul Schroeder for his advice, knowledge, and generosity, especially in allowing me to use his laboratory. Much appreciation is given to John Dowd, who has been an enormous source of support. His door was always open and he is always willing to give guidance and encouragement – tempered with just the right amount of sarcasm. I will always be appreciative of Dave Wenner for his kindness, wisdom, and friendship. I also want to thank the geology department, especially Rob Hawman, Doug Crowe, Mike Roden, and Ashley Moore for their support. Funding from the Geology Department Watts Wheeler Scholarship was essential for the completion of this research.

Throughout grad school, my friends were always there for me. In particular, I would like to thank Tom Camp, Natalie Bond, Parshall Bush, Dan Bulger, Patti Gary, Joey McKinnon, Lina Wayo, Vikenti Gorokhovski, Kathy Schroer, Jeff Chaumba, Jay Austin, and Julie Fiser. I will always remember Jennifer Kyle as the best roommate, friend, and editor that I could have ever asked for.

My family was instrumental in making this project happen. I want thank to my parents, Bonnie Nobles and Derwin Purvis, for their support. Also, my father and mother-in-law, Rich and Marilyn Cary, have been absolutely wonderful throughout my time in grad school. They were always there for me with unending love and understanding.

Most especially, I would like to thank my best friend and incredible husband, Richard, for his unwavering love and support. He is the only reason that my sanity is (somewhat) intact. Thank you, Richard, for riding the roller coaster with me!

TABLE OF CONTENTS

Page

ACKNOWLEDGEMENTS iv

LIST OF TABLES viii

LIST OF FIGURES ix

CHAPTER

1 INTRODUCTION AND LITERATURE REVIEW 1

ABSTRACT 1

INTRODUCTION 1

NON-DESTRUCTIVE TECHNOLOGIES FOR TREATMENT OF PERCHLORATE 4

DESTRUCTIVE TECHNOLOGIES FOR TREATMENT OF PERCHLORATE 31

DUAL TREATMENT OF PERCHLORATE 37

CONCLUSION 38

2 SORPTION OF PERCHLORATE BY SURFACTANT-MODIFIED MONTMORILLONITE 39

ABSTRACT 39

INTRODUCTION 39

MATERIALS AND METHODS 44

RESULTS AND DISCUSSION 52

CONCLUSION 65

3 MODELING 1-DIMENSIONAL TRANSPORT OF PERCHLORATE THROUGH SURFACTANT-MODIFIED MONTMORILLONITE AND SURFACTANT-MODIFIED ZEOLITE....67
ABSTRACT....67
INTRODUCTION....68
METHODS....79
RESULTS AND DISCUSSION....83
CONCLUSION....90
4 TREATMENT OF PERCHLORATE BOUND TO SPENT SURFACTANT-MODIFIED MONTMORILLONITE....92
ABSTRACT....92
INTRODUCTION....92
MATERIALS AND METHODS....98
RESULTS AND DISCUSSION....102
CONCLUSION....109
5 CONCLUSIONS....110
REFERENCES....117
APPENDICES....137
A DATA FROM KINETIC STUDIES OF PERCHLORATE SORPTION BY SMM AND SMZ….....137
B DATA OF LOW PERCHORLATE CONCENTRATION SORPTION BATCH TESTS….....138
C PERCHLORATE SORPTION ONTO SMM AT HIGH INITIAL CONCENTRATIONS....139
D DATA FOR PERCHLORATE SORPTION BY SMM IN DEIONIZED WATER SPIKED WITH NITRATE....140

E DATA FOR PERCHORLATE SORPTION BY SMM IN GROUNDWATER SPIKED WITH NITRATE 141

F PERCHLORATE ADSORPTION BY SMM FROM BRINE 142

G PARAMETERS USED TO MODEL MASS TRANSPORT THROUGH SMM 143

H PARAMETERS USED TO MODEL MASS TRANSPORT THROUGH SMZ 144

I MODELED MASS TRANSPORT THROUGH SMM 145

J MODELED MASS TRANSPORT THROUGH SMZ 149

K BIOLOGICAL TREATMENT OF SPENT CLAY USING COLUMN EFFLUENT 152

L BIOLOGICAL TREATMENT OF SPENT CLAY USING MUSHROOM COMPOST TEA 153

M CONTROL BIODEGRADATION DATA FROM TREATMENT OF SMM USED TO ADSORB PERCHLORATE FROM DEIONIZED WATER 154

N BIOLOGICAL TREATMENT OF SMM USED TO FILTER BRINE 155

LIST OF TABLES

Page

Table 1.1: Studies on the use of HDTMA-montmorillonite to remove contaminants. 7

Table 1.2: Methods used to produce organoclays. 13

Table 2.1: Adsorption parameters and root mean square errors (RMSE) for equilibrium batch tests 56

Table 2.2: Composition of LHAAP groundwater....59

Table 2.3: Concentrations of anions in groundwater from LHAAP after treatment with 0.5g SMM and SMZ 60

Table 2.4: Anions in groundwater from LHAAP that was spiked with nitrate prior to treatment with 0.5g SMM 61

Table 2.5: Constituents measured in full-strength brine from a Los Angeles, California water treatment plant. 62

Table 2.6: Percent removal of co-constituents after treatment of 100mL of brine with 0.5g SMM 64

Table 2.7: Hydration energies of common anions (Custelcean and Moyer, 2007) 65

Table 3.1: Properties of SMM and SMZ. 80

Table 4.1: Experimental Set-up for preparation of spent SMM. 100

LIST OF FIGURES

Page

Figure 1.1: Structure of perchlorate (Webster's, 2008).....2

Figure 1.2: Structures of some short-chain and long-chain quaternary ammonium cations (QAC's) that are commonly used to create geosorbents 10

Figure 1.3: Structure of HDTMA (He *et al*., 2006a) 11

Figure 1.4: Release of cations from Na-montmorillonite and Ca-montmorillonite during HDTMA loading (revised from Lee and Kim, 2003a) 16

Figure 1.5: Energy dispersive X-ray spectrum for HDTMA-smectite (revised from Lee and Kim, 2002b).....17

Figure 1.6: Possible arrangements of HDTMA in montmorillonite (Bonczek *et al*., 2002). 20

Figure 1.7: HDTMA arrangements in montmorillonite considering charge heterogeneity of the clay (Lee and Kim 2002a) 21

Figure 1.8: XRD patterns for HDTMA-montmorillonite (Bonczek *et al*., 2002) 22

Figure 1.9: Images of HDTMA-montmorillonite loaded at 500% CEC (He *et al*., 2006a) 23

Figure 1.10: Images of HDTMA-smectite (Lee and Kim, 2002b) 24

Figure 1.11: Schematic of Na- and HDTMA-montmorillonite at high HDTMA loading rates (He *et al*., 2006b). 25

Figure 1.12: Changes in d-spacings as function of HDTMA loading and the amount of relative humidity (Lee and Kim, 2002a) 26

Figure 1.13: D-spacing variations as a result of temperature (Lee and Kim, 2003b) 27

Figure 1.14: Schematic of possible surfactant/water orientations in montmorillonite (Lee and Kim, 2003b) 28

Figure 1.15: Schematic of proposed variations in montmorillonite structure with HDTMA loading (He *et al*., 2006a).....29

Figure 1.16: Modified and unmodified smectite (Lee and Kim, 2003a).....30

Figure 1.17: Degradation pathway of perchlorate (Rikken *et al*., 1996).....33

Figure 2.1: Kinetic study of perchlorate sorption by SMM and SMZ.....54

Figure 2.2: Isotherms of SMM and SMZ with initial perchlorate concentrations of 0-24mg/L) 55

Figure 2.3: Isotherm of perchlorate sorption by SMM using initial perchlorate solutions of 0-470mg/L fit with the Freundlich model.....56

Figure 2.4: Effect of nitrate on perchlorate adsorption by SMM in deionized water……58

Figure 2.5: Effect of nitrate on perchlorate sorption by SMM in groundwater from LHAAP.....60

Figure 2.6: SMM adsorption of perchlorate from full-strength (100%) and half-strength (50%) brine 61

Figure 2.7: Isotherms of perchlorate sorption by SMM in deionized water, half-strength brine, and full-strength brine 63

Figure 2.8: Example of the Hofmeister series of anaions at the octadoceylamine monolayer at the air/salt solution interface (revised from Zhang and Cremer, 2006) 64

Figure 3.1: Solute transport through a column of porous media.....71

Figure 3.2: Causes of mechanical dispersion at the pore scale (modified from Fetter, 2001). 73

Figure 3.3: Breakthrough curves for a perfect tracer with varying values of dispersivity.. 73

Figure 3.4: Breakthrough curves for a perfect tracer and for a solute that undergoes first order decay....75
Figure 3.5: Examples of Langmuir, Freundlich, and linear isotherms....77
Figure 3.6: Breakthrough of perchlorate (a) and a perfect tracer (b) flowing through SMM....85
Figure 3.7: Breakthrough of perchlorate (a) and a perfect tracer (b) flowing through SMZ....86
Figure 3.8: Pore volumes treated before 1% perchlorate breakthrough flowing through SMM (a) and SMZ (b)....88
Figure 3.9: Range of values of permeability and hydraulic conductivity (Freeze and Cherry, 1979)....90
Figure 4.1: Structure of perchlorate (Webster's 2008)....95
Figure 4.2: Chemical reduction of perchlorate using stabilized zero-valent iron nanoparticles....103
Figure 4.3: Treatment of spent SMM with biologically active column effluent....104
Figure 4.4: Treatment of spent SMM with biologically active mushroom compost tea....107
Figure 4.5: Bioremediation of spent SMM from filtration of perchlorate from brine.....108

CHAPTER 1

INTRODUCTION AND LITERATURE REVIEW

ABSTRACT

Perchlorate (ClO_4^-), a powerful oxidant mainly used in rocket fuel and munitions, has been detected in 4% of public drinking water sources in the United States of America. Perchlorate has been shown to be hazardous to humans, mainly due to passively reducing iodide uptake in the thyroid gland. A review of the currently available literature involving removal of perchlorate from contaminated water revealed that an optimal method of removing perchlorate may involve two phases of treatment. First, the perchlorate is quickly and efficiently removed from water using a filtration media, such as hexadecyltrimethylammonium (HDTMA)-exchanged montmorillonite. Then, the perchlorate bound to spent media is biologically or chemically reduced, resulting complete degradation to the following non-hazardous byproducts: Cl^-, O_2, and clay.

INTRODUCTION

Perchlorate (ClO_4^-) (Figure 1.1) has been detected in at least 45 states and in 4% of public drinking water sources in the United States (USEPA, 2011; USGAO, 2010). This contaminant has been shown to be hazardous to humans, mainly due to competitively reducing iodide uptake in the thyroid (USEPA, 2005).

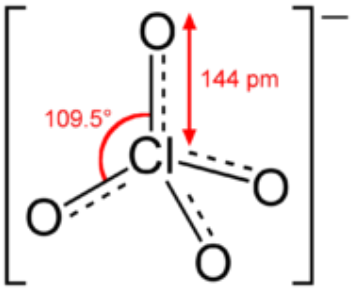

Figure 1.1. Structure of perchlorate (Webster's 2008). The central chlorine atom is in its most oxidized state (+7 valence) and is surrounded by four oxygen atoms.

Many methods have been evaluated to remove perchlorate from solution, including ion exchange resins, membrane-based technologies, and surfactant-modified geosorbents. While many of these methods can remove perchlorate quickly and efficiently, the perchlorate is merely transferred from the solution to solid filtration media. The perchlorate contaminated media still requires treatment or disposal as a hazardous waste.

Perchlorate can be chemically or biologically degraded to innocuous chloride and oxygen with little to no build up of intermediate breakdown products (Rikken *et al*., 1996; Logan, 2001; Kim and Logan, 2001; Cao *et al*., 2005; Xiong *et al*., 2007; Wang *et al*., 2010; Bardiya and Bae, 2011). While the large kinetic barriers associated with chemical reduction of perchlorate can be overcome using techniques such as increasing temperatures and using electrodialysis (Cao *et al*., 2005; Xiong, *et al*., 2007; Wang and Huang, 2008; Wang *et al*., 2010), these requirements greatly increase expense of this technology.

Ex situ biological treatment of perchlorate typically involves bioreactors, which, although effective, have a negative public perception that greatly hinders use of this method for treatment of drinking water (Li, 2008; Dugan *et al*., 2009; Bardiya and Bae, 2011; WRF, 2011). In general, the public is wary of secondary contamination of water

with microbial cells and disinfection by-products (Li, 2008; Dugan *et al*., 2009; Bardiya and Bae, 2011; WRF, 2011). Additionally, biological treatment of perchlorate may result in elevated sulfide, ammonia, microbial products, and acetate, which could negatively impact water quality by causing odors, increasing biological activity, increasing the amounts of chlorine necessary for disinfection, and producing more disinfection byproducts (Brown *et al*., 2003; Dugan *et al*., 2009).

One possible method to optimally remove perchlorate from water is a duel treatment process, in which perchlorate is first quickly removed from solution using a filtration media, such as surfactant-modified montmorillonite, and the perchlorate bound to the spent media is either chemically or biologically degraded. Such a process would take advantage of the benefits of both technologies: fast and efficient removal of perchlorate from solution and degradation of the perchlorate so that only non-hazardous wastes remain.

Study Objectives

This research examined the use of surfactant-modified montmorillonite (SMM) and surfactant-modified zeolite (SMZ) as adsorbents of perchlorate. Several surfactant molecules were evaluated to determine which most enhanced perchlorate adsorption by modified montmorillonite. Kinetic studies were conducted with both SMM and SMZ to determine the time required for the approach to perchlorate sorption equilibrium. Perchlorate mass loading onto each filtration media was evaluated using sorption equilibrium tests. The kinetics and sorption equilibrium data were used to identify the most efficient sorbent for perchlorate. The effects of co-constituents in solution on perchlorate loading onto the media were evaluated using both groundwater from a contaminated site and the brine produced during regeneration of ion exchange resins. The transport of perchlorate and nonreactive tracers through both SMM and SMZ was

modeled using the advection-dispersion equation under a variety of conditions. Finally, chemical reduction and microbial degradation of perchlorate bound to the spent filtration media was investigated.

NON-DESTRUCTIVE TECHNOLOGIES FOR TREATMENT OF PERCHLORATE

Ion Exchange Resins

Both non-selective and perchlorate-selective ion exchange resins can be utilized to remove perchlorate from solution. Non-selective resins are only efficient at sites that either contain very high perchlorate concentrations or extremely low concentrations of other ions (Coates and Jackson, 2009). These resins are typically regenerable, which produces an excessive amount of regeneration brine (Coates and Jackson, 2009).

Generally, perchlorate-selective resins are composed of hydrophobic support matrix that has been modified using quaternary ammonium surfactants (Coates and Jackson, 2009). Large amounts of these resins are typically required for removal of perchlorate because they tend to have low sorption rates (Coates and Jackson, 2009). Although traditional methods to regenerate ion exchange resins using NaCl are ineffective at removing perchlorate, tetrachloroferrate can be used to regenerate perchlorate-selective resins (Gu, *et al*., 2001). Gu *et al*. (2007) developed a method that uses ferrous iron to reduce perchlorate bound to resins. For the latter regeneration method to be efficient a thermoreactor set at 190°C is required, which significantly increases the energy costs.

Membrane Technologies

While membrane technologies such as ultrafiltration, nanofiltration, and reverse osmosis are capable of removing perchlorate from solution, the presence of ionic components decreases the efficiency of these processes by reducing the negative

electrostatic charge of the membrane (Yoon *et al*., 2000; Yoon *et al*., 2004; Lee *et al*., 2008; Yoon *et al*., 2009). Enhancement of ultrafiltration using polyelectrolyte has been shown to increase its selectivity for perchlorate (Huq *et al*., 2007). Modification of the ultrafiltration membrane with cationic surfactants increases the removal of perchlorate from solution, due to increased steric restrictions caused by the reduced pore space resulting from the addition of surfactants (Yoon *et al*., 2003). In all cases, membrane technologies are nondestructive and leave behind high-strength waste streams that require further treatment (ITRC, 2008).

Surfactant-Modified Geosorbents

Surfactants have been used to modify geosorbents so that the removal of perchlorate is enhanced. For instance, Zhang *et al*. (2007) showed that zeolite modified with hexadecyltrimethylammonium (HDTMA) has a strong selectivity for perchlorate, even in the presence of co-constituents. While activated carbon (AC) is not efficient at removing perchlorate from solution (Na *et al*., 2002; Parette and Cannon, 2005; Patterson *et al*., 2011), its selectivity for perchlorate increases after modification with cationic surfactants (including HDTMA), iron and oxalic acid, and cationic polymers (Na *et al*., 2002; Parette and Cannon, 2005; Coates and Jackson, 2009; Xu *et al*., 2011). Surfactant-modified montmorillonite can also remove perchlorate from solution (Kim *et al*., 2011; Seliem *et al*., 2011; Chitrakar *et al*., 2012). For instance, Chitrakar *et al*. (2012) reported that the perchlorate sorption capacity of montmorillonite modified with hexadecylpyridinium was 1.02mmol/g and that sorption equilibrium was approached within 4 hours.

Hexadecyltrimethylammonium (HDTMA)-Montmorillonite

Montmorillonite is able to swell, which enables contaminants to exchange deeply into the clay layers, resulting in a higher effective surface area. Research to enhance sorption capacity and selectivity of montmorillonite for organic and inorganic contaminants, has focused on modifying montmorillonite with quaternary ammonium surfactants, such as tetramethylammonium (TMA), trimethylphenylammonium (TMPA), benzyldimethyltetradecylammonium (BDTDA), and HDTMA. This modification occurs as surfactants exchange with inorganic cations naturally found in interlayer regions of clays (Boyd *et al*., 1988a; Zhang *et al*., 1993; Mizutani *et al*., 1995; Bonczek *et al*., 2002; Lee and Kim, 2002a). The selectivity for surfactant molecules over inorganic ions and for progressively larger surfactant molecules is due to the differences in salvation energies (Maes *et al*., 1980; Mizutani *et al*., 1995; Teppen and Aggarwal, 2007). The surfactant modified montmorillonite becomes increasingly hydrophobic and, therefore, is able to adsorb higher quantities of many contaminants compared to unmodified clays (Table 1.1).

Table 1.1. Studies on the use of HDTMA-montmorillonite to remove contaminants.

Contaminant Type	Contaminant of Interest	Study
Organic	Phenol and chlorophenols	Mortland *et al*., 1986
	Trichloroethene (TCE) and benzene	Boyd *et al*., 1988a
	Pentachlorophenol (PCP)	Boyd *et al*., 1988b; Brixie and Boyd, 1994
	Tetrachloromethane	Smith *et al*., 1990
	Benzene, toluene, ethyl benzene propylbenzene, butylbenzene, naphthalene, and biphenyl	Jaynes and Boyd, 1991a
	Benzene, toluene, ethyl benzene, and xylenes	Jaynes and Vance, 1996
	Diuron and naphthalene	Nzengung *et al*., 1996
	Tetrachloride and nitrobenzene, TCE	Sheng *et al*., 1996
	Dicamba (herbicide)	Zhao *et al*., 1996
	Zearalenone (toxin produced by mold on cereal crops)	Lemke, *et al*., 1998
	Imazamox (pesticide)	Celis *et al*., 1999
	Dichlorobenzene	Sheng and Boyd, 2000
	Sodium dodecylbenzene sulfonate	Rodríguez-Sarmiento and Pinzón-Bello, 2001
	Chlorobenzene	Lee *et al*., 2002c
	Sulfometuron (herbicide)	Mishael *et al*., 2002
	Sulfentrazone (herbicide)	Polubesova *et al*., 2003
	2,4-dinitrotoluene, 1,3-dinitrobenzene, and naphthalene	Roberts *et al*., 2006
	Nitrobenzene	Patel *et al*., 2009
Oxyanion	Nitrate and chromate	Li, 1999
	Chromate	Krishana *et al*., 2001; Majdan *et al*., 2005
	Perchlorate	Seliem *et al*., 2011; Kim *et al*., 2011

Unmodified montmorillonite is hydrophilic due to the presence of strongly hydrated inorganic cations exchanged into the clay gallery. As these inorganic cations are exchanged for very weakly hydrated surfactants, the clays become increasingly hydrophobic (Boyd *et al*., 1988a; Jaynes and Boyd, 1991b; Maes *et al*., 1980; Zeng *et al*., 2000; Zhang *et al*., 1993). Jaynes and Boyd (1991b) found that this increase in hydrophobicity was also partially due to the large organic cations covering the siloxane surface and impeding water from interacting directly with the hydrophilic surface of the modified clay.

Due to the high sorption capacity of organoclay for a variety of contaminants, several environmental applications for organoclays have been proposed. For instance, Boyd *et al*. (1988a) suggested the use of HDTMA-montmorillonite in clay landfill liners and bentonite slurry walls to enhance contaminant sequestration. Organoclays have also been proposed as filtration media for water purification (Zhao and Vance, 1998), industrial wastewater treatment (Groisman *et al*., 2004), and as pre-polishers to extend the bed life of activated carbon (Alther, 2004).

Natural Montmorillonite structure

Montmorillonite has an ideal structure of $[(R_{0.33}{}^{+}(Al_{1.67},Mg_{0.33})Si_4O_{10}(OH)_2$, where R is the exchangeable cation located in the clay interlayer]. It has an expandable dioctahedral 2:1 structure in which the low negative layer charge is primarily due to isomorphic substitution of Mg^{2+} for Al^{3+} in the octahedral sheet (Moore and Reynolds, 1997). The resultant charge imbalance is compensated by exchangeable inorganic cations, typically Na^{+} and Ca^{2+}, which are held in the ditrigonal cavity of the clay interlayer site. The hydration spheres surrounding these exchangeable cations cause the clay to be naturally hydrophilic (Boyd *et al*., 1988a; Jaynes and Boyd, 1991b; Maes *et al*., 1980; Zeng *et al*., 2003; Zhang *et al*., 1993).

Structure and Properties of Quaternary Ammonium Cations (QAC's)

Quaternary ammonium cations (QAC's) contain a positively charged head-group and a neutral carbon tail. The structures of a few commonly used quaternary ammonium ions (generic formula: $[RN(CH_3)_3]^{+}$, where R is either an alkyl or aromatic hydrocarbon) are shown in Figure 1.2 (Nzengung *et al*., 1996). QAC's are generally divided into two groups, those with short chains (<12 carbons) and those with long chains (≥12 carbons). Organoclays in which the inorganic cations were exchanged with short-chain QAC's are

generally called adsorptive clays, while those modified with long-chain QAC's are termed organophilic clays (Azejjel, *et al*., 2010; Yariv *et al*., 2011). Surfactants in adsorptive clays act as pillars, which prop clay layers open, leaving spaces where organic contaminants readily bind to the clay's siloxane surface (Bonczek *et al*., 2002; Nzengung *et al*., 1996). Surfactants adsorbed to organophilic clays are believed to behave as a gel-like partition medium into which organic contaminants migrate (Bonczek *et al*., 2002; Boyd *et al*., 1988a; Nzengung *et al*., 1996).

Montmorillonite that is modified with short chain surfactants are not likely to adsorb large quantities of perchlorate because these surfactants do not contain long hydrophobic tails that produce a hydrophobic gel in the clay interlayer. Modification of montmorillonite with long-chain surfactants, such as BDTDA and HDTMA, result in clay interlayers becoming more hydrophobic, which would increase the partitioning of very weakly hydrated anions, such as perchlorate (ClO_4^-). BDTDA ions have long hydrophobic tails, and a head group that includes a benzene ring. The presence of this ring in the interlayer would likely cause steric restrictions, which would reduce the amount of perchlorate adsorbed. HDTMA consists of a 3-methyl quaternary amine head group with a monovalent charge connected to a 16-carbon chain tail (Figure 1.3).

Compared to clay modified with short-chain surfactants, HDTMA-montmorillonite would most likely have the largest perchlorate adsorption capacity due to the high loading rates of positively charged HDTMA molecules onto montmorillonite and the hydrophobic interlayer produced by the long hydrophobic tails of HDTMA molecules. Also, unlike BDTDA molecules, HDTMA does not include benzene rings, which are likely to reduce the space in the clay gallery that is available for perchlorate sorption sites. Due to all of these reasons, HDTMA-montmorillonite has the most potential as a perchlorate filtration media, therefore, this research focuses on the perchlorate adsorption by this organoclay.

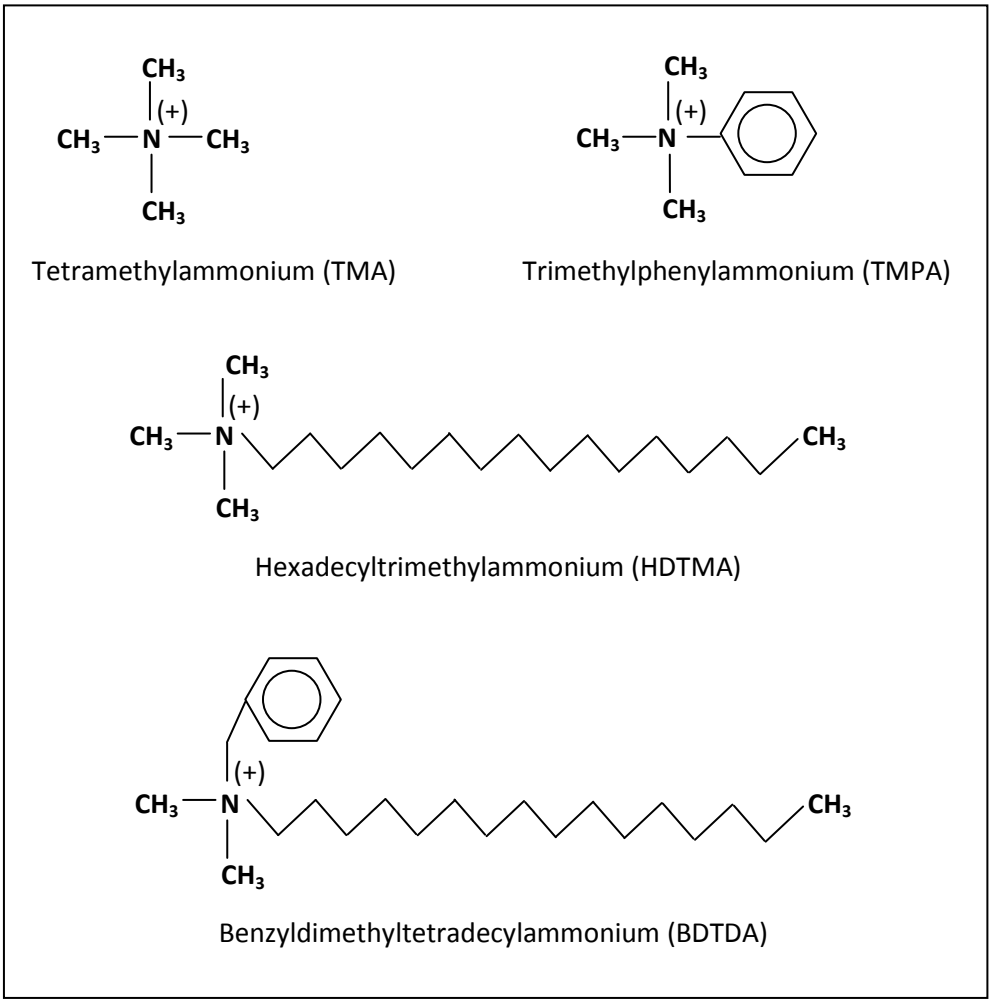

Figure 1.2. Structures of quaternary ammonium cations that are commonly used to create geosorbents (Nzengung *et al*., 1996). Modification of montmorillonite with short-chain surfactants, such as TMA and TMPA, result in adsorptive clays. Montmorillonite modification with more hydrophobic surfactants, such as HDTMA and BDTDA, produce organophilic clays.

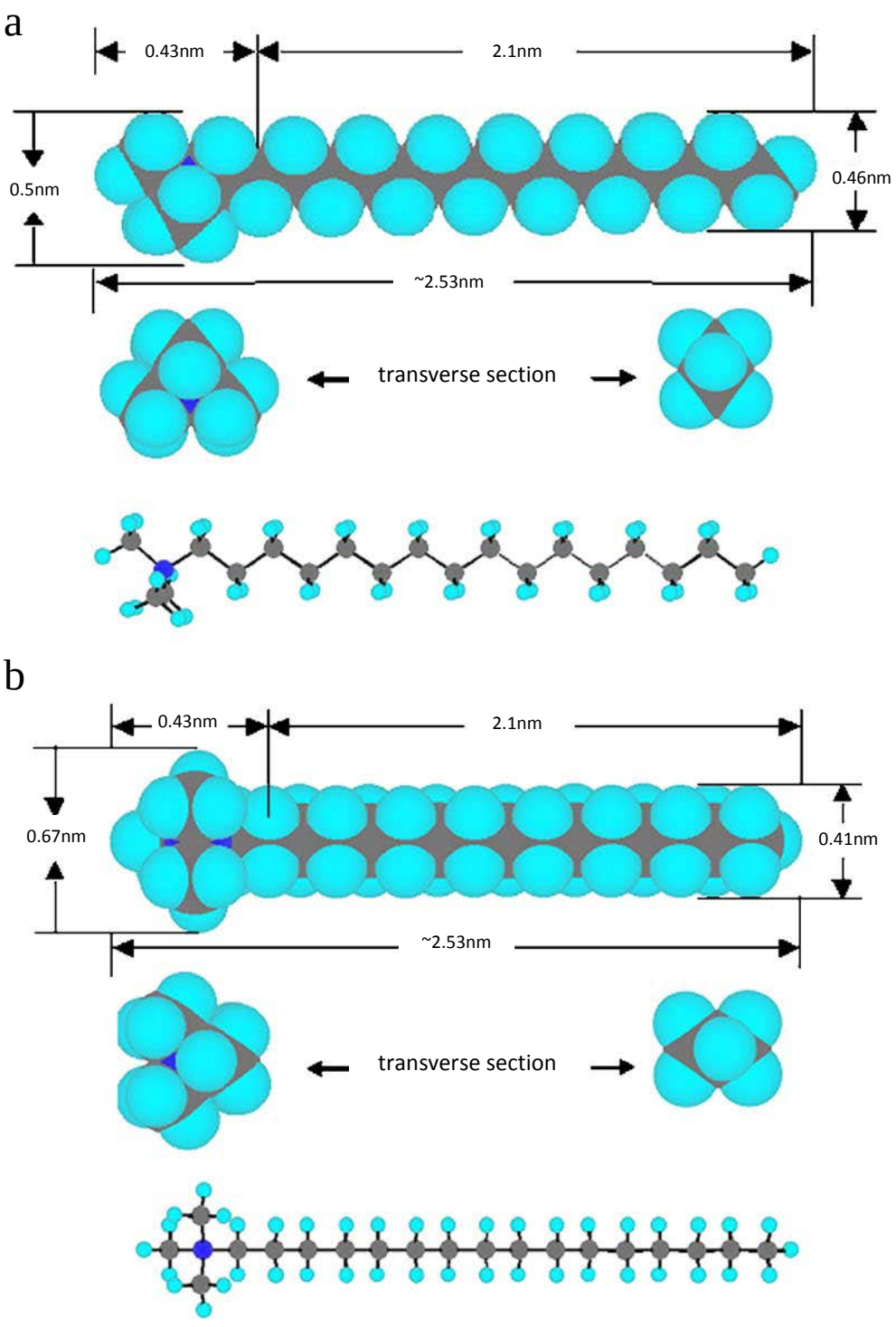

Figure 1.3. Structure of HDTMA (He *et al*., 2006a). (a) depicts view from side of zigzag arrangement of carbon atoms in the surfactant tail and (b) is the top view of the plane of the zigzag arrangement.

Modification of Clay with Cationic Surfactants

General Clay Modification Process

While many methods have been published (Table 1.2) , generally the preparation of organoclays involves the following steps: 1) using ion exchange to replace inorganic cations with surfactant ions at some percentage of the clay cation exchange capacity (CEC), 2) separating the organoclay from the solution, 3) washing the organoclay, and 4) drying the organoclay.

Montmorillonite selectivity for QAC's

Montmorillonite is highly selective for QAC's. Inorganic cations naturally found in montmorillonite interlayers are readily exchanged for cationic surfactants, as the positively charged head groups electrostatically bind to the negatively charged sites in the clay interlayer (Mizutani *et al*., 1995; Zhang *et al*., 1993; Lee and Kim, 2002a; Boyd *et al*., 1988a; Bonczek *et al*., 2002). During preparation of HDTMA-modified clays, the amount of both Na^{+} and Ca^{2+} released into solution increases as the concentration of HDTMA in solution is increased (Figure 1.4) (Lee and Kim, 2003a). Energy dispersive X-ray analysis of HDTMA-montmorillonite conducted by Lee and Kim (2002b) measured only trace amounts of sodium in the modified clay, confirming its exchange with surfactants in the clay interlayer (Figure 1.5). At low HDTMA loading rates, Bonczek *et al*. (2002) concluded that adsorption onto montmorillonite is dominated by electrostatic forces (between the positively charged head and the negatively charged sites in the clay layer), with some van der Waals interactions between the surfactant chains and the siloxane surfaces. As the weakly hydrated surfactants replace strongly hydrated inorganic cations, the clay gallery becomes dehydrated, which causes an even stronger selectivity for cations that are less hydrated (Maes *et al*., 1980).

Table 1.2. Methods used to produce organoclays.

Clay Pre-treatment	Percentage of CEC	Equilibration (Mixing) Time	Separation Method	Washing Method	Drying Method	Post-Treatment	Reference
Settled out >0.5 µm	Unknown	Overnight	Unknown	Unknown	Unknown	Unknown	Maes *et al*., 1980
Settled out quartz and heavy minerals; exchanged with Ca^{+2}; washed; freeze-dried	30% or 70%	Unknown	Filtered	Distilled water	Freeze-dried	None	Boyd *et al*., 1988a
Settled out >2µm fraction; exchanged with Mg^{+2}, frozen; freeze-dried	100%	4 hours	Centrifuged	Centrifuged with distilled water	Frozen and freeze-dried	None	Jaynes and Boyd, 1991a
Settled out >2µm fraction; exchanged with Mg^{+2}, frozen; freeze-dried	500%-1000%	4 hours	Unknown	Dialysis in distilled until negative $AgNO_3^-$ test	Unknown	Unknown	Jaynes and Boyd, 1991b
Unknown	100%	Unknown	Unknown	DI water until negative $AgNO_3^-$ test	Unknown	Unknown	Ogawa *et al*., 1992
Settled out >2µm fraction; exchanged with Ca^{+2}; washed until negative Cl^- test; freeze-dried	200%	Unknown	Unknown	Distilled water until negative $AgNO_3^-$ test	None	Stored suspended in water at 5°C	Fusi *et al*., 1993
Exchanged with Na^+ when surfactants <100% CEC	50% - 100%	At least 48 hours	Centrifugation	None	Unknown	Unknown	Zhang *et al*., 1993
Unknown	100%	2-4 hours	Centrifugation	DI water	Frozen and Freeze-dried	None	Jaynes and Vance 1996
Settled out >2µm fraction; exchanged with Ca^{+2}; washed, frozen; freeze-dried	Unknown	Unknown	Centrifugation	Distilled-DI water	Frozen and Freeze-dried	None	Nzengung *et al*., 1996
Settled out >2µm fraction; exchanged with Ca^{+2}	100%	Overnight	Unknown	Distilled water until negative $AgNO_3^-$ test	Frozen and Freeze-dried	None	Sheng *et al*., 1996
Unknown	60% - 300%	8 hours	Centrifugation	Ethanol/Water (1:1)	Freeze-dried	None	Hsu *et al*., 2000
Settled out >2µm fraction	100%	Unknown	Unknown	Dialysis until free of salts	Frozen and freeze-dried	None	Zhao and Vance, 1998
None	HDTMA sorption plateau	24 hours	Centrifuged	Type I water (electric resistance >18MΩ)	Air dried	Unknown	Li, 1999

Clay Pre-treatment	Percentage of CEC	Equilibration (Mixing) Time	Separation Method	Washing Method	Drying Method	Post-Treatment	Reference
Unknown	200%	4 hours	Unknown	Dialysis with distilled-DI water until salt free	Frozen and Freeze-dried	None	Sharmasarkar *et al*., 2000
Settled out >2µm fraction	100%	Overnight	Unknown	Distilled water until negative $AgNO_3^-$ test	Frozen and Freeze dried	None	Sheng and Boyd, 2000
None	100% (final percent) in acetone	1 hour (after kinetic test of 1hr – 7 days)	Centrifugation	Distilled	Unknown	Unknown	Krishna *et al*., 2001
Settled out >2µm fraction; exchanged with Na^+; washed	20%-200%	Overnight	Centrifugation	"Washed thoroughly"	Freeze-dried	None	Bonczek *et al*., 2002
Settled out >2µm fraction; exchanged with Na^+; washed with DI water until negative $AgNO_3^-$ test; frozen; freeze-dried	1%-600%	2 days	Centrifugation	Washed with DI water	Frozen and Freeze-dried	None	Lee and Kim, 2002a
Settled out >2µm fraction; exchanged with Na^+; washed with DI water until negative $AgNO_3^-$ test; frozen; freeze-dried	100% - 250%	2 days	Centrifugation	Washed with DI water"	Frozen and freeze-dried	None	Lee and Kim, 2002b
Unknown	30% - 100%	8 hours	Gravity Sedimentation	Distilled water until "free of Br"	Oven dried (40°C)	Ground	Yang *et al*., 2002
Unknown	2% - 100%	7 days	Centrifugation	DI water	Unknown	Unknown	Lee and Kim, 2003a
Settled out >2µm fraction; exchanged with Na^+; washed with DI water until negative $AgNO_3^-$ test	1% - 300%	2 days	Centrifugation	DI water	Unknown	Unknown	Lee and Kim, 2003b
Unknown	30-100%	5 hours	Gravity Sedimentation	DI water until no Br- detected	Unknown	Ground to pass through 80 mesh sieve	Yang *et al*., 2003
Unknown	100%	48 hours	Centrifugation	Distilled water until negative $AgNO_3^-$ test	Freeze-dried	None	Groisman *et al*., 2004

Clay Pre-treatment	Percentage of CEC	Equilibration (Mixing) Time	Separation Method	Washing Method	Drying Method	Post-Treatment	Reference
None	20%-400%	30 minutes (sonication at 60°C)	Unknown	"Washed" until negative $AgNO_3^-$ test	Dried at room temperature	Ground	Xi *et al*., 2004
Unknown	2% - 300%	7 days	Centrifugation	DI water	Unknown	Unknown	Lee *et al*., 2005
Heated to 110°C for 48 hours, washed with DI water	150%	~6 hours	Vacuum Filtration	Water or ethanol/water (1:1) mixture until negative $AgNO_3^-$ test	Unknown	Unknown	Vasquez *et al*., 2008
Settled out >2µm fraction; Exchanged with Na+; Centrifuged; washed with DI water until pH = 7; dried at 105°C; ground <200 mesh sieve;	50%-500%	10 hours (80°C)	Unknown	Washed until negative $AgNO_3^-$ test	Unknown	Unknown	He *et al*., 2006a
Settled out >2um fraction; Exchanged with Na+; Centrifuged; washed; dried at 105°C; ground <200 mesh sieve;	50%-250%	10 hours (60°C)	Unknown	Washed until negative $AgNO_3^-$ test	Oven (80°C)	Ground until <200 mesh sieve	He *et al*., 2006b
Unknown	25% - 200%	1 day	Unknown	DI water	Unknown	Unknown	Volzone *et al*., 2006
Unknown	150%	24 hours	Filtration	DI water	Oven dried (65°C)	Unknown	Erdem *et al*., 2010
Unknown	100% - 140%	6 hours (100°C)	Centrifugation	Distilled water and ethanol	Oven dried (60°C)	Unknown	Kim *et al*., 2011
Exchanged with Na+ overnight; washed, dried (80°C), ground (100 mesh)	100%	24 hours	Vacuum filtration	Unknown	Oven dried (80°C)	Activated for 1 hour at 80°C; Ground to pass through 100 mesh sieve	Xin *et al*., 2012

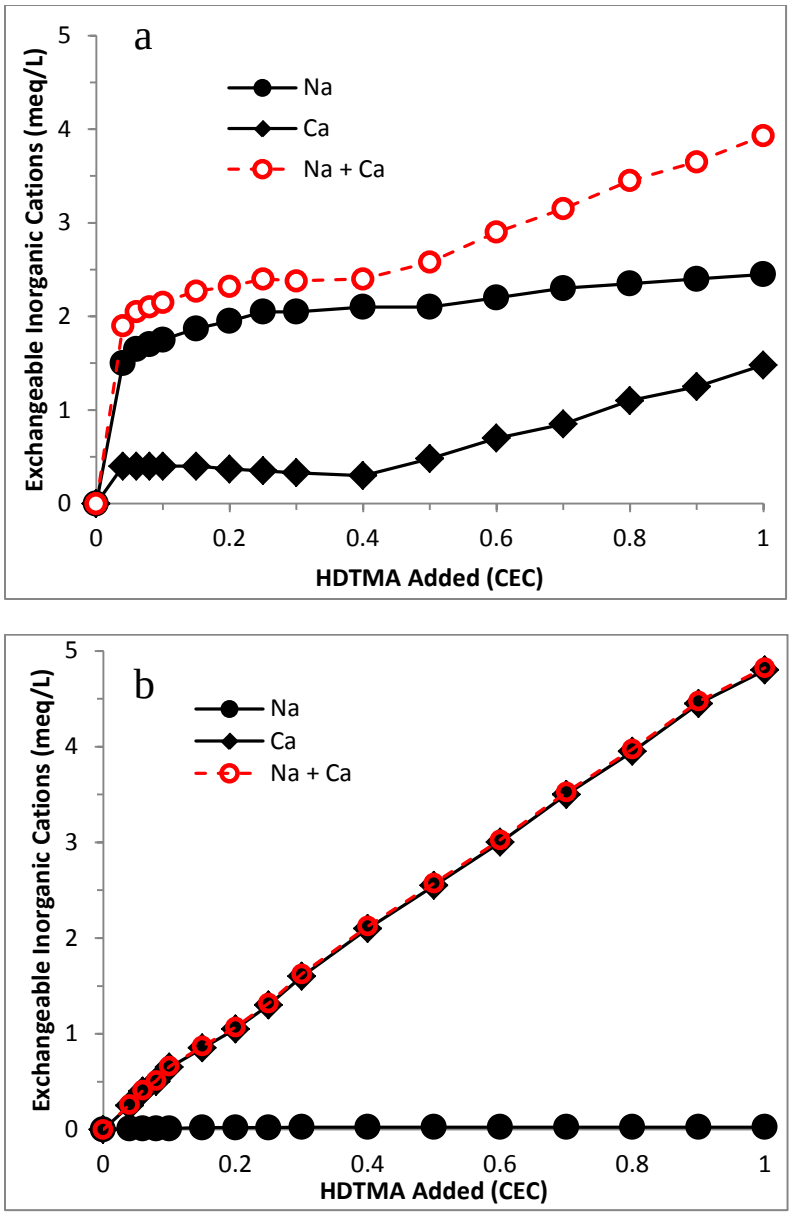

Figure 1.4. Release of cations from Na-montmorillonite and Ca-montmorillonite during HDTMA loading (revised from Lee and Kim, 2003a)

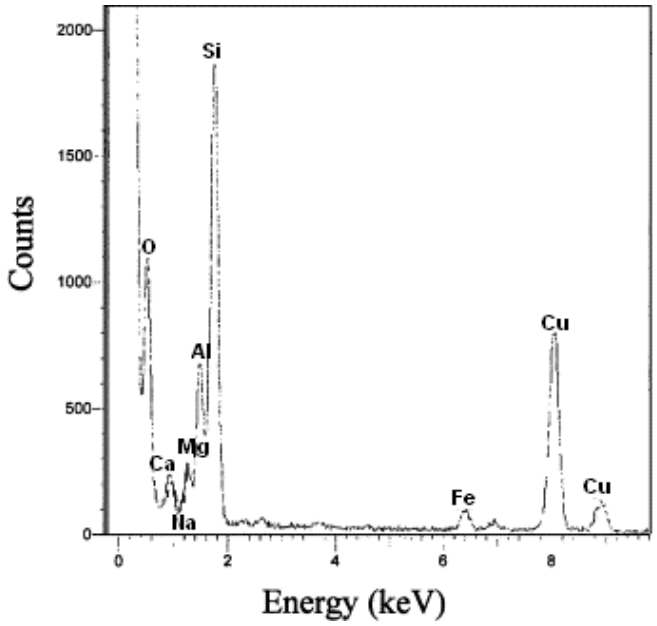

Figure 1.5. Energy dispersive X-ray spectrum for HDTMA-smectite (revised from Lee and Kim, 2002b). Copper peaks are remnant of the analysis, rather than a component of the clay.

Role of Solution Chemistry

While much clay-modification research has focused on interactions between clays and surfactants (Bonczek *et al*., 2002; He *et al*., 2006a; Zhang, *et al*., 1993; Zeng *et al*., 2003), other studies have taken into account the importance of solution chemistry during adsorption of QAC's (Maes *et al*., 1980; Mizutani *et al*., 1995; Teppen and Aggarwal, 2007). Cation hydration energies are extremely important in the selectivity of clay for QAC's over inorganic cations and also for QAC's of increasing size (Maes *et al*., 1980; Mizutani *et al*., 1995; Teppen and Aggarwal, 2007). The amount of space in the interlayer limits the extent of hydration of large cationic surfactants, which causes the energy requirement of dehydrating the cations to play a significant role in QAC selectivity. In their thermodynamic study of organoclay, Teppen and Aggarwal (2007) reported that the free energy of hydration of surfactants with identical head-groups was the dominant force behind cation exchange. When comparing surfactants with identical

head groups, the charge density is lower for larger surfactants, resulting in less hydration. The authors concluded that the cation with the lowest hydration energy exchanges onto the clay because the more strongly hydrated cation tends to remain in solution, where it can remain fully hydrated. The more easily dehydrated cation will enter the clay gallery because the free energy of the entire system will be lowest in this configuration. (Essentially both the clay and the solution "prefer" the smaller organic cation, but the decrease in free energy of the system is most when the smaller cation can be fully hydrated in solution so the larger cation is exchanged into the clay interlayer.) The affinity of montmorillonite for surfactants with the lowest hydration energy is similar to the selectivity shown by many clay minerals for cesium over potassium due to its lower hydration energy (Hendricks, *et al*., 1940; Krishnamoorthy and Overstreet, 1950; Marshall and Garcia, 1959; Sawhney, 1969).

Furthermore, as weakly hydrated surfactants replace strongly hydrated inorganic cations in the interlayer, the clay gallery becomes more dehydrated, leading to an even stronger selectivity for cations with less hydration (Maes *et al*., 1980). Teppen and Aggarwal's research supported a study by Mizutani *et al*. (1995), which found that the selectivity of montmorillonite for larger rather than smaller QAC's in an aqueous solution reversed with experiments involving organic solvents. Mizutani *et al*. (1995) concluded that this reversal was due to the differences in dehydration energies causing the least solvated ion to enter the clay interlayers.

Effect of QAC Loading Rates

QAC's exchange into clay interlayers so effectively that sorption of surfactants can exceed the cation exchange capacity (CEC) of the clay (Jaynes and Boyd, 1991b; Lee and Kim, 2002b; Lee and Kim, 2003b; He *et al*., 2006a; Bonczek *et al*., 2002; Zeng *et al*., 2003). At high surfactant loading rates adsorption is primarily due to hydrophobic

reactions between carbon chains of surfactants (Bonczek *et al*., 2002, Lee and Kim, 2002a; Lee and Kim, 2002b; Lee and Kim, 2003b; Teppen and Aggarwal, 2007; Zeng *et al*., 2003). In their thermodynamic study of cation exchange in montmorillonite, Teppen and Aggarwal (2007) concluded that, at high loading rates, van der Waals interactions between the surfactants exchanged into the clay gallery become increasingly significant and account for approximately 50-60% of total attractive force (with dehydration energies accounting for the majority of the remainder). They also reported that, as the interlayers are filled with surfactants, the clay gallery becomes an organic phase into which large organic cations selectively partition.

QAC Arrangement in HDTMA-Montmorillonite

Many previous research studies have documented the changes in basal spacings of QAC modified clays (Bonczek *et al*., 2002; Boyd *et al*., 1988a; He *et al*., 2006a; Lee and Kim, 2002b; Lee and Kim, 2003b, Nzengung *et al*., 1996). This research has shown that with increasing surfactant loading rates, the arrangement of surfactants in clay interlayers changes progressively from monolayers to bilayers to pseudotrilayers and finally to paraffin-type structures (Bonczek *et al*., 2002; Boyd *et al*., 1988a; He *et al*., 2006a; Lee and Kim, 2002b; Lee and Kim, 2003b, Nzengung *et al*., 1996). Although Figure 1.6 is an idealized schematic of these arrangements that is typically referred to in organoclay studies, Figure 1.7 may be more accurate because it takes into account the possible effects of charge heterogeneity in the montmorillonite. In the monolayer arrangement (with low surfactant concentrations), HDTMA ions are oriented parallel to the siloxane surface, often with some areas dominated by the “original” inorganic cation. As loading rates increase, more of the inorganic cations are replaced by QAC’s. Once the siloxane surface is covered, the surfactants form a bilayer, in which two surfactants lie one-atop-the-other, parallel to the surface of the clay interlayer. At even higher

concentrations, the surfactants form a pseudotrilayer in which the QAC's are kinked and interlaced, but still remain oriented fairly parallel to the clay surface. At very high surfactant concentrations (≥ 250% CEC) the surfactants are arranged in a paraffin-type arrangement, having the highest packing density, where surfactants are arranged at an acute angle to the clay surface. He *et al*. (2006a) calculated that in montmorillonite (modified at 500% CEC) the HDTMA ions were in a paraffin-type arrangement at an angle of 31° with the siloxane surface.

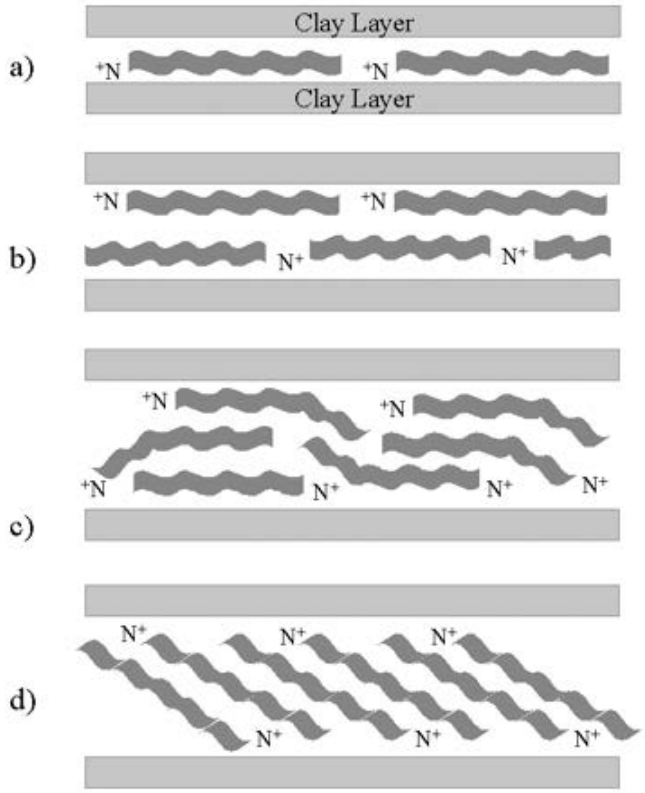

Figure 1.6. Possible arrangements of HDTMA in montmorillonite (Bonczek *et al*., 2002). Schematic of HDTMA in interlayers of montmorillonite as (a) monolayers (13.7Å), (b) bilayers (17.7Å), (c) pseudotrilayers (21.7Å), and (d) paraffin-type (>22Å) (Bonczek *et al*., 2002). Surfactants are represented by N^+, which symbolizes the positively charged head group and wavy lines, representing the carbon chain tails.

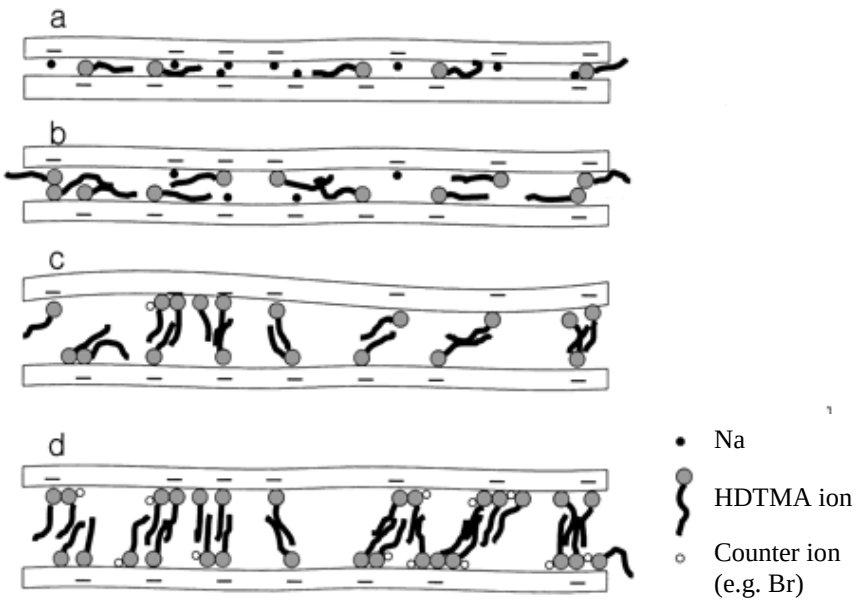

Figure 1.7. HDTMA arrangements in montmorillonite considering charge heterogeneity of the clay (Lee and Kim 2002a).

Transitions between these arrangements are typically stepwise with sudden leaps in d-spacings (Bonczek *et al*., 2002; Lee and Kim, 2002a). Additionally X-ray diffraction (XRD) patterns for HDTMA-montmorillonite often have “shoulders” as the surfactants transition between arrangements. For example, XRD patterns from a study by Bonczek *et al*. (2002) shows the stepwise transition from monolayer at 14.7Å (40% CEC coverage) to bilayer at 17.7 Å (90-100% CEC coverage) (Figure 1.8). At 70% CEC HDTMA coverage, there are two peaks of equal size for each configuration (monolayer and bilayer). Note the distinct shoulders that “grow and disappear” as increased surfactant loading causes the HDTMA ions to rearrange from predominantly monolayer to mainly bilayer.

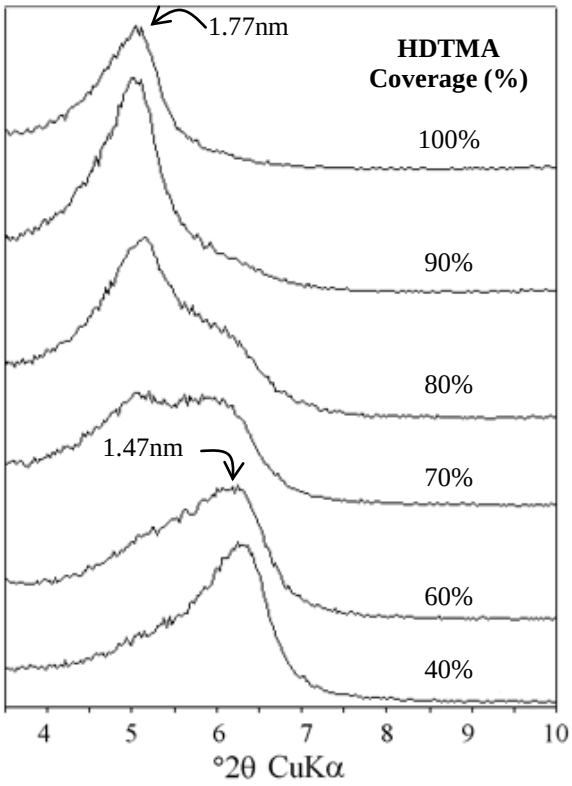

Figure 1.8. XRD patterns for HDTMA-montmorillonite (Bonczek *et al*., 2002). Percents are relative to montmorillonite CEC. D-spacings are labeled. Note the transition from monolayer to bilayer surfactant arrangement with increasing surfactant concentrations**.**

Although the transition between surfactant arrangements is stepwise, there is slight variability in the montmorillonite d-spacings, as indicated by the broad XRD peaks typical of HDTMA-montmorillonite (He *et al*., 2006a). This variability is likely due to surfactant concentrations (transitions between arrangements of HDTMA) and charge heterogeneity within the clay layers. High–resolution transmission electron microscopic (HRTEM) images of HDTMA-montmorillonite depict the complexity of this variability (Figure 1.9). While the distance between montmorillonite layers (with HDTMA in paraffin-type arrangements) was typically 2.2 and 2.3nm, there was variability between layers, including differences in thickness within the same layer (He *et al*., 2006a).

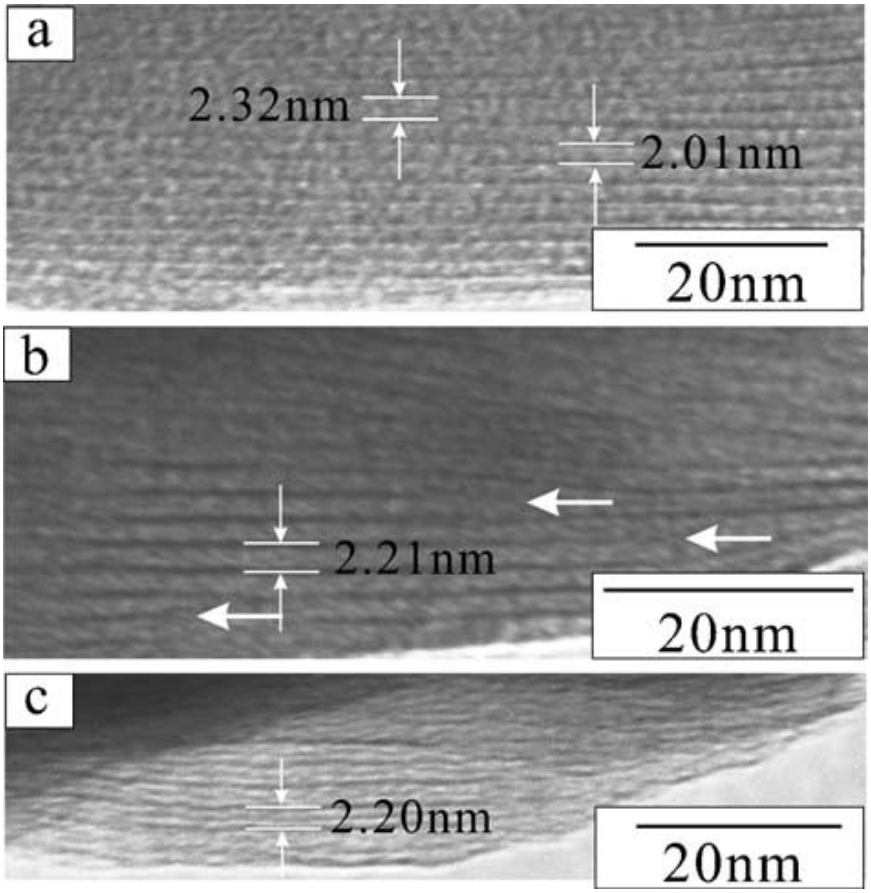

Figure 1.9. Images of HDTMA-montmorillonite loaded at 500% CEC (He *et al*., 2006a). Note variability in clay particle width (a) and the most layers with dimensions 2.2- 2.3nm (b & c). Large arrows indicate layers that have variable thickness.

When low charge montmorillonite was modified with very high HDTMA loading rates (250 % CEC), the d-space expansion of >40 Å caused destabilization of portions of the clay layers (Lee and Kim, 2002b) (Figure 1.10). The likely explanation for this is that charge heterogeneity within the clay (which is common) can cause areas of very high surfactant concentration, which create openings by prying the layers even farther apart. This effect occurs even more readily in low-charge clays, where the forces holding the layers together are weaker than those in higher charged clays.

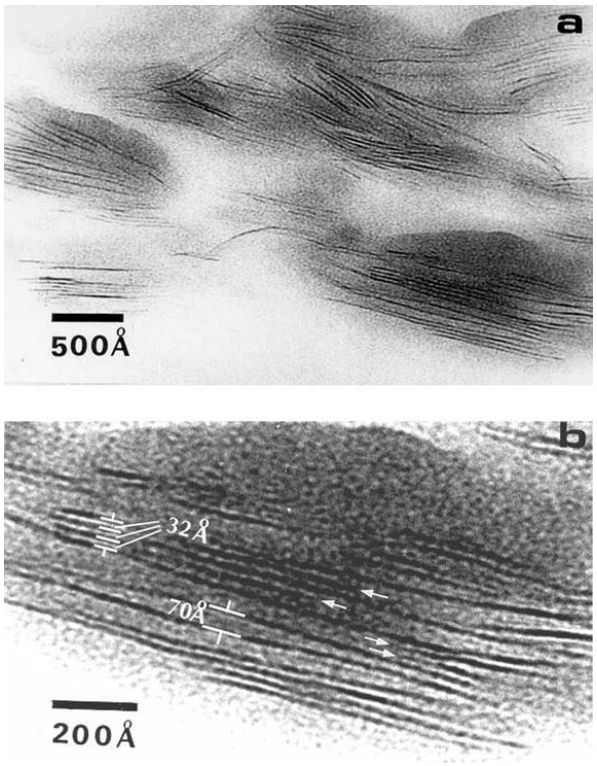

Figure 1.10. Images of HDTMA-smectite (Lee and Kim 2002b). HDTMA-smectite modified with 250% CEC (a) and enlarged view with expanded layers and terminating layers (marked with arrows) (b).

Additionally, He *et al*. (2006b) found that, when loading rates were equal to or less than the CEC, HDTMA was found primarily in the montmorillonite interlayer instead of the outer clay surface), leaving the outer surface hydrophilic and the inner layers organophilic. Conversely, their study showed that, at loading rates equal to or greater than 150%CEC, the surfactant was found in both the clay interlayer and on the exterior of the clay surface, which caused a decrease in porosity (Figure 1.11).

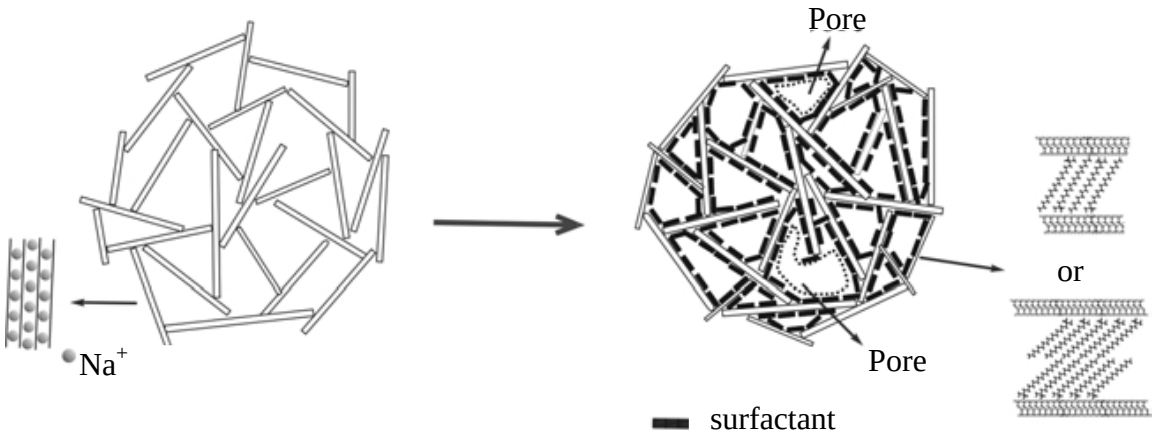

Figure 1.11. Schematic of Na-and HDTMA-montmorillonite at high HDTMA loading rates (He *et al*., 2006b).

Saturation and Dehydration of Organoclays

While the height of the HDTMA-modified clay gallery is dependent on the surfactant concentration, d-spacing also relies on the amount of water in the sample (Bonczek *et al*., 2002; Lee and Kim, 2002a). Bonczek *et al*. (2002) found that as long as sodium was present in the clay gallery, hydration of these inorganic cations caused a uniform increase in d-spacings, suggesting that the amount of hydration was due to the presence rather than the quantity of sodium. Lee and Kim (2002a) reported that, at loading rates between 1% and 150% of the CEC, the d-spacing of HDTMA-montmorillonite was ~4-5Å larger for water-saturated samples compared to samples analyzed at 40% relative humidity and <5% relative humidity (Figure 1.12). At surfactant loading rates >150% CEC, the degree of hydration produced little variation in HDTMA-montmorillonite d-spacings. Based on the large d-spacings for wet <150% CEC HDTMA-montmorillonite, Lee and Kim (2002a) concluded that surfactants in the interlayers of

these organoclays are more disorganized and loosely arranged than the monolayer and bilayer arrangements typically reported for analysis of dry clays (Figure 1.6).

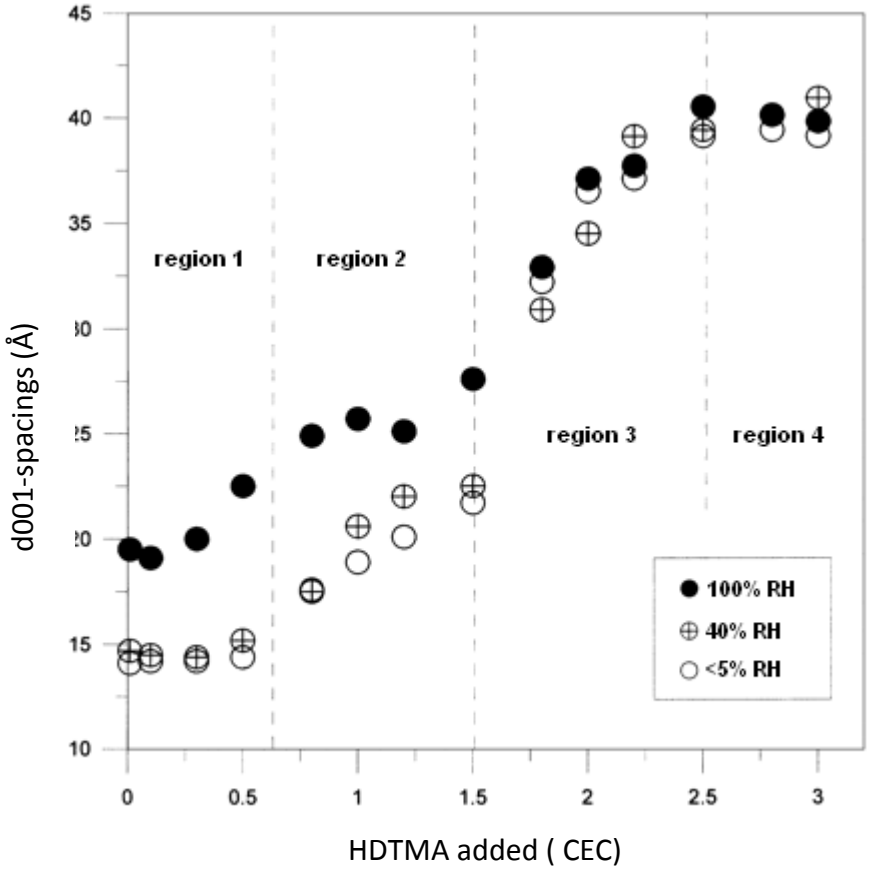

Figure 1.12. Changes in d-spacings as function of HDTMA loading and the amount of relative humidity (Lee and Kim, 2002a). HDTMA was added to water saturated clay (100% RH), montmorillonite at 40% relative humidity, and clay dried in a desiccator to <5% relative humidity.

HDTMA-montmorillonite can be heated to cause dehydration. This leads to changes in basal spacings that vary with the amount of surfactant found in the clay. A study by Lee and Kim (2003b), which evaluated changes in HDTMA-montmorillonite as it was heated to 500°C, found that dehydration of 120% CEC HDTMA-montmorillonite led

to a decrease in d-spacing as water was driven out (Figure 1.13). They concluded that removing water allowed the surfactant tails to become more orderly and to lie horizontally to the hydrophobic siloxane surface (Figure 1.14a and b). However, dehydration of organoclays with paraffin-type arrangements caused the d-spacing to slightly increase (Figure 1.13). Authors interpreted that this was caused by the decrease in water allowing more hydrophobic interactions between surfactant tails, permitting them to straighten, thus increasing the gallery height (Figure 1.14c and d).

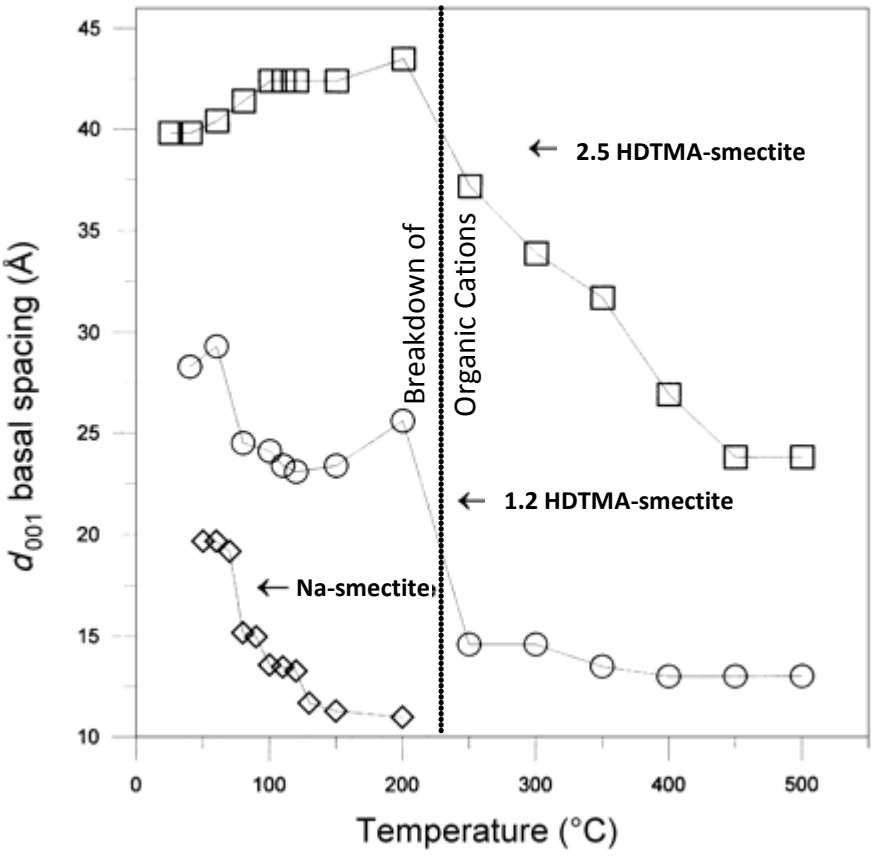

Figure 1.13. D-spacing variations as a result of temperature (Lee and Kim, 2003b). The dramatic decrease at temperatures higher than 200°C for HDTMA-montmorillonite is due to surfactant breakdown.

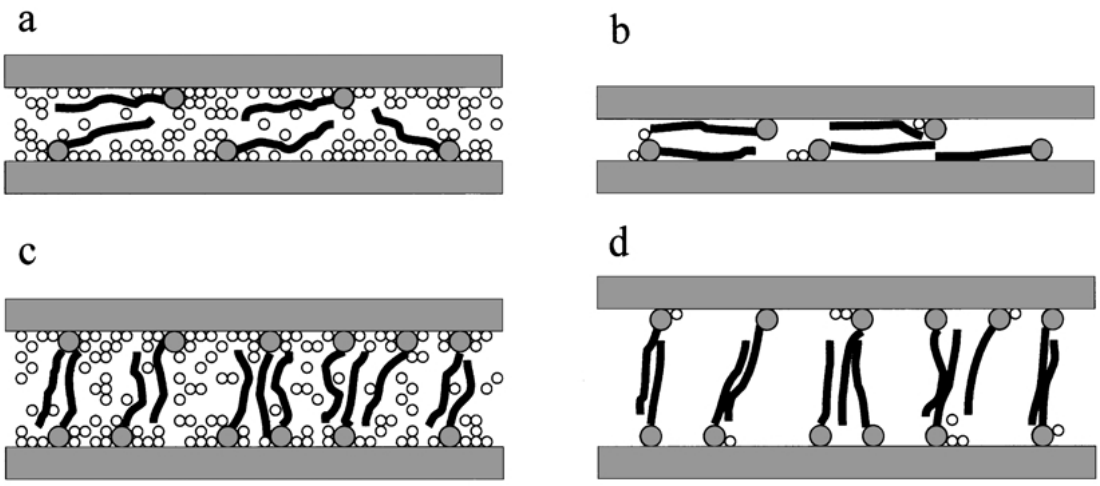

Figure 1.14. Schematic of possible surfactant/water orientations n montmorillonite (Lee and Kim, 2003b). Arrangements of hydrated (a) and dehydrated (b) 120% CEC HDTMA-montmorillonite and hydrated (c) and dehydrated (d) 250% CEC HDTMA-montmorillonite proposed by Lee and Kim (2003b). Surfactants are represented with dark circles and lines and water molecules are depicted by unfilled circles.

Changes in Montmorillonite Morphology due to HDTMA Loading

As HDTMA exchanges into montmorillonite, the clay begins to lose its natural curvature and to become increasingly aggregated (He *et al*., 2006a; Lee and Kim, 2003a) (Figure 1.15). Lee and Kim (2003a) used scanning electron micrographs (SEM) to directly view the morphological changes caused by exchanging inorganic cations with HDTMA. They reported that HDTMA-modification of Na-montmorillonite caused a change in clay structure from “entrails”-like to “cornflake”-like (Figure 1.16a, b, and c). The smooth, dispersed nature of natural Na-montmorillonite was attributed to dispersion caused by the presence of strongly hydrated sodium ions in the interlayers. SEM images of Ca-montmorillonite appear as “irregular aggregates” (Figure 1.16d). Exchange of inorganic cations with HDTMA molecules caused the aggregates to grow larger (Figure 1.16e and f). In the modification of both Na- and Ca-montmorillonite, loading of HDTMA caused the clays to flocculate, presumably because they became more hydrophobic.

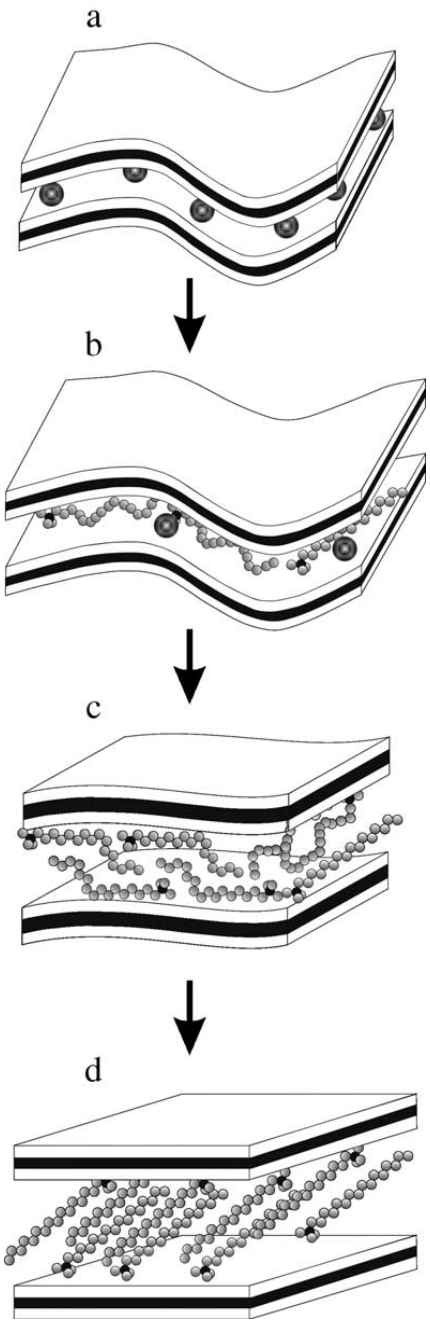

Figure 1.15. Schematic of proposed variations in montmorillonite structure with HDTMA loading (He *et al*., 2006a). Montmorillonite plates transition from (a) Na-montmorillonite to (b) monolayer, to (c) pseudotrilayer, to (d) paraffin-type arrangement (He *et al*., 2006a). The double circles (in a and b) represent sodium ions. Dark filled circles represent methyl heads of HDTMA and lighter circles symbolize surfactant methyl groups.

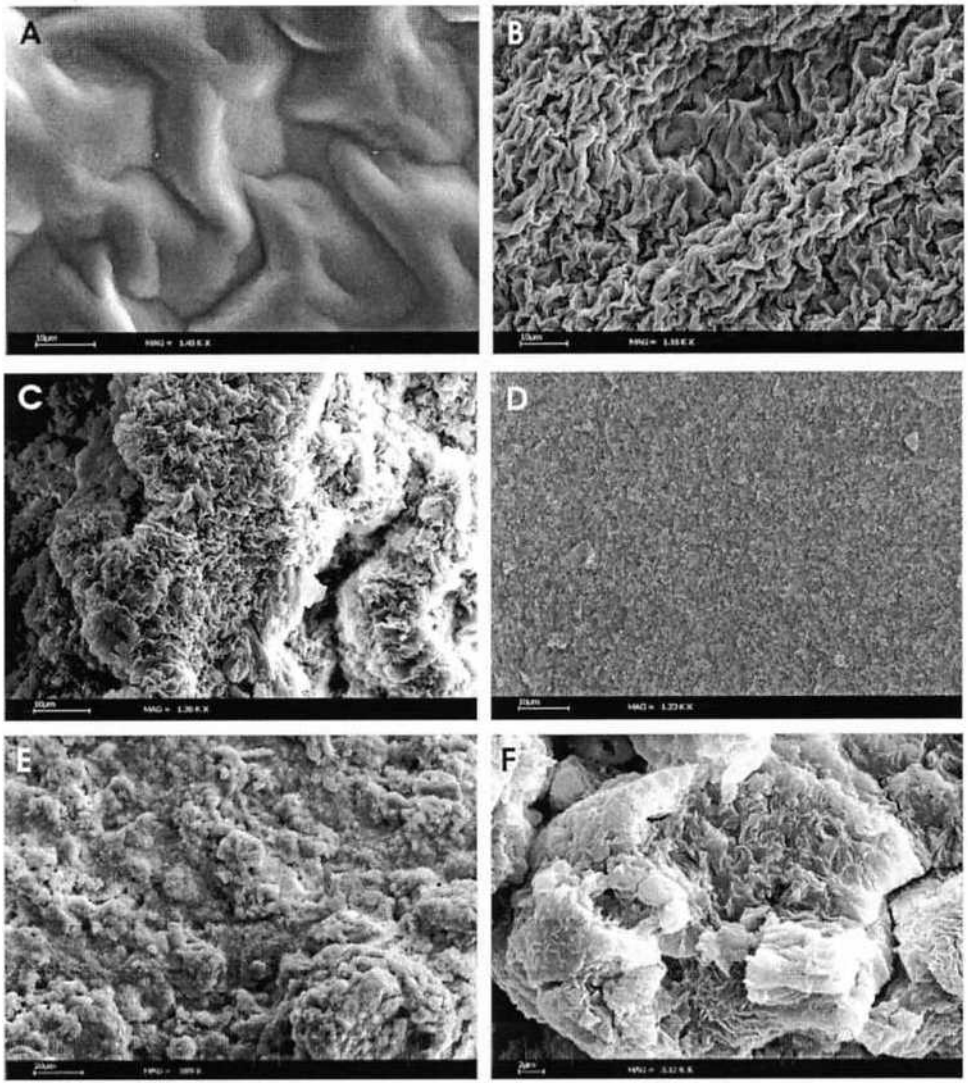

Figure 1.16. Modified and unmodified smectite (Lee and Kim, 2003a). Scanning electron micrographs (SEM) of (a) raw Na-montmorillonite and Na-montmorillonite exchanged with HDTMA to (b) 15% CEC and (c) 90% CEC. SEM micrographs of (d) raw Ca-montmorillonite and Ca-montmorillonite exchanged with HDTMA (e) to 15% CEC and (f) to 90% CEC.

He *et al*. (2006a) suggested that the repulsive forces between the hydrophilic surface and the hydrophobic surfactant tails caused the clay layers to become less curved. However, the clay surface is hydrophobic and it is the inorganic cations that cause unmodified montmorillonite to behave hydrophilically (Sposito *et al*., 1983; Jaynes and Boyd, 1991b). Additionally, interactions between the surfactant tails and the siloxane

surface are attractive (Lee and Kim, 2003b). As more HDTMA molecules are exchanged with inorganic cations (which are strongly hydrated), the clay interlayer contains fewer water molecules, which makes the interlayer increasingly hydrophobic. A possible explanation for the decrease in the curvature of clay particles could be that the water is driven out, causing more hydrophobic interactions between the carbon tails allowing them to straighten--as seen by Lee and Kim (2003b), who used high temperatures to dehydrate organoclays. Further study and comparison is required because the research of Lee and Kim (2003b) was conducted at very high temperatures (up to 500°C) that caused extreme dehydration, unlike the analysis of He *et al*. (2006a). Although there is little research focusing on why the clay layers become less curved with increased loading of QAC's, this phenomenon may be due to steric conditions—the interlayer is forced to straighten out with increased loading of the large surfactant molecules.

DESTRUCTIVE TECHNOLOGIES FOR TREATMENT OF PERCHLORATE

Chemical Reduction

While thermodynamically favored, the chemical reduction of perchlorate involves large kinetic barriers and is very slow under typical conditions (Urbansky, 1998; Moore *et al*., 2003; Cao *et al*., 2005; Brown and Gu, 2006). Furthermore, commonly used reducing agents, such as sulfite, dithionite, and zero-valent iron fail to reduce perchlorate (Brown and Gu, 2006). Cao *et al*. (2005) showed that perchlorate could be reduced by nanoscale iron particles within 24 hours at 75°C. Xiong *et al*. (2007) showed that zero-valent iron stabilized with starch or sodium carboxylmethyl cellulose reduced perchlorate to chloride with the accumulation of no intermediate species. However, trace amounts of metals hindered perchlorate reduction and the process was significantly more efficient at temperatures of 110°C (Xiong, *et al*., 2007). Ti(III) in the presence of β–alanine was able to chemically reduce perchlorate within 2.5 hours, at 50°C and pH > 2.3 (Wang *et al*.,

2010). Perchlorate was also reduced with metallic iron in the presence of UV light (Gurol and Kim, 2000). Direct electrochemical reduction of perchlorate is currently not an effective method of treating contaminated waters due to slow reaction rates and the reduced efficiency caused by the presence of other species (Brown and Gu, 2006; Coates and Jackson, 2009). Although electrodialytically assisted catalytic reduction of perchlorate is possible in concentration ranges of 10-100mg/L, this technique was inefficient at concentrations of <1mg/L (Wang and Huang, 2008).

Biodegradation

Perchlorate-Reducing Bacteria (PRB) in General

Perchlorate-reducing bacteria (PRB) have been identified since the mid 1960's (Hackenthal, *et al*., 1964). Most perchlorate and chlorate reducing bacteria are Gram-negative, non-spore-forming, non-fermenting, facultative anaerobes or microaerophiles (Wallace *et al*., 1998; Coates, *et al*., 1999; Waller *et al*., 2004; Coates and Jackson, 2009; Bardiya and Bae, 2011). These bacteria are phylogenetically diverse, typically members of the genus *Dechloromonas* or *Azospira* (previously *Dechlorosoma),* found in the β subclass of the *Proteobacteria (Achenbach et al*., *2001; Coates and Achenbach, 2004; Coates et al*., *1999).* All identified prokaryotes capable of respiration using perchlorate or chlorate as the electron donor are classified within the α, β, γ and ε subclasses of the *Proteobacteria* (Achenbach *et al*., 2001; Bardiya and Bae, 2011; Coates *et al*., 1999; Wallace *et al*., 1998). Most of these organisms are members of the genus *Dechloromonas* or *Dechlorosoma,* found in the β subclass of the *Proteobacteria* (Achenbach *et al*., 2001; Coates *et al*., 1999), although a study by Waller *et al*. (2004) found a significant number of α*-Proteobacteria* in a study of the diversity of PRB in both contaminated and pristine sites.

Pathway of Perchlorate Reduction

Perchlorate degradation follows the pathway: perchlorate (ClO_4^-) → chlorate (ClO_3^-) → chlorite (ClO_2^-) → Cl^- + O_2 (Rikken, *et al*., 1996; Wallace *et al*., 1998) (Figure 1.17). No transitional phases (chlorate and chlorite) typically accumulate in solution, as the initial reduction of perchlorate is the rate limiting step (Logan, 2001; Kim and Logan, 2001; Bardiya and Bae, 2011). The reduction of chlorite to chloride and oxygen, which is catalyzed by chlorite dismutase, is common to all identified PRB. Chlorite is toxic to bacteria; therefore, the presence of chlorite dismutase is necessary for bacterial germination even though no cell growth is associated with this reaction (Coates *et al*., 1999). Studies indicate that while the outer membranes of all PRB contain chlorite dismutase, this enzyme is only expressed in anaerobic conditions and in the presence of perchlorate or chlorate (Chaudhuri *et al*., 2002; O'Connor and Coates, 2002). Oxygen does not accumulate in the system because most PRB are facultative anaerobes, and quickly reduce any oxygen that is produced (Bardiya and Bae, 2011).

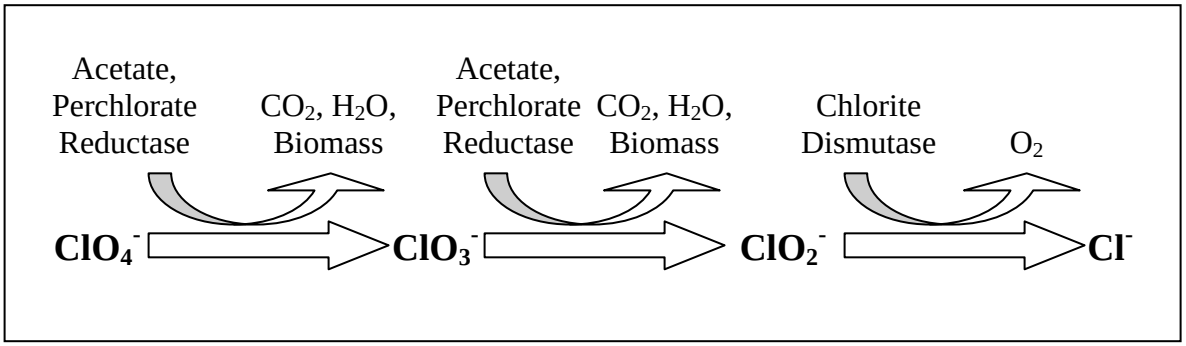

Figure 1.17. The degradation pathway of perchlorate (Rikken *et al*., 1996).

Diversity/Ubiquitousness of PRB

PRB are found in a variety of environments, including pristine areas (Coates *et al*., 1999; Waller *et al*., 2004). For instance, Coates *et al*. (1999) discovered between

2.31×10^3 to 2.4×10^6 cells of PRB per gram of sample from each of the following environments: aquatic sediments, paper mill waste sludges, animal waste lagoons, industrial sites and both pristine and hydrocarbon-contaminated soils.

Research indicates that PRB are capable of growth via a variety of metabolisms, including oxidation of simple organic acids (Achenbach *et al*., 2001; Bruce *et al*., 1999; Coates *et al*., 1999), volatile fatty acids (Coates *et al*., 1999), reduced humic substances (Bruce *et al*., 1999; Coates *et al*., 2002), hydrogen (Nozawa-Inoue, *et al*., 2005), sulfide (Bruce *et al*., 1999), iodate (Kengen *et al*., 1999), bromate (Kengen *et al*., 1999), and ferrous iron (Bruce *et al*., 1999; Chaudhuri *et al*., 2001; Coates *et al*., 1999). Additionally, most PBR are capable of reducing nitrate (Achenbach *et al*., 2001; Coates *et al*., 1999; Nozawa-Inoue *et al*., 2005).

Bioreactors to Treat Perchlorate Contamination

Removal of perchlorate can be completed using a variety of bioreactor configurations, including fixed-bed (Miller and Logan, 2000; Logan and LaPoint, 2002; Brown *et al*., 2003; Min *et al*., 2004), fluidized-bed (McCarty and Meyer, 2005; Fuller *et al*., 2007), and membrane biofilm (Nerenberg and Rittmann, 2004; Nerenberg *et al*., 2008; van Ginkel *et al*., 2008; Ziv-El and Rittmann, 2009). Bioreactors for perchlorate degradation typically include additives of either acetate or H_2, which serve as the electron donor (Bardiya and Bae, 2011). Issues with the use of organic electron donors, such as acetate, include the risk of elevated organic electron donors in treated water and increased biomass production, both of which result in higher total suspended solids (Hatzinger, 2005). The use of H_2 may raise concerns related to its low solubility in water and the possible detonation of any H_2 that vents out of the system (Hatzinger, 2005; Logan and LaPointe, 2002; Miller and Logan, 2000).

Although bioreactors are efficient at degrading highly concentrated waste streams, this method has not been applied to treat drinking water (Bardiya and Bae, 2011; WRF, 2011). This lack of utilization is due the generally negative public perception of microbial treatment of drinking water, which is typically attributed to the threat of contamination of treated water with microbial cells and disinfection by-products (Li, 2008; Dugan *et al*., 2009; Bardiya and Bae, 2011; WRF, 2011). Another obstacle to the application of this method is the potential negative impact to water quality that results from elevated levels of sulfide, ammonia, microbial products, and acetate (Brown *et al*., 2003; Dugan *et al*., 2009). These constituents may cause odors, increase biological activity, increase the amount of chlorine necessary for disinfection, and produce more disinfection byproducts (Brown *et al*., 2003; Dugan *et al*., 2009). Additional concerns with biological treatment are the exorbitant cost of operation and the potential for excess biomass accumulation (Bardiya and Bae, 2011).

In situ Treatment of Perchlorate Contamination

Biostimulation

PRB are ubiquitous in the environment, and, therefore, contaminated sites generally do not require bioaugmentation for successful treatment of perchlorate-contaminated sites (Coates *et al*., 1999; Coates and Achenbach, 2004; Coates and Jackson, 2009; Hatzinger *et al*., 2009; Borden and Lieberman, 2009). Often the only site requirement is the successful application of suitable electron donors (Hatzinger *et al*., 2002; Nzengung *et al*., 2001; Wu *et al*., 2001). This addition could be completed using several methods, including active bioremediation, semi-active bioremediation, and passive bioremediation (Cox, 2009; Hatzinger *et al*., 2009). Active bioremediation involves actively mixing the electron donor and groundwater using a system of injection and pumping wells to constantly recirculate water (Cox, 2009; Hatzinger *et al*., 2009).

Semi-active bioremediation is similar to active; however, the system is actively pumped for a short period of time (usually for days to weeks) followed by a longer period in which natural groundwater flow resumes and continues to mix the system (Cox, 2009; Hatzinger *et al*. 2009; Krug and Cox, 2009). Passive bioremediation entails injecting slow-release electron donors into the subsurface and utilizing the natural flow of groundwater to mix the system (Borden, 2007; Borden and Lieberman, 2009; Cox, 2009; Hatzinger *et al*., 2009). One passive bioremediation technique involves constructing biowalls, which are trenches filled with a solid electron donor (e.g. mulch, compost, or wood particles) that are sometimes recharged with semi-soluble amendments, such as vegetable oil (Henry, *et al*., 2009; Stroo and Norris, 2009; Robertson *et al*., 2009). Using this method, mulch and compost can promote perchlorate-reducing conditions for 3-5 years (Henry *et al*., 2009).

Prior to adopting a method of *in situ* remediation, laboratory experiments must be conducted to determine the optimal electron donor for the site (Hatzinger *et al*., 2002; Nzengung *et al*., 2001). Recently, the injection of gaseous electron donors has been shown to enhance biodegradation of perchlorate (Evans and Trute, 2006; Evans *et al*., 2011). Additionally, pH buffers may be required to allow or optimize perchlorate biodegradation (Cramer *et al*., 2004).

While the low cost of *in situ* biodegradation of perchlorate makes it an attractive remediation option for contaminated sites, there are some potential drawbacks with this technology. These include the application of excess electron donors into the aquifer, reduction of hydraulic conductivity through biofouling of the aquifer matrix (particularly near where electron donors are applied), and a decline in water quality caused by variations in pH, changes to redox potential, mobilization of heavy metals and phosphate, and the production of Fe(II), HS^-, and CH_4 (Coates and Jackson, 2009).

Additionally, site specific characteristics may reduce the effectiveness of *in situ* biodegradation in some cases.

Phytoremediation

Phytoremediation is another option for *in situ* treatment of perchlorate found in shallow groundwater (Susarla *et al*., 1999; Nzengung *et al*., 1999; van Aken and Schnoor, 2002; Yifru and Nzengung, 2008). Numerous plant species have been found to remove perchlorate from groundwater, including smartweed, pickleweed, water-lily, willow, eastern cottonwoods, poplar trees, eucalyptus, sweet gum, tarragon, blue-hyssop, perennial glasswort, and parrot-feather (Nzengung *et al*., 1999; Susarla *et al*., 1999; Susarla *et al*., 2000; van Aken and Schnoor, 2002; Shrout *et al*., 2006; Yifru and Nzengung, 2008; Stuckhoff, 2009). Phytoremediation of perchlorate is generally attributed to two processes: 1) uptake and phytodegradation and 2) rhizodegradation (Nzengung, *et al*., 1999; Nzengung *et al*., 2004). Rhizodegradation occurs when microbial degradation of perchlorate in root zones is enhanced because microbes associated with plant roots utilize electron donors produced by plants and excreted by root systems to degrade a contaminant (Shrout *et al*., 2006). This degradation in the rhizosphere can be enhanced by adding electron sources, such as dissolved organic carbon (Yifru and Nzengung, 2008). Krauter (2001) and Krauter *et al*. (2005) developed an *in situ* wetland bioreactor that effectively removed perchlorate from groundwater.

DUAL TREATMENT OF PERCHLORATE

While microbial degradation of perchlorate results in the complete breakdown of perchlorate into non-hazardous byproducts, the negative public perception of biodegradation due to fear of biological components entering drinking water reduces its viability as a treatment for drinking water. Chemical reduction of perchlorate generally

requires high temperatures that greatly reduce its cost efficiency. Filtration technologies are much more favorable to the public but consist of transferring perchlorate from the solution to the solid phase, with no degradation of perchlorate molecules. An optimal method for treatment of perchlorate-contaminated water will take advantage of the benefits of both processes by first using a filtration media, such as HDTMA-montmorillonite, to quickly remove perchlorate from solution, followed by biological or chemical reduction of perchlorate bound to the filtration media. This combination would result in complete degradation of perchlorate, with only non-hazardous byproducts (Cl^- and O_2) remaining.

CONCLUSION

Many technologies can be utilized to treat perchlorate contamination, including biodegradation, chemical reduction, ion exchange resins, membrane technologies, surfactant modified geosorbents, such as HDTMA-montmorillonite. Nondestructive technologies are generally more widely accepted methods of drinking water treatment. However, these processes merely transfer the perchlorate from the liquid to the solid phase. Biodegradation achieves complete degradation of perchlorate, but the public is less accepting of the application of this technology to treat drinking water. Chemical reduction is another destructive technology. However, chemical reduction typically requires high temperatures and the expense of heating large quantities of water becomes prohibitive. Perhaps the best method to treat perchlorate-contaminated water, particularly for drinking water and industrial waste streams, is the use of a two step process. First the perchlorate can be efficiently and quickly removed using a filtration media, such as HDTMA-montmorillonite. In the second phase, the perchlorate bound to the clay is biologically or chemically reduced so that only non-hazardous waste products remain.

CHAPTER 2

SORPTION OF PERCHLORATE BY SURFACTANT-MODIFIED MONTMORILLONITE

ABSTRACT

Surfactant-modified montmorillonite (SMM) was created by exchanging the inorganic cations naturally found in clay interlayers with hexadecyltrimethylammonium (HDTMA) ions. SMM was evaluated as a filtration media for perchlorate-contaminated waters. Sorption batch tests showed that SMM has a relatively larger sorption capacity for perchlorate compared to surfactant-modified zeolite (SMZ). Kinetic studies revealed that SMM and SMZ approached sorption equilibrium within 1 and 3 hours, respectively. Although co-contaminants reduced perchlorate uptake by SMM, the filtration media remained selective for perchlorate in groundwater from Longhorn Army Ammunition Plant (LHAAP) and in brine created during the regeneration of ion exchange resin used to treat perchlorate-contaminated water.

INTRODUCTION

Prior to 1997, perchlorate was not considered to be a common drinking water contaminant. However, when the California Department of Health Services developed a method to measure perchlorate with a detection limit of 4ppb, much lower than the 400ppb detection limit of previous techniques (Logan, 2001; Motzer, 2001; Srinivasan and Sorial, 2009), researchers and the environmental community began detecting the contaminant in many areas, including many sources of municipal drinking water supplies (Pontius *et al*., 2000; Logan, 2001; Motzer, 2001). The development of this new

analytical technique eventually led to the detection of perchlorate in at least 45 states and in 4% of public drinking water sources in the United States (USEPA, 2011; USGAO, 2010), with concentrations greater than 5,000ppb reported in Alabama, Arkansas, Arizona, California, Nevada, Texas, Utah, and West Virginia (USGAO, 2010). Perchlorate has also been detected in dairy milk (Kirk *et al.*, 2003; USFDA, 2009; Kirk *et al*., 2005; Sanchez *et al*., 2008), infant formula (Pearce *et al*., 2007), human breast milk (Kirk *et al*., 2005; Pearce *et al.*, 2007), wine and beer (El Aribi *et al*., 2006), dietary supplements (Snyder *et al*., 2006), forage crops (Sanchez *et al*., 2008); lettuce (USFDA, 2009; Sanchez *et al.*, 2005a; Sanchez *et al*., 2005b, Seyfferth and Parker, 2007), and many other fruits and vegetables (USFDA, 2009; Jackson *et al*., 2005; El Aribi *et al*., 2006). Additionally, Blount *et al*. (2007) found detectable levels of perchlorate in urine from each of the nearly 3000 people studied in research conducted by the Center for Disease Control in Atlanta, Georgia.

Perchlorate has a wide variety of anthropogenic uses. The majority of manufactured ammonium perchlorate in the United States is utilized as an additive in solid rocket propellant (Urbansky and Schock, 1999; Logan, 2001), where it has a limited shelf life and has to be replaced periodically (Motzer, 2001; Pontius *et al.*, 2000; Cunniff *et al*., 2006). Much of the man-made perchlorate contamination in the United States was likely caused when high-pressure water was used to wash the propellant out of containers during this replacement process (Urbansky, 1998; Logan, 2001). This process often resulted in discharges of high-concentration effluent directly onto the ground surface or into evaporation ponds, both of which were legal at the time. Perchlorate salts are used in a wide variety of additional products and activities, such as munitions, pyrotechnics (including fireworks, matches, photographic flash powder, and flares), blasting agents, lubricating oils, tanning leather, electroplating, rubber manufacturing, paint production, automobile air bag inflators, magnesium batteries, and

medications to treat hyperthyroidism (ITRC, 2002; Cunniff *et al*., 2006; Aziz *et al*., 2006; Sturchio *et al*., 2006; Mattie *et al*., 2006; Srinivasan and Sorial, 2009). Also, perchlorate is created as a byproduct during the production of herbicides that contain sodium chlorate (Cunniff *et al*., 2006). Both the manufacturing and use of these products are potential sources of perchlorate releases into the environment.

Perchlorate is also naturally occurring in the environment. The nitrate-rich caliche deposits in the Atacama Desert, Chile contain measureable quantities of perchlorate (Bao and Gu, 2004; Urbansky *et al*., 2001) and were long thought to be the only naturally formed perchlorate deposit. For over a century (peaking in the 1930's), this ore was imported to the United States for use as a fertilizer, with a variety of names including Chile saltpeter, Bulldog soda, nitrate saltpeter, sodium nitrate, nitratine, sodia niter, and nitrate of soda (Aziz *et al*., 2006; Urbansky *et al*., 2001). Although the mechanism of perchlorate formation in these deposits was a mystery for many decades (Jackson *et al*., 2006), more recent research indicates that the primary mechanism of formation was likely deposition of perchlorate created by photochemical reactions in the atmosphere (Michalski *et al*., 2004; Bao and Gu, 2004; Rajagopalan *et al*., 2006; Sturchio *et al*., 2006; Kang *et al*., 2008; Rao *et al*., 2010). Non-anthropogenic perchlorate has been detected in the High Plains of Texas and New Mexico (Rajagopalan *et al*., 2006). Perchlorate has been measured in potash ore from Saskatchewan, Canada and New Mexico, in mineral samples of hanksite from Searles Lake, California, and in playa crust samples from Bolivia and California (Orris *et al*., 2003). Groundwater samples from "pristine" areas across the United States contained measurable quantities of perchlorate (Parker *et al*., 2008). In two separate studies by Dasgupta *et al*. (2005) and Parker *et al.* (2008), perchlorate was detected in the majority of rainwater samples taken during rainfall events from throughout the Southwestern United States.

Numerous adverse health effects have been associated with perchlorate exposure in humans. Most issues are caused by the reduction of thyroid function, which is the result of perchlorate competitively blocking iodide uptake by the sodium/iodide symporter (USEPA, 2005b). Iodide is crucial for the synthesis of thyroid hormones (L-triiodothyronine (T_3) and L-thyroxine (T_4)); therefore, a reduction in iodide uptake can result in lower production of these hormones (USEPA, 2005b). In addition to being important for oxygen metabolism and regulation of gene expression, T_3 and T_4 are vital for functioning of tissues, for proper bone growth, and for proper cell growth, differentiation and metabolism (Galfore *et al.*, 2009; Videla and Fernandez, 2009; Capen and Martin, 1989). Low levels of thyroid hormones in fetuses may result in irreversible neurological effects and mental retardation (Galfore *et al*., 2009). Pregnant and lactating women, fetuses, and infants are generally regarded as populations that are sensitive to the effects of perchlorate intake (USEPA, 2010).

In 1998, the United States Environmental Protection Agency placed perchlorate on the contaminant candidate list (USEPA, 2009) and later established a reference dose of 0.7µg/kg/day. This corresponds to a drinking water equivalent level of 24.5ppm assuming that all perchlorate is supplied from drinking water (USEPA, 2005a). Several states (e.g. Massachusetts, California, and Texas) have set lower regulatory levels for perchlorate (Srinivasan and Sorial, 2009). In February 2011, USEPA decided to regulate perchlorate in drinking water under the Clean Water Act (Federal Registry, 2011). The USEPA is currently preparing a proposed National Primary Drinking Water Regulation (NPDWR) for perchlorate, which is scheduled to be published by February 2014 and finalized within 18 months of publication (Federal Registry, 2011).

Ion exchange is the most commonly used method to treat perchlorate-contaminated drinking water. Both non-selective and perchlorate-selective ion exchange resins are capable of removing perchlorate from water (Coates and Jackson, 2009; Gu,

et al., 2001; Gu *et al*. 2007). After use, the resins still contain perchlorate and, therefore, require either regeneration or treatment as a hazardous waste. If the resins are regenerated, the perchlorate is transferred to high concentration brines, which also requires either treatment or disposal as a hazardous waste.

In an effort to develop low-cost techniques to treat wastewater and to remediate contamination in the environment, many studies have focused on the modification of geologic materials for use as filtration media. One area of increasing interest is the use of zeolite and swelling phyllosilicate minerals, particularly montmorillonite, as sorption media to filter contaminants from water. In order to enhance the sorption capacity of geologic materials, “geosorbents” have been created by treating zeolite and clays with surfactants, particularly quaternary ammonium cations (QACs), such as hexadecyltrimethylammonium (HDTMA). HDTMA consists of a positively charged 3-methyl quaternary amine head group with a positive monovalent charge connected to a neutral 16-carbon tail. Modification of montmorillonite with HDTMA occurs as the surfactant molecules exchange with inorganic cations naturally found in interlayer regions of clays (Boyd *et al*., 1988a; Bonczek *et al*., 2002; Mizutani *et al*., 1995; Lee and Kim, 2002a; Zhang *et al*., 1993). When HDTMA is added to zeolite, the positively charged head is attracted to the negatively charged surface, creating a layer of surfactants surrounding the zeolite surface (Haggerty and Bowman, 1994). Surfactant-modified montmorillonite (SMM) and surfactant-modified zeolite (SMZ) are hydrophobic and, therefore, are able to adsorb higher quantities of many contaminants compared to unmodified materials (Bonczek *et al*., 2002; Boyd *et al*., 1988a; Brown and Burris, 1996; Luthy *et al*., 1997; Nzengung *et al*., 1996).

Both Kim *et al*. (2011) and Seliem *et al*. (2011) found that montmorillonite modified with HDTMA is capable of adsorbing perchlorate from water. However, neither of these studies further examined perchlorate sorption by SMM through the development

of sorption isotherms nor did they conduct kinetic experiments to evaluate the amount of time required for sorption equilibrium to occur.

The objective of this research is to evaluate SMM and SMZ as low-cost adsorbents of perchlorate. Kinetic studies were utilized to determine the amount of time required for perchlorate loading onto the filtration media. Isotherms were developed to investigate the amount of perchlorate adsorption by both SMM and SMZ. Additionally, the effect of 13 co-contaminants on perchlorate sorption by was also examined to identify potential interferences to the uptake of perchlorate by SMM.

MATERIALS AND METHODS

Materials

Sodium-montmorillonite (Swy-2) from Crook County, Wyoming, USA, was purchased from the Clay Minerals Society Source Clay Repository. A thorough list of published research involving Swy-2 can be found on the Clay Minerals Society website at www.clays.org. Hexadecyltrimethylammonium bromide (HDTMA) was obtained from Tokyo Kasei Kogyo Co and benzyldimethyltetradecylammonium chloride dihydrate (BDTDA) was obtained from Aldrich Chemical Co. (Milwaukee, WI). Sodium perchlorate, potassium nitrate, tetramethylammonium chloride (TMA) and trimethylphenylammonium chloride (TMPA) were purchased from Fisher Chemical, Fisher Scientific, Fair Lawn, New Jersey. California NELAC Perchlorate Standards were obtained from AccuStandard Wet Chemistry Reference Standard. Groundwater was obtained from a monitoring well at an open burn/open detonation site at Longhorn Army Ammunition Plant (LHAAP), Karnack, Texas. The perchlorate-contaminated brine was provided by a Los Angeles, California drinking water treatment plant that uses regenerable ion exchange resin to treat perchlorate contaminated groundwater.

Preparation of Organoclays

Organoclays were prepared as described by Nzengung (1993) by exchanging the inorganic cations found in the montmorillonite interlayer with the following cationic surfactants: TMA, TMPA, BDTDA, and HDTMA. Briefly, Na-montmorillonite was converted to organoclay by ion exchange with aqueous solutions that contained surfactants concentrations equal to the CEC (76.4meq/100g) and mixed using a magnetic stir plate for 24 hours. Next, the organoclay was separated via centrifugation. Finally, the organoclay was washed until the $AgNO_3$ test was negative for bromide in the supernatant, separated by centrifugation, quick frozen, and freeze-dried.

Preparation of Surfactant-Modified Zeolite

SMZ was provided by Mr. Richard Helferich of Columbus, OH, where the SMZ was created using the following steps: 1) zeolite was acquired from the St. Cloud Mine in Winston, NM in the size range of 0.297 to 0.595 mm (30–50 mesh); 2) the natural zeolite was placed in columns (15cm long and 2.5cm diameter); 3) 2L of 40mM HDTMA-Br solution flowed through the column at 3mL/min; 4) zeolite was rinsed with water at 3.0mL/min for 4.5 pore volumes; and 5) SMZ was air dried overnight in a fume hood (Zhang *et al*., 2007).

Methodology

Comparison of Perchlorate Sorption by Organoclays

Batch tests were conducted to compare perchlorate loading onto each type of organoclay. Two reactors were prepared for each type of organoclay and for unmodified Na-montmorillonite. Each reactor contained 0.2g of each organoclay or Na-montmorillonite to which 100mL of 10mg ClO_4^-/L solution was added. The vials were shaken by hand and placed on an end-over-end rotating shaker for 24 hours at ambient

temperature. The vials were centrifuged and 15mL samples of the solution were collected. Prior to perchlorate analysis, the solution was passed through a 0.22µm filter to remove most all of the clay particles. Based on the results of this experiment, the organoclay that adsorbed the most perchlorate was determined and utilized in all further experiments. For simplicity, the selected organoclay was called surfactant-modified montmorillonite (SMM) and was investigated in the remainder of the research.

Kinetic Batch Tests

In order to determine the amount of time required for perchlorate sorption equilibrium to be approached, kinetic batch tests were conducted with both SMM and SMZ, using 0.1g of sorbent and 50mL of solution. The initial concentrations of perchlorate used in the tests were 380µg/L and 1,200µg/L for SMM and 700µg/L for SMZ. After dosing, the vials were placed on an end-over-end rotating shaker. Periodically, during the duration of the test (12 and 13.5 hours for SMM and SMZ, respectively), the aqueous perchlorate concentrations were analyzed in duplicate vials. The first set of vials sacrificed for analysis were shaken by hand and centrifuged for 40 minutes at 2,000rpm (rotor diameter of 30cm), and filtered through a 0.22µm screen prior to perchlorate analysis. The remaining samples incubated at ambient temperature for longer equilibration periods and were placed on an end-over-end rotating shaker until 45 minutes prior to the time of analysis, when two vials of each treatment were centrifuged, filtered, and immediately analyzed via ion chromatography. The times reported for the kinetic studies cover the time from when the stock solution was added to the vial until when the sample was filtered.

Equilibrium Batch Tests

The batch reactors consisted of borosilicate glass that was threaded at the top to allow closure with aluminum screw top seal lined with a silicone face septum. In the lower concentration batch test, 0.2g of SMM or SMZ was dosed with 100mL of aqueous solutions with initial perchlorate concentrations ranging from 0-24mg/L. Triplicate vials were dosed with each concentration for a total of 18 vials per isotherm. Immediately after dosing, the vials were sealed, shaken by hand, and placed on an end-over-end rotating shaker where they were mixed continuously for the duration of the equilibrium period, as previously determined from batch sorption kinetic tests. After the equilibration period, the reactors were centrifuged and the solution was decanted and filtered with a 0.2µm filter to remove most all residual clay particles prior to analysis.

An additional batch sorption test was performed at high perchlorate loading on SMM. For this equilibrium sorption test, each vial was completed in duplicate and contained 0.5g SMM, 50mL of solution, and initial perchlorate concentrations ranging from 0-470mg/L. The batch samples were equilibrated and sampled as previously described.

Effects of Nitrate and Other Co-constituents in Groundwater

Additional batch sorption tests were performed to evaluate the effects of co-constituents in water on perchlorate sorption by SMM. A more intensive investigation focused on competition by nitrate for two reasons: 1) both nitrate and perchlorate have relatively low hydration energies compared to many other anions that are commonly found in the environment and 2) ammonium perchlorate is frequently the type of perchlorate salt that is utilized in many applications. In the environment, ammonium is often oxidized to nitrate, resulting in elevated nitrate concentrations (compared to background levels) associated with ammonium perchlorate contamination.

The effect of nitrate alone on perchlorate sorption by SMM was evaluated in sorption a batch test using deionized water spiked with perchlorate and nitrate. Another batch sorption test was conducted with groundwater from LHAAP, which contained 32.4mg ClO_4^-/L and numerous other compounds, including 1,1,2-trichloroethane, methyl tert-butyl ether (MTBE), aluminum, arsenic, chromium, cadmium, sodium, magnesium, chloride, and sulfate. In both batch tests, the vials contained 0.2g SMM and 100mL of either deionized water or groundwater. The initial perchlorate concentration was constant at 32 ±1mg/L. The initial nitrate concentrations in the deionized water solution were varied between 0 to 20.0mg NO_3^-/L. In the batch test with groundwater, the initial nitrate concentration ranged from 0.9 to 20.8 mg NO_3^-/L. In both cases, triplicate vials of 0.2g SMM and 100mL of the solution were prepared for at least 5 initial concentrations. After dosing, the vials were placed on an end-over-end rotating shaker and allowed to equilibrate at room temperature for 24 hours. The vials were centrifuged and 15mL samples of the solution were collected from each vial. The samples were passed through a 0.2µm filter prior to analysis.

Treatment of Perchlorate-Contaminated Brine with SMM

To measure perchlorate adsorption from the brine, batch tests were conducted using both full-strength and half-strength (diluted by 50% with deionized water) brine solutions. The brine, which was produced during the regeneration of ion exchange resin from a Los Angeles, California, drinking water treatment plant, contained 5.6mg/L perchlorate. Brine solutions were spiked with perchlorate so that perchlorate concentrations ranged from 5.6mg/L to 26.4mg/L and 2.8mg/L to 36.1mg/L, for the full-strength and the half strength batch tests, respectively. The batch tests consisted of adding 100mL of the brine solution to vials containing 0.5g of SMM and mixing the

reactors on an end-over-end rotating shaker at ambient temperature for 24 hours. The vials were centrifuged and 15mL samples of the solution were collected for analysis.

Analytical Methods

Analysis of Perchlorate

Perchlorate was measured using a Dionex DX500 Ion Chromatography System (IC) with a 500µL sample loop. Samples were diluted to between 0.002 to 1.5 mg/L and placed in 5mL Dionex auto-sampling vials. The IC setup utilized an IONPAC AS16 analytical column (4x250mm), an AG16 guard column (4x50mm), an ASRS-Ultra II Self Regenerating Suppressor (4mm) set at 300mA, and an AI-450 Chromatography Automation System with the Advanced Computer Interface Module. The samples were analyzed via either the high concentration (standards ranging from 0.1-1.5mg/L) or the low concentration (standards ranging from 10 to 500µg/L) methods. The eluent was made with J.T. Baker 50% (w/w) sodium hydroxide solution and deionized water, which was degassed using a VWR Scientific Aquasonic Sonicator, model 150D. The eluent was applied at a flow rate of 1mL/min and consisted of 100mM and 50mM sodium hydroxide solutions for the high and low concentration methods, respectively.

A new calibration curve was created each time eluent was changed (every 1-2 days) or when the recovery of standards was either <95% or >105%. Calibration of the IC utilized a 4-point calibration curve made for the high-concentration IC method and a 6-point calibration curve for the low concentration method. Blanks of deionized water, along with check standards, were analyzed every 5 samples to test for hold-over and instrumental drifting, respectively. If the blanks detected perchlorate or if the check standard was more than 5% off, the IC was recalibrated and the samples were reanalyzed. All samples were analyzed in duplicate.

Analysis of Groundwater and Brine

The Laboratory for Environmental Analysis, Department of Crop and Soil Sciences, University of Georgia, Athens, Georgia analyzed total organic carbon (TOC), total dissolved solids (TDS), total suspended solids (TSS), MTBE, 1,1,2-trichloroethane, and metals. TOC was analyzed using EPA method 9060A with catalytic conversion. TDS and TSS were determined gravimetrically using EPA test methods 160.1 and 160.2, respectively. MTBE and 1,1,2-trichloroethane were analyzed with a GC/MS equipped with purge-and-trap, using EPA test methods 8260A and 524.2, respectively. Metals (Al, Fe, As, Pb, Cr, Cd, Na, and Mg) were analyzed using ICP/MS with EPA test method 200.8. Anions (nitrate, phosphate, sulfate, and chloride) were analyzed via IC using EPA test method 300.1. The brine is not an ideal solution; therefore, ionic strength was calculated using:

$$I = \frac{1}{2}\sum_{i=1}^{n} b_i z_i^2 \tag{2.1}$$

where I is the ionic strength, b_i is the molality (mol/kg), z_i is the charge of that ion, and the sum is of all ions in solution.

Data Analysis

The amount of adsorbate sorbed to the SMC and SMZ was calculated using mass balance:

$$C_{ADS} = (C_0 - C_{aq})\left(\frac{V}{m}\right) \tag{2.2}$$

where C_{ADS} is the mass adsorbed to the solid phase (mg/kg), C_0 is the initial solution concentration (mg/L), C_{aq} is the equilibrium solution concentration (mg/L), V is the volume of solution (L), and m is the mass of adsorbent (kg).

Sorption isotherms were generated for the batch test studies by plotting the measured equilibrium solution concentration versus the calculated adsorbed concentration using a custom program called Isotherm. The program was developed by John Dowd, University of Georgia Geology Department, Athens, Georgia using Borland C++ 2007. The specific programming libraries utilized were LMD-Tools produced by LMD innovative (Mainz, Germany), TeeChart Pro produced by Steema Software (Catalonia, Spain), and MtxVec and Stats Master both produced by Dew Research (Slovenske Konjice, Slovenia). A Windows version of the Isotherm program is available upon request.

The best fit isotherm model was selected from the linear, Freundlich, and Langmuir models. The simplest batch sorption model is the linear model:

$$C_{ADS} = K_D C_{aq} \tag{2.3}$$

where K_D is the partition coefficient. The Freundlich equation is as follows:

$$C_{ADS} = K_F C_{aq}{}^{N} \tag{2.4}$$

where K_F is the Freundlich sorption coefficient constant [(mg/kg)/(mg/L)^N] and N is the Freundlich exponent relating to the sorption intensity. In order to determine Freundlich sorption parameters, the equation is linearized as follows:

$$\log C_{ADS} = \log K_F + N \log C_{aq} \tag{2.5}$$

A plot of log C_{ADS} verses log C_{aq} yields the sorption parameters K_F and N, which are the log of the y-intercept and the slope, respectively. Note that if N=1, the Freundlich reduces to Equation 2.3. Another model commonly used in sorption studies, the Langmuir isotherm, is as follows:

$$C_{ADS} = \frac{Q_{\max} b C_{aq}}{1 + b C_{aq}} \tag{2.6}$$

where Q_{max} is the maxim adsorption capacity with monolayer coverage (mg/kg) and b is a coefficient relating the extent of adsorption (L/kg).

The linear model was selected to describe the isotherm data if the coefficient of determination (r^2) was greater than 0.97. When the r^2 was less than 0.97, the model with the lowest root mean square error (RMSE) of C_{ads} was used to fit the data. The RMSE is defined as:

$$RMSE = \sqrt{\frac{\sum_{j=1}^{n} (y_j - \hat{y}_j)^2}{n}} \tag{2.7}$$

where n is the number of observations, y is the observed adsorbed concentration, ŷ is the estimated adsorbed concentration corresponding to y. RMSE is often utilized to compare the fits of nonlinear isotherms (Kinnlburgh, 1986; Tsai and Juang, 2000; Tsai *et al*., 2005; Bilgili, 2006; Özkaya, 2006; Padmesh, *et al.,* 2006; Vijayaraghavan *et al*., 2006; Chen *et al*., 2008; Chowdhury and Das, 2010) and is presented in the same units as the y-axis (mg/kg in this case). Smaller values of RMSE indicate a better fit.

RESULTS AND DISCUSSION

Perchlorate Sorption by Unmodified Montmorillonite and Organoclays

Na-montmorillonite did not adsorb perchlorate. This was due to the net negative charge of natural montmorillonite, which makes it unlikely to adsorb an anion. Additionally, perchlorate loading by both TMA- and TMPA-modified montmorillonite was negligible. While BDTDA-montmorillonite was capable of adsorbing appreciable amounts of perchlorate, the sorption was much lower than that observed with HDTMA-montmorillonite. The most perchlorate sorption by far was observed with HDTMA-montmorillonite. Due to this, further investigations utilized this organoclay and HDTMA-montmorillonite was referred to as surfactant-modified montmorillonite (SMM).

The variability in perchlorate uptake between the organoclays was due to the differences in the structure of the surfactants and the resultant organoclay properties. TMA and TMPA are short chain surfactants (Figure 1.2) and tend to act as pillars that prop open montmorillonite interlayers (Bonczek *et al*., 2002; Nzengung *et al*., 1996). This varies drastically from montmorillonite that is modified with long chain surfactants, such as BDTDA and HDTMA. The long chain surfactants act as hydrophobic gel-like partition media inside the clay interlayer (Bonczek *et al*., 2002; Boyd *et al*., 1988a; Nzengung *et al*., 1996). Additionally, hydrophobic attractions between surfactant molecules can result in surfactant loading that is in excess of the cation exchange capacity, causing the organophilic clay to become positively charged (Jaynes and Boyd, 1991b; Lee and Kim, 2002b; Lee and Kim, 2003b; He *et al*., 2006a; Bonczek *et al*., 2002; Zeng *et al*., 2003). Perchlorate is a weakly hydrated anion; therefore, it is attracted to the hydrophobic, positively charged interlayer that results from modification of montmorillonite with long-chain surfactants, such as BDTDA and HDTMA. The positively charged BDTDA head group includes a benzene ring that may reduce the space available for perchlorate sorption (Figure 1.2), producing steric restrictions that reduce the amount of perchlorate loading onto this organoclay compared to HDTMA-montmorillonite. Therefore, the structure of HDTMA makes it the most well suited surfactant to increase perchlorate uptake by montmorillonite.

Kinetic Batch Tests

The results of the approach to sorption equilibrium for both SMM and SMZ indicate that the time required to reach equilibrium is relatively short (Figure 2.1 and Appendix A). The batch kinetic tests for SMM show that sorption equilibrium with perchlorate at different initial concentrations (380 and 1,200µg/L) was approached within an hour. While the initial concentration of perchlorate had no effect on the rate of

approach to equilibrium, the initial concentration did alter the final equilibrium concentration of the solution. The batch test using an initial concentration of 1,200µg/L resulted in an equilibirium concentration of 33µg/L and the test that utilized 380µg/L as the intitial perchlroate concentration resulted in equilibrium concentrations of 13µg/L. The sorption test conducted with SMZ indicated that sorption equilibrium is approached after approximately 3 hours (Figure 2.1). The difference in the time to approach sorption equilibrium for the two sorbents is due to the different particle sizes and surface areas associated with them. The smaller size of SMM allows for faster diffusion of perchlorate to sorption sites. Additionally, SMM particles have a much higher surface area compared to SMZ, therefore more exchange sites are exposed, which allows perchlorate to sorb perchlorate more rapidly to SMM than to SMZ.

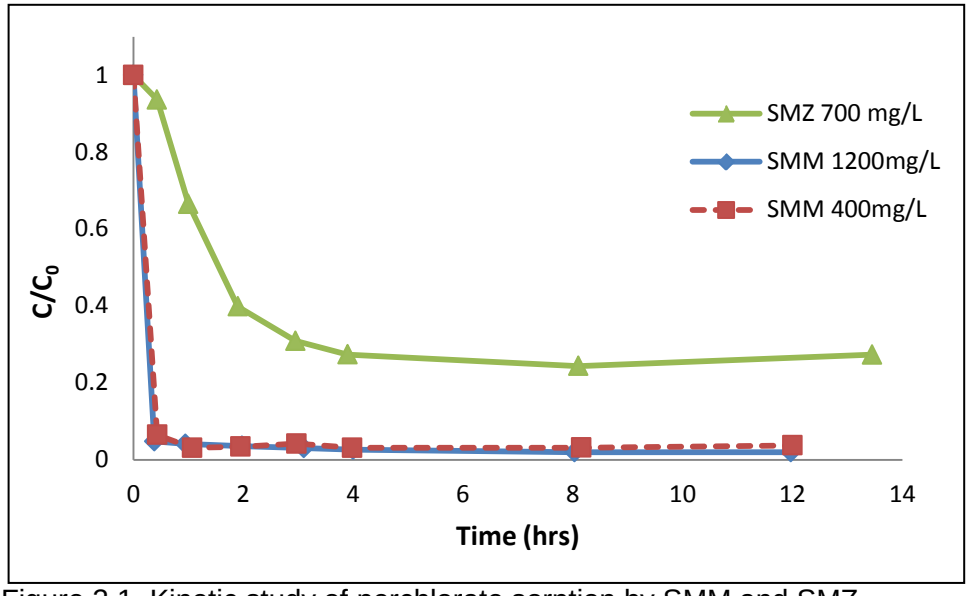

Figure 2.1. Kinetic study of perchlorate sorption by SMM and SMZ.

Equilibrium Batch Tests

Results of the low-concentration isotherm tests revealed that SMM was best modeled with the linear isotherm equation, with a partition coefficient of 17,100L/kg and an r^2 of 0.98 (Figure 2.2 and Appendix B). The goodness of fit of the linear isotherm model suggests that the loading of perchlorate onto SMM did not approach the sorption capacity. At higher perchlorate loading (Figure 2.3), the perchlorate sorption isotherm data was best described with the Freundlich equation, as indicated by the RMSE of 717mg/kg (Table 2.1). The Freundlich sorption parameters, K_F and N were 6,394 mg/kg/(mg/L)^N and 0.11, respectively. At these higher concentrations, the capacity for perchlorate adsorption by SMM was approached (Appendix C).

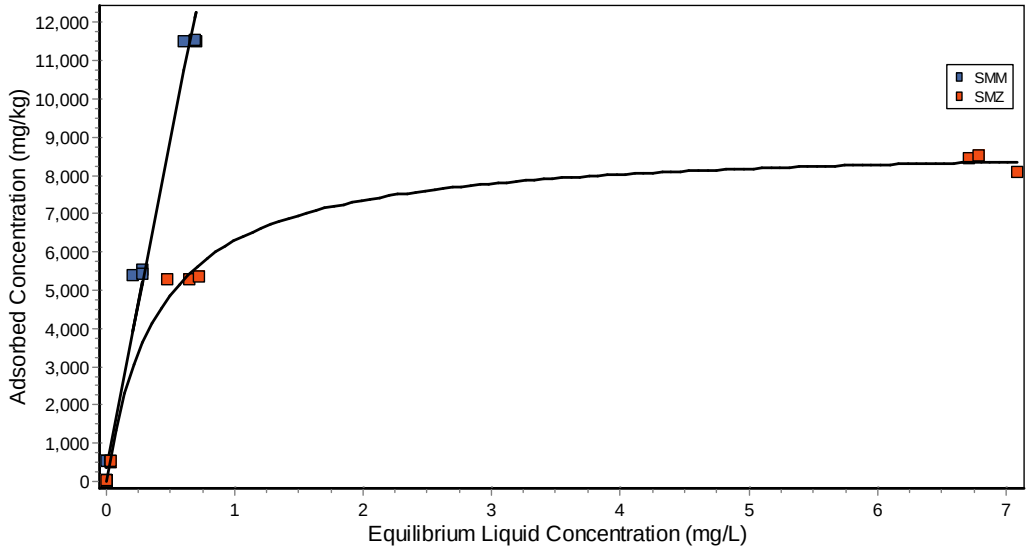

Figure 2.2. Isotherms of SMM and SMZ with initial perchlorate concentrations of 0-24mg/L.

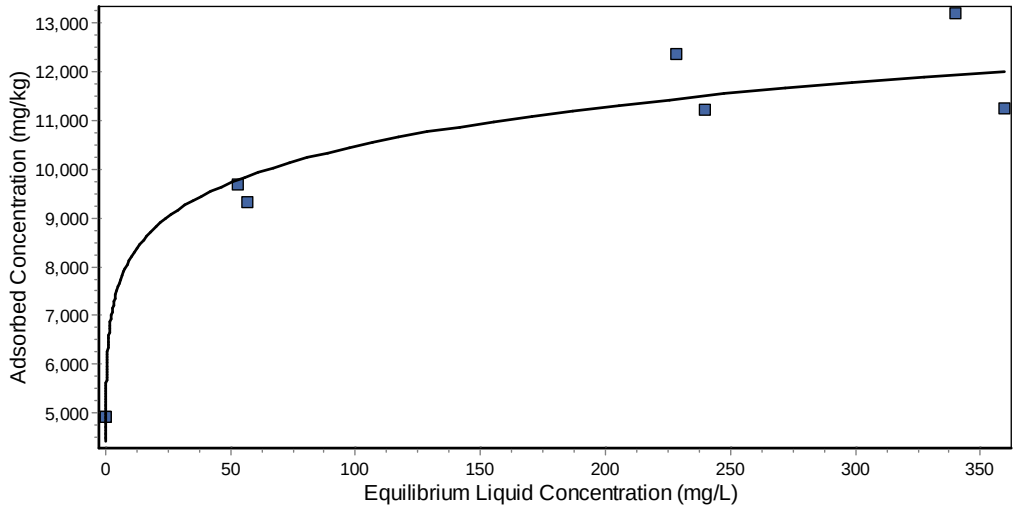

Figure 2.3. Isotherm of perchlorate sorption by SMM using initial perchlorate solutions of 0-470mg/L fit with the Freundlich model.

Table 2.1. Adsorption parameters and root mean square errors (RMSE) for equilibrium batch tests. DNC indicates that the model did not converge on a solution.

Sorbent	Initial Concentration range	**Linear**			**Freundlich**			**Langmuir**		
		K_d (L/kg)	RMSE (mg/kg)	r^2	K_F (mg/kg)/(mg/L)^N	N	RMSE (mg/kg)	b (L/kg)	Q_{max} (mg/kg)	RMSE (mg/kg)
SMM	0 – 24 mg/L	**17,100**	**555**	**0.98**	15,400	0.74	418	0.73	35,200	418
SMZ	0 – 24 mg/L	1,080	1,750	0.73	4,070	0.52	1,578	**2.5**	**8,840**	**192**
SMM	0 – 470 mg/L	18	1,560	0.73	**6,394**	**0.11**	**717**	0.0708	12,470	2,474
SMM	100% Brine	**245**	**300**	**0.89**	353	0.80	364	DNC	DNC	DNC
SMM	50% Brine	**505**	**239**	**0.98**	463	1.01	268	DNC	DNC	DNC

Low-concentration equilibrium batch test results showed that SMZ sorption isotherms were best described by the Langmuir isotherm model, indicating that the number of perchlorate adsorption sites limited sorption (Figure 2.2). The isotherm was best described with the Langmuir model, with b and Q_{max}, of 2.5L/kg and 8,840mg/kg, respectively (Table 2.1). The perchlorate sorption capacity of SMZ determined in these batch tests was roughly twice that determined by Zhang *et al*. (2007). The differences

between the measured sorption capacities, is most likely due to the differences in zeolite grain sizes. Zhang *et al*. used SMZ which was 2.4–1.4mm (8-14 mesh) which is signifcantly larger than the 0.297-0.595mm (30–50 mesh) size range used in this study. The smaller SMZ grain size utilized in these tests resulted in a higher surface area that can be modified with HDTMA, producing more perchlroate sorption sites.

The disparity in perchlorate sorption by SMM and SMZ are likely due to the differences in the amount of surface area associated with each sorbent. The effective surface area of SMM and SMZ are $10m^2/g$ and $6.9m^2/g$, respectively (Frost *et al*., 2008; Leyva-Ramos *et al*., 2008). Only the external surface area of SMZ is relevant for perchlorate adsorption because HDTMA molecules are too large to enter the pores inside the zeolite structure (Haggerty and Bowman, 1994). When scaled by their respective surface areas, SMM and SMZ had similar amounts of perchlorate sorption. For instance, when the initial perchlorate concentration was 24mg/L, the actual sorption by SMM and SMZ was 11,514mg/kg and 8,357mg/kg, respectively. However, after scaling these amounts by their surface areas, these amounts become $1.15mg/m^2$ and $1.21mg/m^2$ for SMM and SMZ, respectively. Due to the much higher actual perchlorate sorption capacity of SMM compared to SMZ, further work on this project focused on SMM.

Effect of Nitrate and Other Co-Constituents in Groundwater

The batch experiment designed to examine the effect of nitrate on perchlorate sorption to SMM in deionized water revealed that increasing concentrations of nitrate reduced perchlorate adsorption, as shown by the negative slope of adsorbed perchlorate (Figure 2.4 and Appendix D). A linear regression t-test revealed that the slope of adsorbed perchlorate was significantly different from zero.

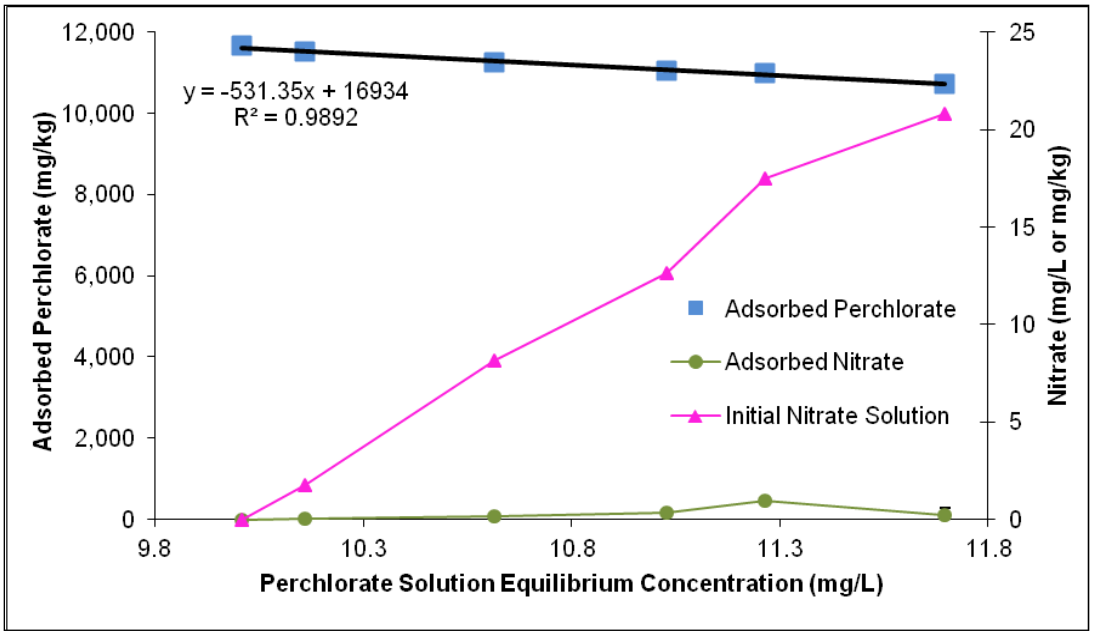

Figure 2.4. Effect of nitrate on perchlorate adsorption by SMM in deionized water. Adsorbed perchlorate was fit using a linear regression.

Similarly, the batch test conducted with groundwater from LHAAP (chemical composition in Table 2.2) also showed that increasing the concentration of nitrate caused a decrease in perchlorate adsorption (Figure 2.5 and Appendix E). A linear regression t-test showed that the slope of adsorbed perchlorate was significantly different from zero. The presence of co-constituents in the groundwater had a slight effect on perchlroate sorption. For the same initial concentration of nitrate in solution, the SMM sorbed 5% (±3%) more perchlorate in deionized water than in groundwater.

Table 2.2. Composition of LHAAP groundwater.

Analyte	**Concentration**
Perchlorate	32.4 mg/L
1,1,2-Trichloroethane	0.16 µg/L
MTBE	6.94 µg/L
Aluminum	0.067 mg/L
Iron	BDL
Arsenic	1.50 mg/L
Lead	BDL
Chromium	0.01 mg/L
Cadmium	1.10 mg/L
Sodium	210.73 mg/L
Magnesium	2.25 mg/L
Chloride	426.02 mg/L
Nitrate	BDL
Phosphate	BDL
Sulfate	23.55 mg/L
TOC	11.3 mg/L
pH	7.48
Alkalinity	200.00 mg/L as $CaCO_3$
TSS	0.06 mg/L
TDS	0.88 mg/L

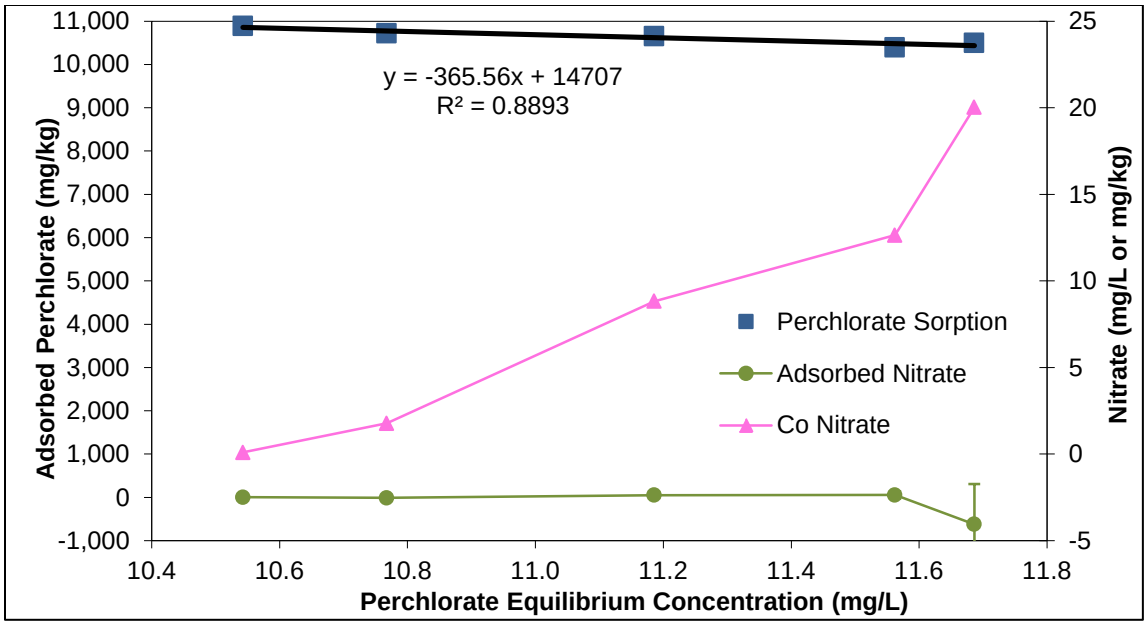

Figure 2.5. Effect of nitrate on perchlorate sorption by SMM in groundwater from LHAAP. Adsorbed perchlorate was fit with a linear regression.

Perchlorate concentrations in groundwater from LHAAP were below the detection limit after treatment of 100mL of groundwater with 0.5g of SMM and SMZ (Table 2.3). SMM removed slightly more sulfate (11%) from solution than SMZ (6%). In both cases, the amount of chloride in solution remained fairly constant. Treatment of groundwater spiked with nitrate (Table 2.4) also showed that SMM was selective for perchlorate.

Table 2.3. Concentrations of anions in groundwater from LHAAP after treatment with 0.5g SMM and SMZ.

Analyte	Initial Groundwater Concentration	Treated with SMM		Treated with SMZ	
		Final Concentration	Percent Difference	Final Concentration	Percent Difference
Perchlorate	32.4 mg/L	BDL	100%	BDL	100%
Chloride	426. mg/L	423	1%	431.54	-1%
Nitrate	BDL	BDL	NA	BDL	NA
Sulfate	23.6 mg/L	20. 9	11 %	22.12	6%

Table 2.4. Anions in groundwater from LHAAP that was spiked with nitrate prior to treatment with 0.5g SMM

Analyte	Initial Groundwater Concentration	Treated with SMM	
		Final Concentration	Percent Difference
Perchlorate	32.4 mg/L	ND	100%
Chloride	426 mg/L	401 mg/L	6%
Nitrate	22.0 mg/L	22.1 mg/L	0%
Sulfate	23.7 mg/L	21.1 mg/L	11 %

Treatment of Brine

In order to further examine the effects co-constituents on perchlorate adsorption by SMM, equilibrium batch tests were conducted using perchlorate-contaminated brine. This brine was created from the regeneration of ion exchange resin from a Los Angeles, California water treatment plant (chemical composition in Table 2.5). The perchlorate sorption isotherm was best described with the linear model and had a K_d of 245L/kg (Figure 2.6 and Appendix F). Although SMM adsorbed less perchlorate from the brine than from deionized water and groundwater, SMM continued to adsorb perchlorate even in the high ionic strength (0.75mol/kg) solution.

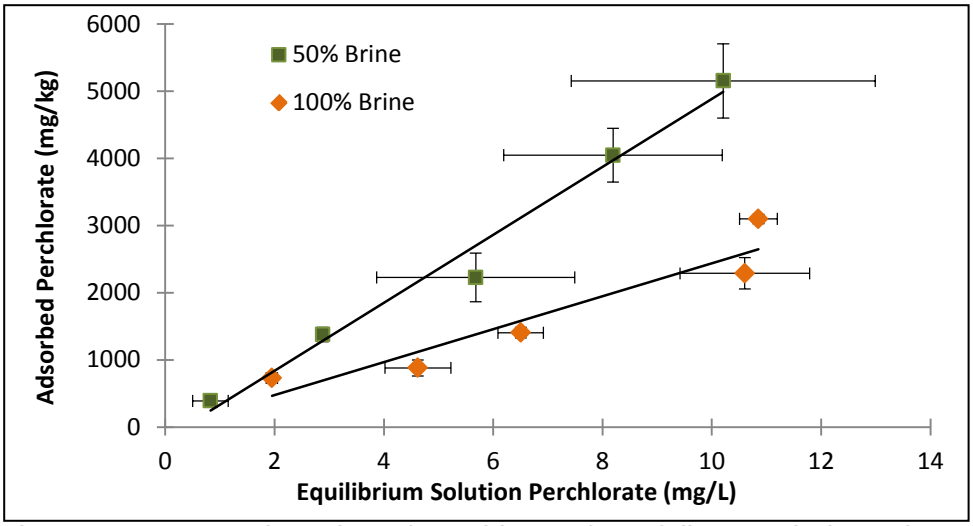

Figure 2.6. SMM adsorption of perchlorate from full-strength (100%) and half-strength (50%) brine. Error bars represent the standard deviation of sample concentrations.

Table 2.5. Constituents measured in full-strength brine from a Los Angeles, California water treatment plant.

Analyte	Concentration
Perchlorate	5.6 mg/L
1,1,2-Trichloroethane	0.15 µg/L
MTBE	1.05 µg/L
Aluminum	0.067 mg/L
Iron	2140 mg/L
Arsenic	157.3 mg/L
Lead	5.06 mg/L
Chromium	1.11 mg/L
Cadmium	1.10 mg/L
Sodium	284 mg/L
Magnesium	2.25 mg/L
Chloride	47472 mg/L
Nitrate	4961 mg/L
Phosphate	BDL
Sulfate	1528 mg/L
TOC	58.20 mg/L
pH	8.27
Alkalinity	5500 mg/L of $CaCO_3$
TSS	0.50 mg/L
TDS	78.50 mg/L
Ionic Strength	0.75 mol/L

To further evaluate the effect of co-constituents on perchlorate sorption by SMM, equilibrium batch tests were also conducted with brine that was diluted by 50% with deionized water. In order to normalize the different initial perchlorate solutions, the perchlorate concentrations in both the full- and half-strength brine were spiked with additional perchlorate so that the 5 initial perchlorate solution concentrations were similar. As was the case with the full-strength brine, the data were best described with the linear model, with a K_d of 505 L/kg (Figure 2.6). These results show that a 50% dilution of the brine caused perchlorate adsorption by SMM to approximately double, as indicated by the value of K_d increasing twofold. Perchlorate removal was highest in deionized water and lowest in full-strength brine (Figure 2.7). As the concentrations of

co-constituents in solution increased, perchlorate sorption by SMM decreased. Although the other species in solution reduced perchlorate uptake, SMM remained selective for perchlorate.

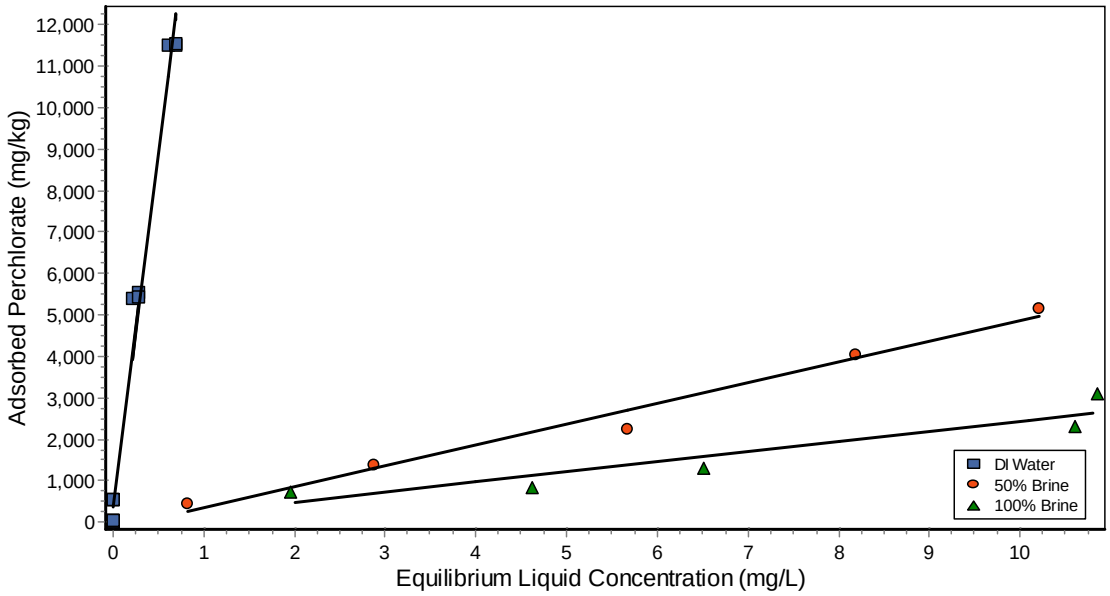

Figure 2.7. Isotherms of perchlorate sorption by SMM in deionized water, half-strength brine, and full-strength brine.

In treatment of brine (Table 2.6), the relative adsorption of perchlorate and other anions to SMM generally followed the Hofmeister anion series: ClO_4^- > I^- > NO_3^- ≈ Br^- > Cl^- > HCO_3^- > F^- >$H_2PO_4^-$ > $S_2O_3^{2-}$ > SO_4^{2-} > CO_3^{2-} (Hofmeister, 1888, translated by Kunz *et al.*, 2004; Zhang *et al*., 2005; Sessler *et al*. 2006). Kosmotropic anions cause water to become more stable and these ions are less likely to pass through surfactant monolayers (Figure 2.8). This type of anion is generally smaller with higher charge density and, therefore, is more strongly hydrated. Chaotropic anions, such as perchlorate, have a lower charge density, are less hydrated and, therefore, are better able to penetrate surfactant monolayers (Zhang and Cremer, 2006). The Hofmeister anionic series is theorized to be closely related to hydration energies (Custelcean and

Moyer, 2007). Perchlorate has a low hydration energy (Table 2.7) and, therefore, is more likely to behave chaotropically and partition into the hydrophobic region created by HDTMA in the SMM interlayer.

Table 2.6. Percent removal of co-constituents after treatment of 100mL of brine with 0.5g SMM.

Analyte	Full-Strength Brine			Half-Strength Brine		
	Initial (mg/L)	Final (mg/L)	Percent Removal	Initial (mg/L)	Final (mg/L)	Percent Removal
Perchlorate	5.6	1.95	65%	2.8	0.83	70%
TOC	58.2	53.0	9%	29.1	19.8	32%
Aluminum	0.067	0.029	57%	0.034	0.0041	88%
Arsenic	157.3	149.3	5%	79	68.0	14%
Lead	5.06	1.37	73%	2.53	0.32	87%
Chromium	1.11	0.95	14%	0.55	0.47	15%
Cadmium	1.10	0.75	32%	0.55	0.35	37%
Sodium	284	260.5	8%	142	213	-50%
Chloride	94,944	85,490	10%	47,472	42,493	10%
Nitrate	4961	3367	32%	2,481	3,097	34%

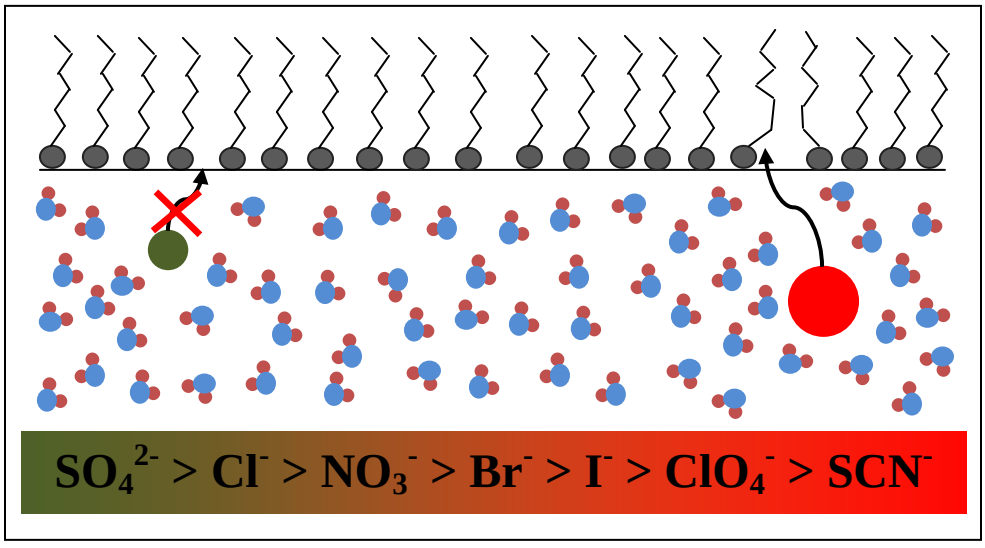

Figure 2.8. Example of the Hofmeister series of anions at the octadoceylamine monolayer at the air/salt solution interface (revised from Zhang and Cremer, 2006). Arrows compare the movement of kosmotropic (green) and chaotropic (red) anions into the headgroup region. The red "x" indicates that the kosmotrope generally does not successfully penetrate the monolayer.

Table 2.7. Hydration energies of common anions (Custelcean and Moyer, 2007).

Anion	Hydration Energy (kJ/mol)
ClO_4^-	-214
I^-	-275
NO_3^-	-306
Br^-	-321
Cl^-	-347
F^-	-472
SO_4^{2-}	-1090
PO_4^{3-}	-2773

The relative sorption of anions from groundwater by SMM did not follow the Hofmeister series very closely and instead ranked in order of decreasing sorption as: $ClO_4^- > SO_4^{2-} > Cl^- > NO_3^-$ (Table 2.4). This difference between groundwater and brine is likely due to the variation in salt concentrations; the Hofmeister effect is much stronger at moderate to high salt content (Collins and Washabaugh, 1985). At lower salt concentrations, the hydration energies are less significant in sorption of anions.

CONCLUSION

This study was successful in establishing basic sorption characteristics of perchlorate to SMM and SMZ. Perchlorate adsorption by SMM was very rapid with equilibrium concentrations approached within 1hr, while results of SMZ indicate that equilibrium is approached within approximately 3 hours. At lower concentrations (≤24mg/L), the isotherm of perchlorate adsorption by SMZ was best fit with the Langmuir model and had a maximum perchlorate adsorption capacity of 8,800mg/kg. Over this same concentration range, the isotherm of SMM was linear, indicating that the number of sorption sites was not limiting. Batch tests of SMM with higher initial perchlorate concentrations were best fit with the Freundlich model.

Although nitrate slightly reduced perchlorate adsorption, SMM successfully removed perchlorate from nitrate-spiked solutions created using deionized water and those made with groundwater from a contaminated site. While increasing the concentrations of other anions in solution reduced the amount of perchlorate adsorbed compared to experiments using deionized water, SMM remained selective for perchlorate even in the presence of high concentrations of competing anions. Adsorption of anions by SMM from both full and half-strength brine followed the order of the Hofmeister series, ClO_4^- > NO_3^- > Cl^-, which indicated that hydration energies play an important role in anion selectivity. The hydrophobic clay interlayer produced by the presence of large concentrations of HDTMA molecules resulted in stronger selectivity for perchlorate, which is a very weakly hydrated anion.

With the recent decision by EPA to create regulations for levels of perchlorate in drinking water, the development of efficient treatments of this contaminant is essential. This study indicates that SMM is an effective sorbent of perchlorate from both freshwater and brines and could be used as a filtration media, for pre-treatment prior to use of a more expensive method, or as an *in situ* reactive barrier (e.g. landfill liner) to remove perchlorate from contaminated water.

CHAPTER 3

MODELING 1-DIMENSIONAL TRANSPORT OF PERCHLORATE THROUGH SURFACTANT-MODIFIED MONTMORILLONITE AND SURFACTANT-MODIFIED ZEOLITE COLUMNS

ABSTRACT

Both surfactant-modified montmorillonite (SMM) and surfactant-modified zeolite (SMZ) are capable of treating perchlorate-contaminated water. Perchlorate transport through SMM and SMZ packed columns was modeled with a custom computer program that used the Ogata solution of the advection-dispersion equation. The retardation factors of SMM and SMZ were calculated using their perchlorate partition coefficients and were 30,480 and 16,380, respectively. A range of advective velocities and dispersions were utilized to determine the time for breakthrough ($C/C_0 = 0.01$) through a 1m long column with a diameter of 0.5m. The fastest breakthrough was predicted to occur with higher values of velocity and dispersion. Due to its very high sorption capacity and low advective velocities, the longest times until breakthrough were predicted for perchlorate transport through SMM. For instance, in a column packed with SMM and with solution that is flowing at an average velocity of 1.008cm/d and with a dispersion of $84cm^2/d$, 1% perchlorate breakthrough would occur after 700 years. Prior to breakthrough, 5,697 pore volumes ($514m^3$) of contaminated water would be treated. In a column packed with SMZ and with solution flowing at an average mean velocity of 10cm/hr with a dispersion of $500cm^2/hr$, breakthrough would occur after 2.5 years. During this time, 4,388 pore volumes ($431m^3$) of solution would be treated.

The physical characteristics of the two sorbents determine their potential applications. Although SMM has a higher sorption capacity than SMZ, its low hydraulic conductivity is more suited for use as landfill liners or as filtration media in fluidized-bed reactors rather than in packed-bed reactors. SMZ has a high hydraulic conductivity that allows it to be more useful in packed-bed reactors or for *in situ* permeable sorption barriers.

INTRODUCTION

Perchlorate (ClO_4^-) has been detected in the soil and water in at least 45 states (USGAO, 2010). This contaminant has been shown to be harmful to humans primarily due to its interference with thyroid function (USEPA, 2005b). In 2011, the USEPA announced that the agency will begin regulating perchlorate in drinking water under the Clean Water Act (Federal Registry, 2011). Currently, the USEPA is developing a proposed National Primary Drinking Water Regulation (NPDWR) for perchlorate. The perchlorate NPDWR is scheduled to be published by February 2014 and finalized within 18 months of publication (Federal Registry, 2011).

Ex situ filtration of contaminants from water is achieved with the use of flow-through packed-bed columns or fluidized-bed reactors operated in series or in parallel. At present many technologies are being developed and used to treat perchlorate-contaminated drinking water. Ion exchange resins are generally the preferred method to remove perchlorate from drinking water. While both non-selective and perchlorate-selective ion exchange resins can be used to filter perchlorate from solution, each type has limitations. For example, non-selective ion exchange resins are only efficient in water with either very high perchlorate concentrations or extremely low levels of other ions (Coates and Jackson, 2009). Generally, these resins are regenerable; however, regeneration must be completed often due to the low sorption potential (Coates and

Jackson, 2009). Additionally, the high frequency of regeneration produces an excessive amount of regeneration brine that requires either treatment or disposal as a hazardous waste (Coates and Jackson, 2009). The use of perchlorate-selective resins typically requires large amounts of resin due to their low sorption rates (Coates and Jackson, 2009). If ion exchange resins are not regenerated, they must be either treated or disposed of as hazardous waste.

In order to filter perchlorate from water, a variety of geosorbents have been developed by modification with surfactants, such as hexadecyltrimethylammonium (HDTMA). For instance, surfactant-modified activated carbon is capable of removing perchlorate from solution (Na *et al*., 2002; Parette and Cannon, 2005; Coates and Jackson, 2009; Xu *et al*., 2011). Additionally, surfactant-modified zeolite (SMZ) and surfactant-modified montmorillonite (SMM) have been shown to have a strong selectivity for perchlorate and to be effective at filtering perchlorate from solution (Zhang *et al*., 2007; Kim *et al*., 2011; Seliem *et al*., 2011; Chitrakar *et al*., 2012). The batch test studies conducted in Chapter 2 have evaluated perchlorate sorption by SMM and SMZ and confirmed that both effectively adsorb perchlorate from solution. However, further modeling is required to evaluate their application as a filtration media for perchlorate-contaminated water.

In situ applications of filtration technologies often involve installation of permeable sorption barriers across the plume. As the contaminated water moves through the barrier, perchlorate binds to the media and treated water flows out. The design of permeable barriers must be such that it is located in the path of the plume and that it is wide enough to encompass entire width of the plume. Additionally, the filtration media must have a higher hydraulic conductivity than the surrounding geology so that the contaminated groundwater flows through (rather than around) the barrier.

Both *ex situ* and *in situ* applications involve the filtration of contaminated water as it flows through the media. Prior to the application of SMM and SMZ as a filtration media, the transport of perchlorate-contaminated waters through these materials must be evaluated. The advection-dispersion model was utilized to predict perchlorate breakthrough as contaminated water flows through packed-bed columns filled with either SMM or SMZ.

Column tests are designed as beds packed with porous media through which a solution flows (Figure 3.1.a). If the solute does not react with the media (i.e. is a perfect or conservative tracer), the solute moves through the column with the flow of water and quickly reaches the outlet. However, if the solute binds to the media, the solute front is delayed compared to a perfect tracer. As the test continues, the media becomes increasingly saturated with sorbate. Breakthrough occurs when the solute first reaches the outlet of the column (i.e. is measurable in the effluent). A perfect tracer will reach the column outlet sooner than a solute that binds with the media (Figure 3.1.b). With continuous treatment, the effluent solute concentration slowly increases until it equals the influent concentration. At this point, all of the active sorption sites have been saturated and the filtration media is ready to be disposed of or recycled.

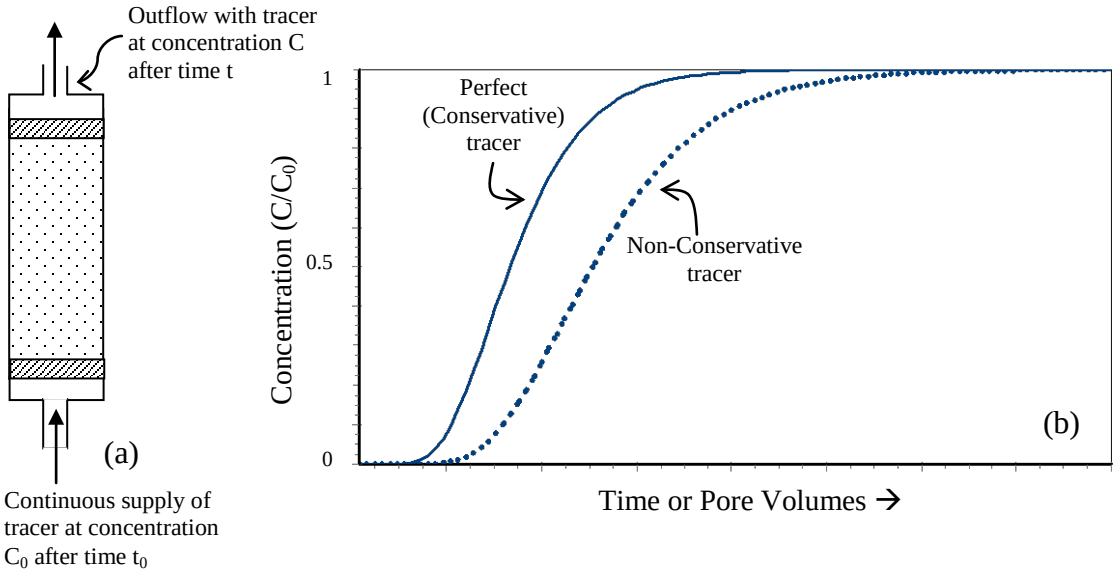

Figure 3.1. Solute transport through a column of porous media. Column filled with porous media and with continuous supply of tracer (a) and comparison of breakthrough curves for a perfect tracer and a solute that binds to the media (b).

Fixed-bed reactors are the preferred mode for filtration of contaminants from water. As the contaminated solution flows through the reactor bed, the effluent concentration slowly increases until it approaches the influent concentration. The flow is stopped when the concentration approaches the operating limit, typically the maximum contaminant limit (MCL). Many systems are designed with multiple reactors in series, which allows more efficient use of the filtration media. Rather than stopping flow and refilling the reactor with fresh filtration media as soon as the operating limit is approached, the column is utilized until the media is completely spent. At which point, it is removed from operation and switched with a new column without interrupting the treatment process. The new column is placed at the end of the filtration columns operated in series, allowing continuous operation.

When flowing through a porous media, the solute concentration is affected by a combination of advection and dispersion. Advection is the transport of solute due to the

average pore water velocity. Dispersivity is a combination of mechanical dispersion and molecular diffusion. The dispersivity is defined as:

$$D_x = \alpha_x \bar{v}_x + D^* \tag{3.1}$$

where D_x is the dispersivity (L^2/T), α_x is the mechanical dispersion (L), which is a characteristic of the porous media and is scale dependent, v_x is the average linear velocity of the fluid (L/T) and D* is the molecular diffusion (L^2/T). Mechanical dispersion is caused by irregular (branching) flow paths, variations in pore sizes, and the velocity profiles within the pore channels (Figure 3.2) and results in "smearing" of the contaminant front (Figure 3.3). These irregularities in pore sizes and path lengths cause variations in travel times for molecules moving through the porous media, depending on their individual routes. Heterogeneity in the porous media results in larger-scale dispersion. Molecular diffusion, which is caused by the movement of a chemical species from areas of high concentration to areas of low concentration (and is independent of flow), results in further spreading of the contaminant front. When the solution is flowing, dispersion processes dominate over diffusion processes. In cases where the velocity is negligible, dispersion processes are insignificant and molecular diffusion processes dominate. Fick's Law describes the diffusion of a solute:

$$F_x = -D\frac{dC}{dx} \tag{3.2}$$

where F_x is the mass flux (M/L^2T) in the x-direction, D is the diffusion coefficient (L^2/T), C is the solute concentration in solution (M/L^3), and dC/dx is the concentration gradient. The negative sign indicates that the flux is in the opposite direction of the concentration gradient (i.e. from high concentration to low).

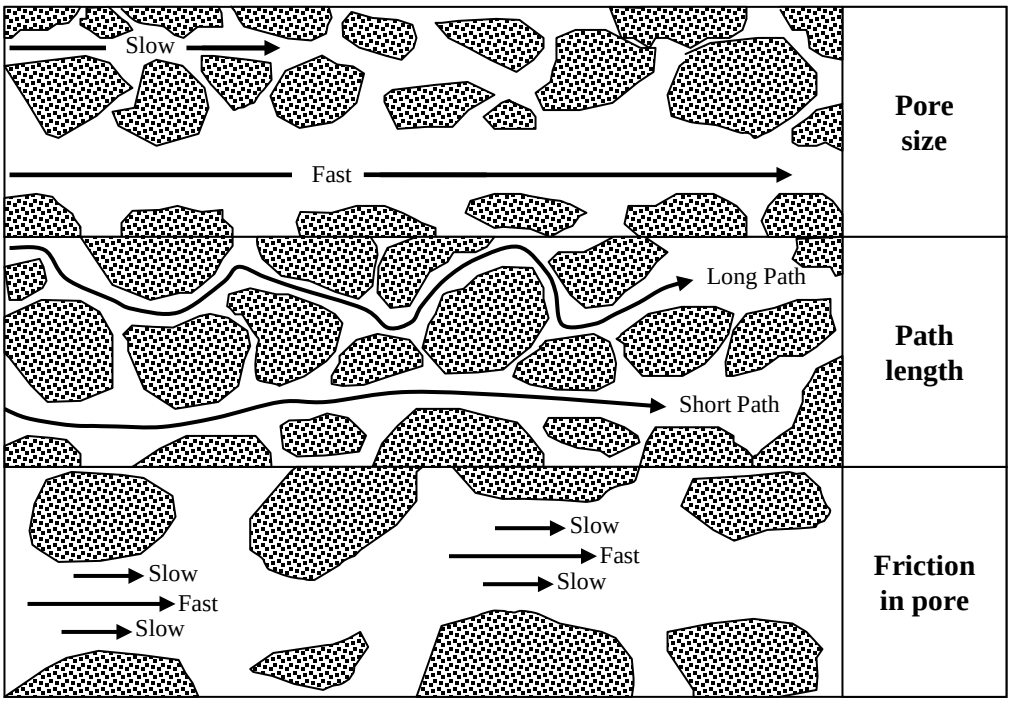

Figure 3.2. Causes of mechanical dispersion at the pore scale (modified from Fetter, 2001).

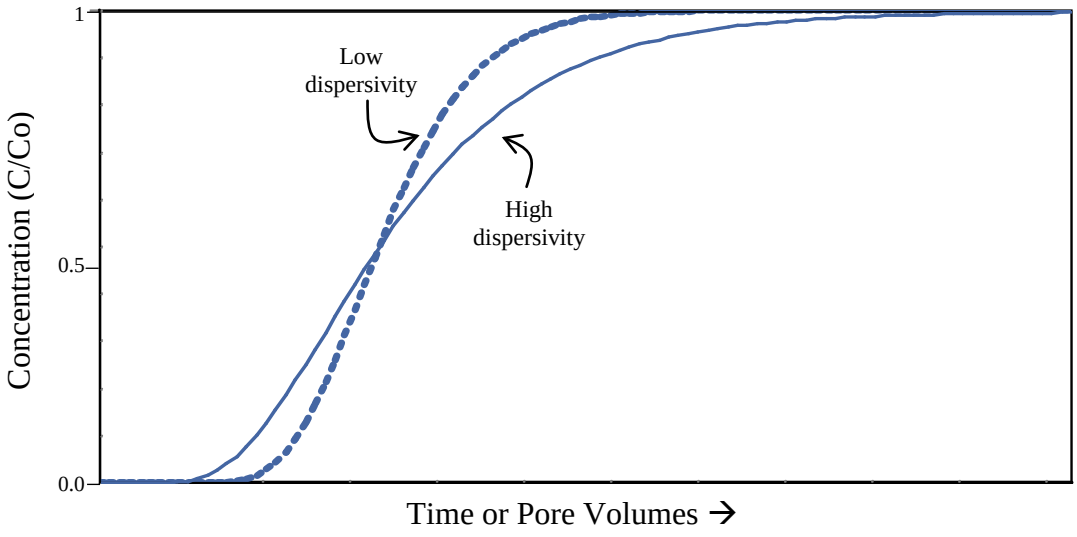

Figure 3.3. Breakthrough curves for a perfect tracer with varying values of dispersivity.

If the solution is flowing, solutes are also transported directly by the flow of solution via advection. The amount of solute in a volume of porous media is equal to $\partial \mathrm{nC}/\partial \mathrm{x}$. The porosity (n) is constant and can be removed so that $\frac{\partial nC}{\partial x} = n\frac{\partial C}{\partial x}$. The mass of solute transported by advection is equal to v_xnCdA, where dA is the elemental cross-sectional area. If advection alone is the only transport mechanism, the solute would move as a plug through the media. In reality, however, this is never the case, because diffusion always occurs. In solutions flowing through porous media, solute transport occurs due to a combination of both advection and dispersion and the mass flux of the solute in one dimension can be described with:

$$F_x = \bar{v}_x nC - nD_x \frac{\partial C}{\partial x} \tag{3.3}$$

where F_x is the mass flux of solute per unit of cross-sectional area per unit time. The law of conservation states that, if the solute is nonreactive, the difference between the solute flux out of and the flux into the elemental volume is equal to the amount of solute inside the volume. The rate of solute mass change can be described as:

$$\frac{\partial F_x}{\partial x} = -n\frac{\partial C}{\partial t} \tag{3.4}$$

Substitution of Equation 3.3 into Equation 3.4 yields:

$$\frac{\partial}{\partial x}(\bar{v}_x nC) - \frac{\partial}{\partial x}\left(nD_x \frac{\partial C}{\partial x}\right) = -n\frac{\partial C}{\partial t} \tag{3.5}$$

Porosity is constant and, therefore, can be removed from the equation. Additionally, if the system is at steady-state, v_x is constant. D_x does not vary in space and, therefore, is constant. These simplifications to Equation 3.5 result in the one-dimensional advection-dispersion equation for a perfect tracer:

$$D_x \frac{\partial^2 C}{\partial x^2} - \bar{v}_x \frac{\partial C}{\partial x} = \frac{\partial C}{\partial t} \tag{3.6}$$

If the amount of a solute decreases at a rate that is directly proportional to its quantity at that same time, it is said to undergo first-order decay. This could occur due to processes such as radioactivity, mineralization or degradation to daughter products. First order decay is described using the equation:

$$C = C_0 e^{-\lambda C} \tag{3.7}$$

where C_0 is the initial concentration, λ is the decay constant which is equal to $0.693/t_{1/2}$ and $t_{1/2}$ is the half-life. In such cases, a decay term is added to the advection-dispersion equation:

$$D_x \frac{\partial^2 C}{\partial x^2} - \bar{v}_x \frac{\partial C}{\partial x} - \lambda C = \frac{\partial C}{\partial t} \tag{3.8}$$

Compared to the breakthrough curve for a perfect tracer, the curve associated with first order decay is altered such that the effluent concentration never reaches the influent concentration due to decay of the solute (Figure 3.4).

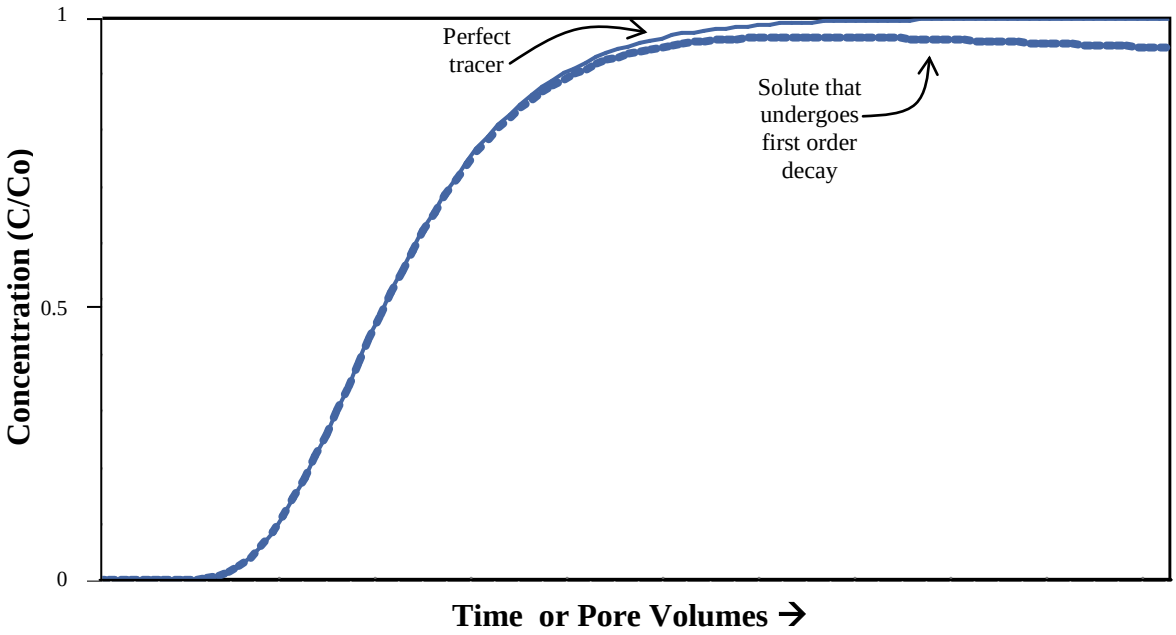

Figure 3.4. Breakthrough curve for a perfect tracer and for a solute that undergoes first order decay.

While traveling through the porous media, the solute has the potential to bind to the media itself, causing the solute to behave non-conservatively. Sorption will retard the migration of the solute front and cause it to reach the column outlet later than a solute that is conservative (Figure 3.1.b). The advection-dispersion equation for a perfect tracer can be modified to take into account the amount of solute adsorbed using:

$$D_x \frac{\partial^2 C}{\partial x^2} - \bar{v}_x \frac{\partial C}{\partial x} - \frac{\rho_b}{n} \frac{\partial C_{ads}}{\partial t} = \frac{\partial C}{\partial t} \tag{3.9}$$

where p_b is the bulk density, n is the porosity, and C_{ads} is the concentration of solute adsorbed (mass of solute/mass of sorbent).

Batch tests are utilized to quickly and efficiently determine the extent of sorption. These tests allow the development of isotherms that reveal the media's sorption capacity and the extent of sorption at different solution concentrations. Three common models utilized to evaluate the relationship between the liquid and solid phases are the Langmuir, Freundlich, and linear models. The Langmuir isotherm is often used when sorption sites become limiting and the amount of sorption approaches an asymptotic upper limit (Figure 3.5):

$$C_{ads} = \frac{Q_{\max} bC}{1 + bC} \tag{3.10}$$

where Q_{max} is the maxim adsorption capacity with monolayer coverage (mass of solute/mass of sorbent) and b is a partition coefficient relating the extent of adsorption (volume of solution/mass of sorbent). Substitution of Equation 3.10 into Equation 3.9 and rearrangement yields:

$$D_x \frac{\partial^2 C}{\partial x^2} - \bar{v}_x \frac{\partial C}{\partial x} = \frac{\partial C}{\partial t} + \frac{\rho_b}{n} \left(\frac{Qb}{(1+bC)^2} \right) \frac{\partial C}{\partial t} \tag{3.11}$$

Simplification by factoring gives:

$$D_x \frac{\partial^2 C}{\partial x^2} - \bar{v}_x \frac{\partial C}{\partial x} = \frac{\partial C}{\partial t}\left(1 + \frac{\rho_b}{n}\left(\frac{Qb}{(1+bC)^2}\right)\right) \tag{3.12}$$

which describes mass transport of a solute that undergoes Langmuir sorption.

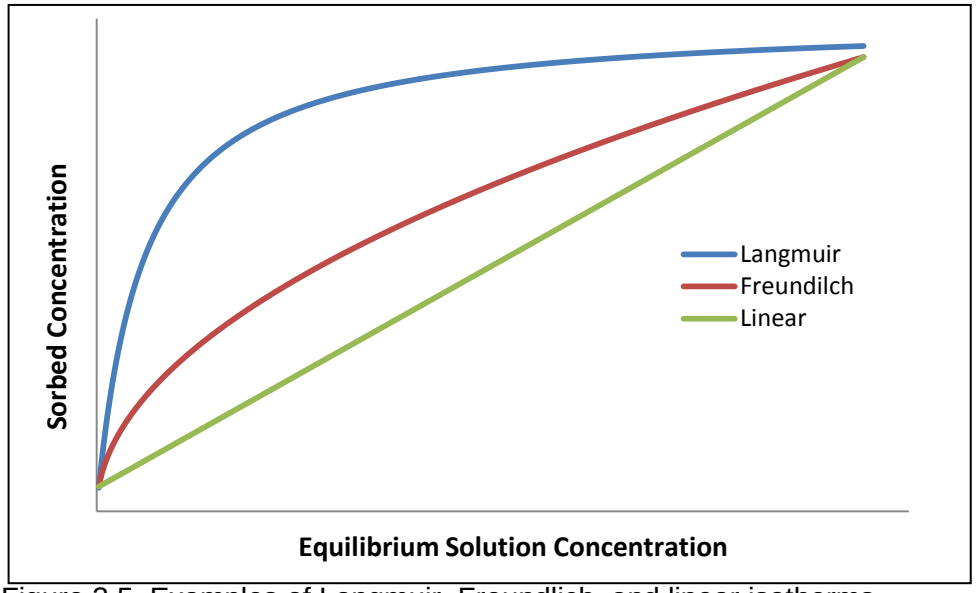

Figure 3.5. Examples of Langmuir, Freundlich, and linear isotherms.

When sorption causes variations in the solution concentration over several orders of magnitude and the sorption capacity is not approached, the Freundlich model is often used to model data (Figure 3.5):

$$C_{ads} = K_F C^N \tag{3.13}$$

where K_F is the Freundlich sorption coefficient constant [(mg/kg)/(mg/L)^N] and N is the Freundlich exponent relating to the sorption intensity. Incorporation of the Freundlich model into Equation 3.9 yields:

$$D_x \frac{\partial^2 C}{\partial x^2} - \bar{v}_x \frac{\partial C}{\partial x} = \frac{\partial C}{\partial t}\left(1 + \frac{\rho_b}{n} K_F N C^{N-1}\right) \tag{3.14}$$

The simplest isotherm sorption model is linear:

$$C_{ads} = K_D C \tag{3.15}$$

where K_D is the partition coefficient. In this case, the liquid and adsorbed concentrations are directly proportional and sorption is reversible. Note that the linear sorption model is equivalent to the Freundlich model with N=1. Incorporation of linear sorption into Equation 3.9 by substitution of C_{ads} yields:

$$D_x \frac{\partial^2 C}{\partial x^2} - \bar{v}_x \frac{\partial C}{\partial x} = \frac{\partial C}{\partial t}\left(1 + \frac{\rho_b K_d}{n}\right) \tag{3.16}$$

For linear sorption, the retardation factor (R_f) is constant and can be defined as:

$$R_f = 1 + \frac{\rho_b}{n} K_d \tag{3.17}$$

Larger values of R_f indicate stronger sorption and longer tracer delays in the column. Incorporation of Equation 3.17 into Equation 3.9 yields:

$$\frac{D_x}{R_f}\frac{\partial^2 C}{\partial x^2} + \frac{\bar{v}_x}{R_f}\frac{\partial C}{\partial x} = \frac{\partial C}{\partial t} \tag{3.18}$$

The type of isotherm used to model contaminant transport through a column is based on both the initial solution concentration and media sorption capacity. In instances where the solution concentrations are very low compared to the sorption capacity, the linear K_d is often utilized. This is typically the case when modeling the sorption of a filtration media for a contaminant. If the linear model is used when the solute concentration is high and the media sorption capacity is relatively low, the time until breakthrough will be overestimated (Freeze and Cherry, 1979). Such an error may result in breakthrough occurring much sooner than predicted, resulting in inadequate treatment of contaminated water. In such cases, nonlinear isotherms are required to more accurately predict breakthrough. When the solute concentration is high compared to the sorption capacity, Langmuir isotherms are often used to model the data. This is

frequently the circumstance when modeling the movement of heavy metals through soil (Hinz and Selim, 1993; Chang *et al., 2001)*. Solute transport modeling through a column with intermediate conditions often requires the use of the Freundlich isotherm, which accounts for nonlinear relationships that vary over multiple orders of magnitude and that do not reach the sorption capacity. The incorrect use of a non-linear model to predict breakthrough will often underestimate the time to breakthrough, which will result in the inefficient use of the filtration media.

METHODS

Transport of both perchlorate and a non-reactive tracer were modeled through surfactant-modified montmorillonite (SMM) and surfactant-modified zeolite (SMZ). The physical structures of the two sorbents are very different (Table 3.1). The particle size of SMM is significantly smaller than that of SMZ, which results in SMM having a much larger surface area than SMZ. Only the external surface area of SMZ is presented because the HDTMA molecules are too large to enter into the zeolite pores (Haggerty and Bowman, 1994). Additionally, the hydraulic conductivity of SMZ is 500% that of SMM. The K_d for perchlorate sorption by SMM was determined with a sorption batch tests described in Chapter 2 (Table 2.1). The K_d for sorption by SMZ was ascertained using the linear portion of the sorption isotherm (Figure 2.2).

Table 3.1. Properties of SMM and SMZ. The external surface area is reported for SMZ because steric restrictions prohibit HDTMA from entering the zeolite pores (Haggerty and Bowman, 1994), which limits perchlorate sorption to the external SMZ surface.

Property	SMM	SMZ
Bulk density (g/cm^3)	0.82 (Jarraya *et al*., 2010)	1.00 (Li *et al*., 1998)
Porosity (unitless)	0.46 (Jarraya *et al*., 2010)	0.5 (Li *et al*., 1998)
K_d for perchlorate (L/kg)	17,100 (Table 2.1)	8,190 (Table 2.1)
Perchlorate retardation factor (unitless)	30,480 (Equation 3.17)	16,380 (Equation 3.17)
Hydraulic conductivity (m/s)	1.8x10^{-8} (Lorenzetti *et al.,* 2005)	10^{-3} (Li *et al.,* 1998)
Surface area (m^2/g)	11.2 (Wibulswas, 2004)	6.9 (Leyva-Ramos *et al.,* 2008)
Particle size (µm)	57 (Wibulswas, 2004)	420 (Leyva-Ramos *et al.,* 2008)

Due to the high sorption capacities of SMM and SMZ for perchlorate, the sorption is linear and, therefore, the following equation was used to model breakthrough curves:

$$\frac{D_x}{R_f}\frac{\partial^2 C}{\partial x^2}+\frac{\bar{v}_x}{R_f}\frac{\partial C}{\partial x}=\frac{\partial C}{\partial t} \tag{3.19}$$

and retardation factors were calculated with:

$$R_f = 1+\frac{\rho_b}{n}K_d \tag{3.20}$$

A custom analytical computer program, OneD, was used to generate breakthrough curves for more than 100 conditions of flow through a 100cm column with mechanical dispersions of 50, 75, 100, 125, and 150cm. The OneD program was developed by John Dowd, University of Georgia Geology Department, Athens, Georgia using Borland C++ 2007. The specific programming libraries utilized were LMD-Tools produced by LMD innovative (Mainz, Germany), TeeChart Pro produced by Steema Software (Catalonia, Spain), and MtxVec and Stats Master both produced by Dew Research (Slovenske Konjice, Slovenia). A windows version of the OneD program is available upon request.

The advective velocity through SMM was severely limited by its low hydraulic conductivity ($K_{hydraulic}$) and the velocities that were modeled for SMM were determined using:

$$v_x = \frac{K_{hydraulic}}{n} * gradient \tag{3.21}$$

with the hydraulic gradient ranging from 1 (no pooling of solution above the column) to 5 (the equivalent of 4m of water above the 1m long column) (Table 3.2). At these flow rates, diffusion is negligible and dispersivity ≈ dispersion and Equation 3.1 can be simplified to:

$$D_x = \alpha_x \bar{v}_x \tag{3.22}$$

which results in values of dispersion that range from 16.8 to 255.6cm^2/d.

The empty bed contact time (EBCT or residence time) was calculated with:

$$EBCT = \frac{V_{column}}{Q} \tag{3.23}$$

where V_{column} is the volume of the empty column and Q is the volumetric flow rate. The hydraulic conductivity of SMZ is significantly higher than SMM, which resulted in kinetic sorption limitations (3 hours) on flow through SMZ columns rather than physical limitations. Empty bed contact times used for modeling flow through SMZ were greater than 6 hours to ensure that equilibrium is approached in the column. In all cases, breakthrough was arbitrarily determined to occur when the effluent concentration was 1% of the influent concentration ($C/C_0 = 0.01$).

The specific parameters used to model transport through SMM and SMZ are listed in Appendices G and H. In all cases, the initial and boundary conditions used were:

$$C(x,0) = 0 x \geq 0$$
$$C(0,t) = C_0 t \geq 0 \quad (3.24)$$
$$C(\infty,t) = 0 t \geq 0$$

where C is the effluent concentration and C_0 is the influent concentration (Freeze and Cherry, 1979). OneD employed the Ogata solution to analytically solve the advection-dispersion equation:

$$\frac{C}{C_0}(x,t) = \frac{1}{2}\left[erfc\left(\frac{x - \bar{v}_x t}{2\sqrt{D_x t}} \right) + \exp\left(\frac{x + \bar{v}_x x}{D_x} \right) erfc\left(\frac{x + \bar{v}_x t}{2\sqrt{D_x t}} \right) \right] \quad (3.25)$$

(Ogata, 1961; Freeze and Cherry, 1979), where the complementary error function (erfc) is defined as:

$$erfc(x) = \frac{2}{\sqrt{\pi}} \int_x^{\infty} -t^2 dt = 1 - \frac{2}{\sqrt{\pi}} \int_0^x -t^2 dt = 1 - erf(x) \quad (3.26)$$

The volume of solution treated prior to breakthrough was calculated from breakthrough using:

$$T_b * \bar{v}_x * A = V_{treated} \quad (3.27)$$

where T_b is the amount of time until breakthrough (C/C_0 = 1% in this case), A is the cross-sectional area of the column, and $V_{treated}$ is the volume of solution treated until breakthrough occurs (L^3). The volume of solution treated can be converted to the number of pore volumes treated by:

$$\frac{V_{treated}}{V_{column} * n} = PV \quad (3.28)$$

where n is the porosity (unitless), V_{column} is the volume of the column (L^3) and PV is the number of pore volumes treated. The complete results of modeling mass transport through SMM and SMZ are listed in Appendices I and J.

RESULTS AND DISCUSSION

The physical differences between SMM and SMZ necessitate the use of very different modeling parameters for each media (Appendices G and H). SMM is a hydrophobic clay with high porosity and low hydraulic conductivity (Table 3.1), which will result in lower advective velocities and smaller values of diffusivity. In contrast, SMZ consists of aggregates of cage-like spheres surrounded by a hydrophobic layer of surfactants; a coarse media through which solution can flow rapidly. Additionally, surfactant molecules both bind to the exterior of the montmorillonite and exchange into the interlayer, which allows perchlorate sorption to occur throughout the structure. On the other hand, steric restrictions prohibit HDTMA molecules from the intra-particle exchange sites inside zeolite (Haggerty and Bowman, 1994), resulting in a lower effective surface area for perchlorate sorption onto SMZ.

SMM has a higher perchlorate sorption capacity than SMZ; therefore contaminant breakthrough would occur sooner with SMZ at the same diffusivity and velocity combination. In fact, the retardation factor of SMM is roughly double that of SMZ; therefore breakthrough of perchlorate flowing through SMM will typically take nearly twice as much time as flow through SMZ if the same advective velocity and dispersivity were used.

For each filtration media, larger values of velocity and dispersion would result in the fastest breakthrough (Figures 3.6 and 3.7). Perchlorate transport through SMM would have the longest time to breakthrough due to both the high sorption capacity and the comparatively low velocities (Figure 3.6). For instance, 1% breakthrough of perchlorate transported in solution through a 1m column of SMM at a velocity of 1cm/d and a dispersion of 84cm^2/d would occur after approximately 260,000 days (700 years). Comparatively, a perfect tracer flowing through the same column under the same conditions would achieve 1% breakthrough on the eighth day. Perchlorate transport

through a 1m long column of SMZ, flowing at the rate of 20cm/hr with a dispersion of 750cm^2/hr, would reach 1% breakthrough around 1.5 years. Under the same circumstances, a perfect tracer flowing through SMZ will achieve breakthrough at approximately 0.8hr. Breakthrough would occur soonest in the case of the perfect tracer transported through SMZ, due to both the lack of sorption and the high flow rates (Figure 3.7.b).

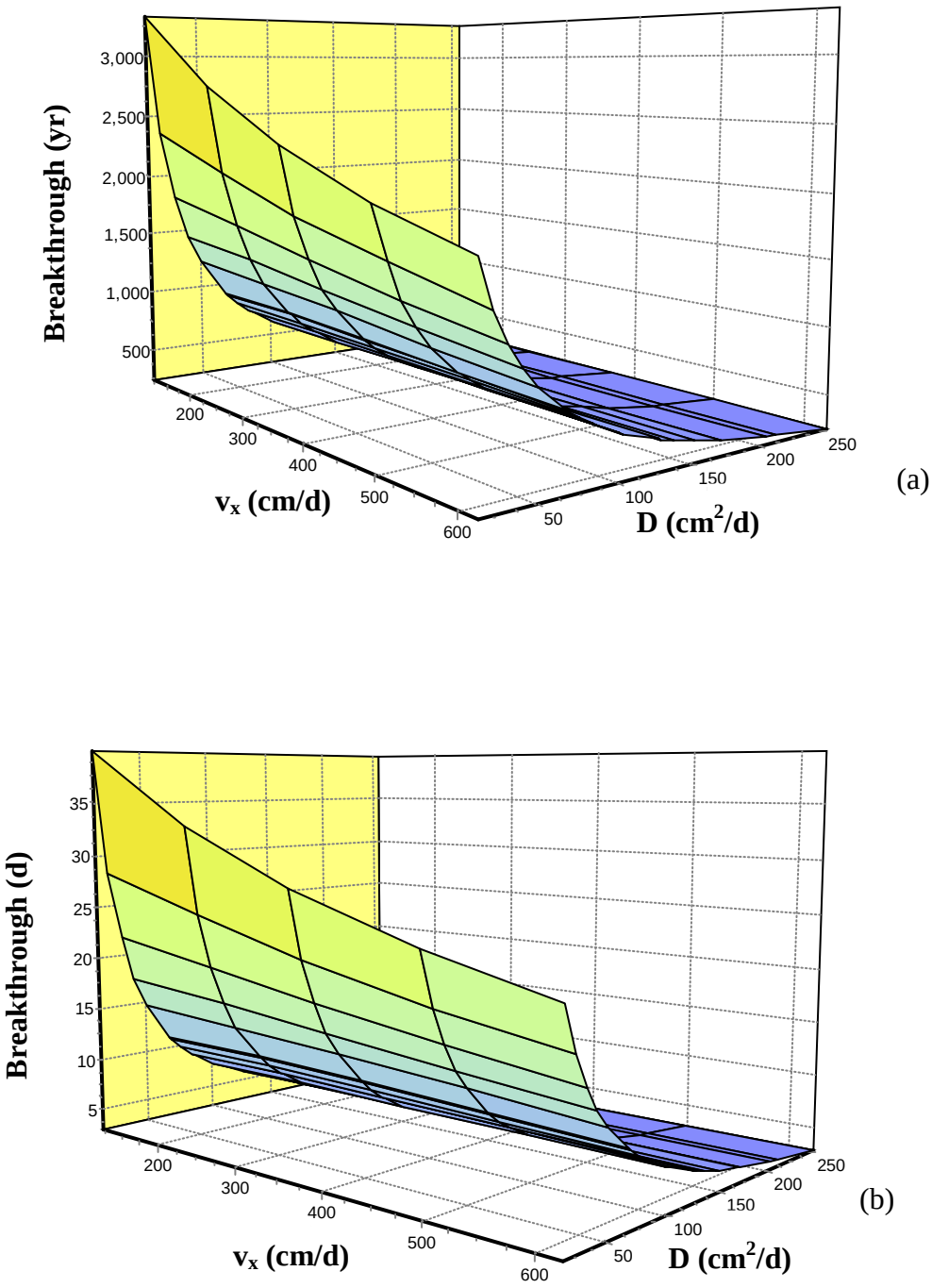

Figure 3.6. Breakthrough of perchlorate (a) and a perfect tracer (b) flowing through SMM.

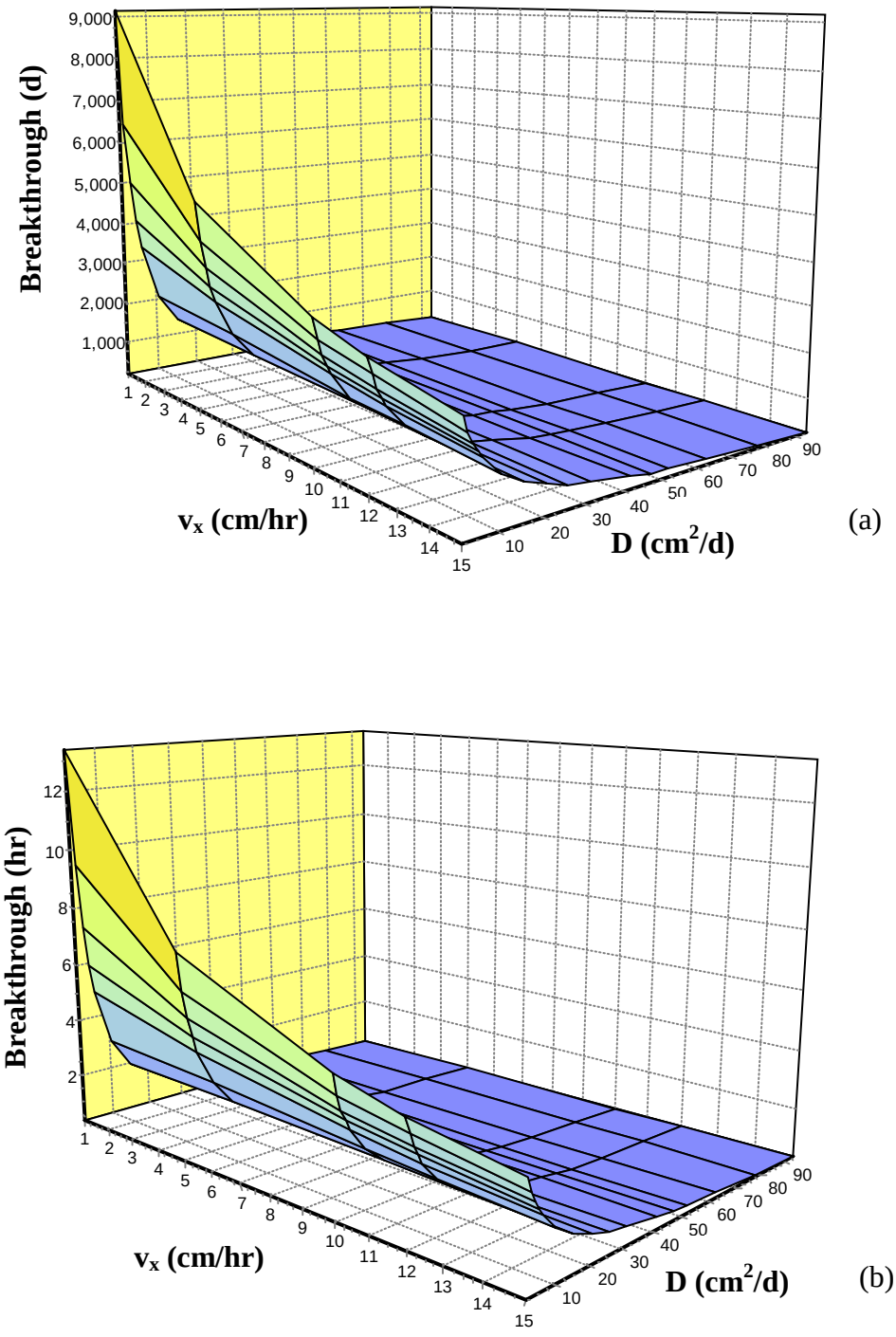

Figure 3.7. Breakthrough of perchlorate (a) and a perfect tracer (b) flowing through SMZ.

The predicted volumes of perchlorate-contaminated solution treated prior to 1% breakthrough for both SMM and SMZ would occur in cases with the largest advective velocity and the lowest dispersivity (Figure 3.8). In an SMM treatment column with an inner diameter of 50cm and length of 100cm and with solution that is flowing at an average mean velocity of 1.008cm/d with a dispersion of 84cm^2/d, perchlorate breakthrough would occur after 712 years. The volume of solution treated would be 514m^3, which is treatment of 5,697 pore volumes (Figure 3.8). In the same column packed with SMZ and solution flowing at an average mean velocity of 10cm/hr with a dispersion of 500cm^2/hr, breakthrough would occur after 914 days. During this time, 4,388 pore volumes (431m^3) of solution would be treated (Figure 3.8).

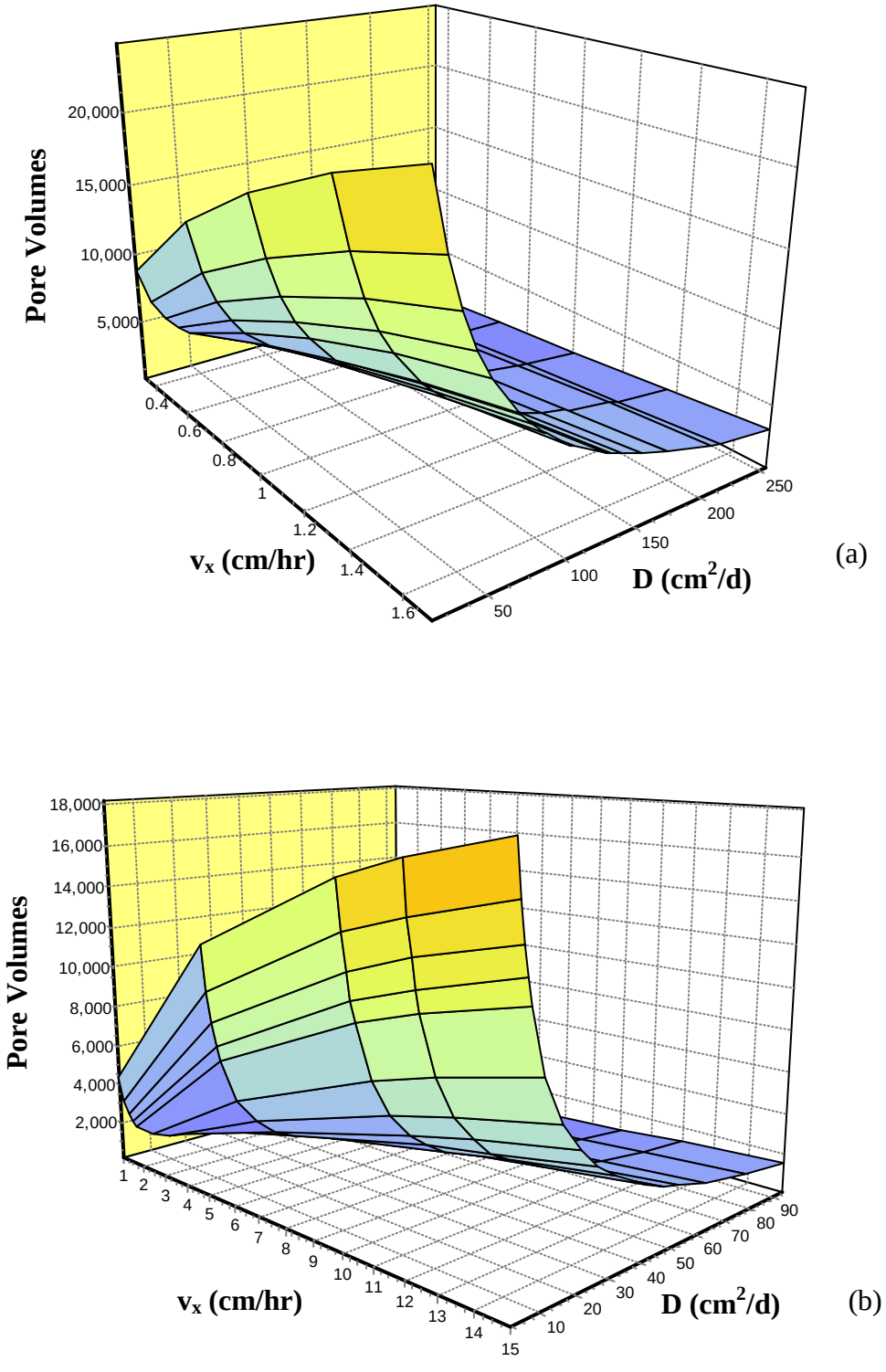

Figure 3.8. Pore volumes treated before 1% perchlorate breakthrough flowing through SMM (a) and SMZ (b). The column has a diameter of 50cm and a length of 100cm.

The hydraulic conductivity of SMZ is 5 orders of magnitude greater than that of SMM, resulting in large differences in the potential applications of these filtration media. SMZ is more suited to packed-bed flow through reactors or *in situ* permeable sorption barriers that are used to remove perchlorate from contaminated plumes in shallow groundwater. In order to treat a contaminated plume of groundwater, permeable sorption barriers must have a lower hydraulic conductivity than the surrounding geologic materials so that the plume will flow through the permeable barrier. With a hydraulic conductivity of 10^{-3}m/s (Li *et al.,* 1998), SMZ could be utilized in permeable sorption barriers to treat perchlorate contamination in a variety of geologic settings (Figure 3.9). However, SMM has a low hydraulic conductivity of 10^{-8}m/s (Lorenzetti *et al.,* 2005), which would drastically limit its effectiveness as a permeable sorption barrier in many geologic settings (Figure 3.9). SMM is much more suited for use as an impermeable liner for landfills, where its low hydraulic conductivity is beneficial. Another application of SMM is as a sorbent in fluidized-bed reactors. Additionally, mixing SMM with a larger-grained sorbent, such as SMZ, will increase the hydraulic conductivity of the mixture and allow utilization of this dual sorbent in fixed-bed reactors. The benefit of this technique is the ability to completely customize the mixtures so that specific contaminants are adsorbed. However, such a configuration may result in the development of preferential flow pathways, which would reduce its efficiency, by reducing contact with sorption sites.

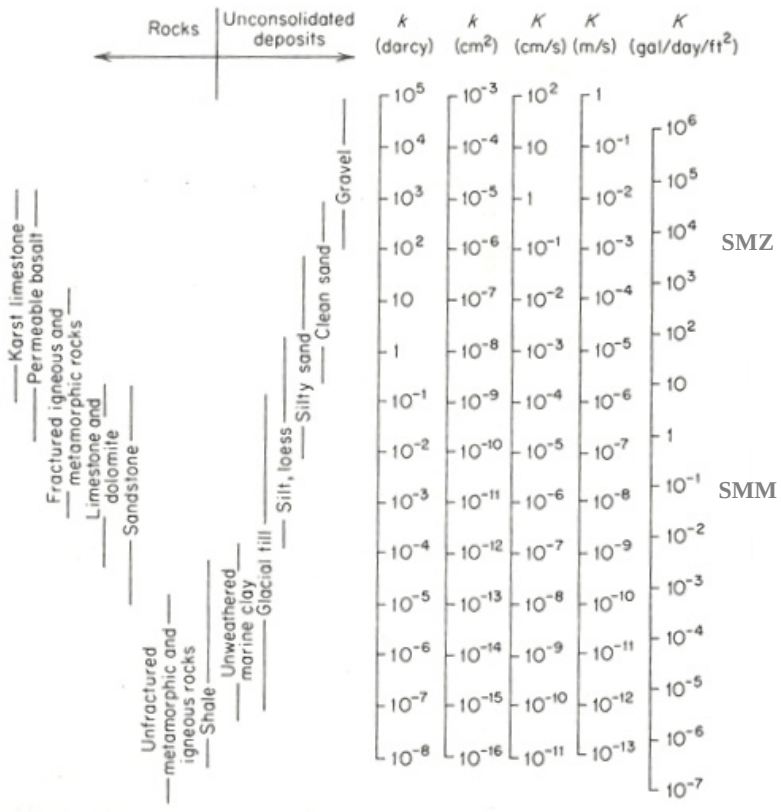

Figure 3.9. Range of values of permeability and hydraulic conductivity (Freeze and Cherry, 1979).

CONCLUSION

The advection-dispersion equation was utilized to model breakthrough times for perchlorate sorption by SMM and SMZ under a variety of circumstances. Perchlorate partition coefficients were used to calculate the retardation factors for SMM and SMZ, which were 30,480 and 16,380, respectively. In a treatment column filled with SMM (1m long and inner diameter of 50cm) and with a solution that is flowing at an average velocity of 1.008cm/d and with a dispersion of 84cm^2/d, 1% perchlorate breakthrough would occur after 712 years. The volume of solution treated prior to breakthrough would be 514m^3, which is treatment of 5,697 pore volumes. In the same column filled with SMZ

and with solution flowing at an average velocity of 10cm/hr and with a dispersion of 500cm^2/hr, breakthrough would occur after 2.5 years. During this time, 431m^3 or 4,388 pore volumes of solution would be treated.

The physical characteristics of the two filtration media are very important in determining their possible applications. The high hydraulic conductivity of SMZ makes it suitable for use as a filtration media in packed-bed reactors or as *in situ* permeable sorption barriers. SMM has a low hydraulic conductivity, which makes it more suited for use as landfill liners or as filtration media in fluidized-bed reactors. A mixture of SMM and a filtration media with relatively larger grain size, such as SMZ, would likely make it a more effective filtration media for use in a packed-bed reactor.

CHAPTER 4

TREATMENT OF PERCHLORATE BOUND TO SPENT SURFACTANT-MODIFIED MONTMORILLONITE

ABSTRACT

Perchlorate (ClO_4^-) contamination is a growing threat to the drinking water and food supplies of millions of people throughout the world. Surfactant-modified montmorillonite (SMM) has been shown to quickly remove perchlorate from aqueous solutions. However, filtration does not destroy perchlorate; it merely transfers it from the liquid phase to the solid phase. In order to both quickly remove perchlorate from solution and to degrade it to inert byproducts (Cl^- and O_2), filtration with SMM should be followed by a second phase of treatment to breakdown the adsorbed perchlorate. Biodegradation and chemical (abiotic) reduction were evaluated as treatment techniques for perchlorate in spent SMM. Within 120 days, the perchlorate concentration in solution that was in contact with spent SMM was reduced to less than 1.1mg/L in all six bioreactors treated with biologically active column effluent; averaging 94% reduction. Attempts to use stabilized zero-valent iron nanoparticles to chemically reduce perchlorate bound to spent SMM were not successful at ambient temperature.

INTRODUCTION

The United States currently faces the challenge of mitigating extensive perchlorate contamination of the drinking water supplies of millions of citizens (USEPA, 2011; USGAO, 2010). Perchlorate is known to bind to the thyroid gland's sodium-iodide

symporter and inhibit iodide uptake by the thyroid gland (USEPA, 2005b). For sensitive populations (fetuses, infants, and children), disruptions in thyroid hormone levels can cause lowered IQ, mental retardation, motor skill deficits, and loss of hearing and speech (Galfore *et al.*, 2009; Videla and Fernandez, 2009; Capen and Martin, 1989).

A variety of techniques have been evaluated as potential methods to remove perchlorate from water. Both ion exchange resins and membrane technologies are capable of removing perchlorate from solution; however, these technologies are non-destructive. Regeneration of the resins and membranes produce large quantities of high-strength brines, which must either be treated or disposed of as a hazardous waste. If not regenerated, the resins and membranes themselves require disposal as a hazardous waste. Filtration media, such as surfactant-modified geosorbents, are also nondestructive and, therefore, spent sorbents also require disposal as a hazardous waste.

Technologies that breakdown perchlorate to Cl^- and O_2 include chemical reduction and biodegradation. Chemical reduction involves the use of reducing agents, such as stabilized zero-valent iron nanoparticles to abiotically reduce perchlorate. This process typically requires heating the solution to high temperatures to overcome large kinetic barriers (Cao *et al*., 2005; Xiong *et al*., 2007), which greatly increases the costs of such treatments. Although bioreactors can be designed to biologically degrade perchlorate, this method has not been used to treat drinking water (Bardiya and Bae, 2011; WRF, 2011). This is attributed to the general public's fear of contamination of treated water by microbial cells and disinfection by-products (Li, 2008; Dugan *et al*., 2009; Bardiya and Bae, 2011; WRF, 2011).

Due to the issues associated with each technology, perhaps the optimal method to treat perchlorate-contaminated water is the use of a filtration media to first remove perchlorate from solution followed by the application of a destructive process to degrade

the perchlorate bound to the media. Surfactant-modified montmorillonite (SMM) has been shown to quickly remove perchlorate from aqueous solutions (Chapter 2). In order to degrade the perchlorate bound to the spent SMM, the used media should undergo a second phase of treatment, such as chemical reduction or biodegradation. By treating the perchlorate bound to the spent SMM, the media can be disposed of as a non-hazardous waste.

Chemical Perchlorate Reduction

As a strong oxidant, the chemical reduction of perchlorate is thermodynamically favored:

$$\mathrm{ClO_4^-} + 8\mathrm{H^+} + 8\mathrm{e^-} = \mathrm{Cl^-} + 4\mathrm{H_2O}$$
$$\mathrm{E_H^0} = 1.389\mathrm{V} \qquad (4.1)$$

(Cao *et al.,* 2005). However, the tetrahedral structure of perchlorate (Figure 4.1) results in a large kinetic barrier to perchlorate reduction, which renders common reductants useless and allows perchlorate to persist in the environment (Srinivasan and Sorial, 2009). Early investigations achieved success in the reduction of perchlorate through the use of trace elements, such as vanadium (King and Garner, 1954); however, the reaction required high temperatures (>40°C) and the byproducts formed hindered the reaction (Duke and Quinney, 1954).

More recent investigations have focused on using iron to reduce perchlorate. Moore *et al.* (2003) found that, while iron surfaces were capable of reducing perchlorate at slightly acidic or near-neutral pH, the reaction rates were prohibitively slow for use in reactors. Additionally, the presence of chloride was found to decrease perchlorate reduction by iron, which is significant because chloride is commonly found in the environment and is a product of the reduction of perchlorate (Moore and Young, 2005). Zero valent iron (ZVI) is capable of reducing perchlorate at temperatures ranging from

125 to 200°C (Oh *et al.,* 2006). Cao *et al*. (2005) found that ZVI nanoparticles (nZVI) were able to reduce perchlorate in the temperature range of 25 to 75°C, with the lag time decreasing from 28 days to 24 hours as the temperature increased. Sodium carboxymethyl cellulose-stabilized nZVI were capable of complete perchlorate degradation at ~95°C (Xiong *et al*., 2007).

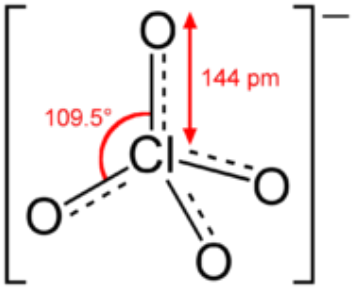

Figure 4.1. Structure of perchlorate (Webster's, 2008)

Requirements of Biological Perchlorate Reduction

Perchlorate-Reducing Bacteria (PRB)

Biological degradation of perchlorate has been studied for almost 50 years (Hackenthal, *et al*., 1964; Hackenthal *et al*., 1965). More recently, bacteria capable of reducing perchlorate (PRB) have been found to be ubiquitous in the environment (Coates *et al*., 1999; Waller *et al*., 2004). For instance, Coates *et al.* (1999) and Coates and Achenbach (2006) found significant numbers of PRB (2.31×10^3 to 2.4×10^6 cells per gram) in hydrocarbon-contaminated soil, aquatic sediments, paper mill waste sludges, and pristine soils. The ubiquity of PRB indicates that bioaugmentation is not usually required for *in situ* biological degradation of perchlorate.

Suitable Electron Donors

Bacteria have been identified that are capable of degrading perchlorate using electron donors similar to those used in chemical reduction (e.g. ZVI). All identified perchlorate reducing bacteria (PRB) require an electron donor for growth (Bardiya and Bae, 2011). Acetate is the most commonly utilized electron donor for reduction of perchlorate (Bardiya and Bae, 2011). Amendments of acetate and hydrogen to PRB found in vadose zone soil reduced the lag time of perchlorate degradation from 63 days (no amendments) to 14 and 41 days, respectively (Nozawa-Inoue, *et al*., 2005). Waller *et al*. (2004) observed that 1.7 moles of acetate are oxidized for each mole of perchlorate reduced. Other electron donors commonly used by PRB include H_2, zero-valent iron, Fe(II), and elemental sulfur (Bruce *et al.*, 1999; Ju *et al*., 2008; Sahu *et al*., 2009; Yu *et al*., 2007; Son, *et al*., 2011).

Molybdenum Requirement

In order for PRB to reduce perchlorate, studies have shown that trace amounts of molybdenum are required, as its absence inhibits perchlorate reduction (Chaudhuri *et al.*, 2002). For example, *Dechloromonas aromatica* and *D. agitata* completely stopped reducing perchlorate when transferred to a media with no molybdenum; however, perchlorate reduction immediately resumed once molybdenum was added to the culture (Chaudhuri *et al*., 2002; Coates and Achenbach, 2006). A molybdenum-dependent chaperone gene that is associated with the genes that encode chlorite dismutase were found within both *Pseudomonas* sp. strain PK and *Dechloromonas aromatic* strain RCB (Bender *et al*., 2002; Chaudhuri *et al*., 2002).

Moderate pH and Temperature

Almost all identified PRB thrive in neutral pH and mesophilic temperatures (Bruce *et al*., 1999; Coates *et al*., 1999; Bardiya and Bae, 2011). Wang *et al*. (2008) found that biological perchlorate reduction occurred throughout the pH range of 5 to 9, with maximum perchlorate degradation at pH 7. Similarly, Wu *et al*. (2008) noted perchlorate reduction occurred between pH 6 and 10, with optimum perchlorate degradation at pH 8. Additionally, neutral-acidic conditions may be maintained due to production of CO_2 as perchlorate is degraded (Figure 1.17) due to the carbonic acid that is produced from dissolution of CO_2 in water.

Competing Electron Acceptors

Most PRB will preferentially reduce oxygen, nitrate, and chlorate before perchlorate (Bardiya and Bae, 2011). For instance, all the PRB identified by Coates *et al*. (1999) were also able to use oxygen as the sole electron acceptor. Additionally, the perchlorate reductase enzyme isolated from Strain GR-1 was sensitive to the presence of oxygen (Kengen *et al*., 1999). *Dechlorosoma suillum* grown in the presence of perchlorate and with even low concentrations of oxygen (as low as 5% saturation) were incapable of reducing perchlorate (Chaudhuri *et al*., 2002). Once oxygen was replaced with nitrogen gas, perchlorate reduction commenced within 15 hours (Chaudhuri *et al*., 2002).

Most identified PRB are capable of growth coupled to the reduction of nitrate. All PRB found in contaminated sites by Waller *et al*. (2004) reduced nitrate either before or simultaneously with perchlorate. In *Dechlorosoma suillum*, neither perchlorate reduction nor chlorite dismutase expression occurred until after the nitrate was consumed (Chaudhuri *et al*., 2002). Nozawa-Inoue *et al*. (2005) found that, while nitrate addition suppressed perchlorate reduction at first, once the nitrate was consumed and the

process of perchlorate reduction began, the initial presence of nitrate enhanced the rate of transformation. While the initial concentration of nitrate did not alter the lag time, higher rates of perchlorate reduction were found in the communities with the highest initial addition of nitrate. Nozawa-Inoue *et al*. (2005) hypothesized that this increased rate of perchlorate reduction can be associated with the numbers of bacteria able to reduce both nitrate and perchlorate. Their conclusion was that the high initial nitrate concentrations induced the growth of large numbers of nitrate-reducing bacteria that were also capable of reducing perchlorate after nitrate depletion.

Objective

Non-destructive techniques, such as the use of SMM to filter perchlorate from solution, merely transfer the contaminant from the liquid to the solid phase. The spent filtration media requires disposal as a hazardous waste. However, the application of a second treatment phase could reduce the perchlorate bound to the SMM into innocuous byproducts (Cl^- and O_2). The effectiveness of both chemical reduction using nZVI and biodegradation were evaluated as a second phase of treatment following perchlorate filtration using SMM.

MATERIALS AND METHODS

Materials

SMM was created as described in Chapter 2 by exchanging the inorganic cations naturally found in montmorillonite with hexadecyltrimethylammonium (HDTMA). Sodium perchlorate was obtained from Fisher Chemical, Fisher Scientific, Fair Lawn, New Jersey. California NELAC perchlorate standards were purchased from AccuStandard Wet Chemistry Reference Standards, New Haven, Connecticut. Sodium acetate and sodium hydroxide were purchased from JT Baker, Phillipsburg, New Jersey. Palladized

zero-valent iron nanoparticles (Pd/nZVI) were obtained from Dr. Dongye Zhao, Civil Engineering Department, Auburn University (Zhao *and Xu*, 2009). Pd/nZVI was created by stabilizing nZVI with carboxymethyl cellulose and potassium hexachloropalladate (K_2PdCl_6) (Xiong, 2007). Column effluent was collected from a treatment column used for over a year to biodegrade perchlorate-contaminated waters generated in the laboratory. The treatment column was created by filling a 4.5ft long tube (4.5in inner diameter) with compost and sand and biostimulating perchlorate reduction. Sodium acetate and mushroom compost tea were periodically added to the column in order to enhance perchlorate reduction. Organic mushroom compost tea was acquired from Advantage Organic Products, Duncanville, TX. Brine was obtained from the regeneration of resin used to treat perchlorate-contaminated groundwater at a Los Angeles, California treatment plant (Table 2.5). The initial perchlorate concentration in the brine was 5.6mg/L and was spiked to 2,000mg/L.

Preparation of Spent SMM

Prior to application of the perchlorate-destructive treatment, spent SMM was prepared by adding perchlorate solutions to SMM (Table 4.1). The vials were placed on an end-over-end rotating shaker at ambient temperature for 24 hours, when it was centrifuged. The solution was decanted and analyzed. The adsorbed perchlorate concentration was calculated using mass balance:

$$C_{ads} = (C_0 - C_{aq})\left(\frac{V}{m}\right) \quad (4.2)$$

where C_{ads} is the mass adsorbed to solid phase (mg/kg), C_0 is the initial solution concentration (mg/L), C_{aq} is the equilibrium solution concentration (mg/L), V is the volume of solution (L), and m is the mass of adsorbent (kg).

Table 4.1. Experimental Set-up for preparation of spent SMM.

Description/ Additive		Vial ID	C_0 (mg/L)	C_{aq} (mg/L)	Volume (mL)	Mass of SMM (mg)	C_{ads} (mg/kg)
Freshwater	Pd/nZVI	ZVI 1	2,000	1,370	50	1.4707	21,420
		ZVI 2	2,000	1,370	50	1.4634	21,530
		ZVI 3	2,000	1,370	50	1.4903	21,140
	Control - DI Water	ZVI Control	2,000	1,370	50	1.4805	21,280
	Column Effluent	CE 1	2,240	30.66	93	10.0092	20,550
		CE 2	2,240	30.85	93	10.0063	20,550
		CE 3	2,240	31.75	93	10.0079	20,540
		CE 4	2,240	30.37	93	10.0255	20,550
		CE 5	2,240	30.80	93	10.0040	20,560
		CE 6	2,240	32.12	93	10.0054	20,540
	Mushroom Compost	MC 1	2,240	1.408	93	10.0819	20,670
		MC 2	2,240	1.533	93	10.0194	20,800
		MC 3	2,240	1.453	93	10.0207	20,800
		MC 4	2,240	1.449	93	10.0172	20,800
		MC 5	2,240	1.312	93	10.0301	20,780
	Control - DI Water	FW Control 1	2,240	23.83	93	10.0160	20,610
		FW Control 2	2,240	25.25	93	10.0061	20,610
Brine	Column Effluent	Brine CE 1	1,900	223.5	93	9.9367	15,690
		Brine CE 2	1,900	228.9	93	9.9454	15,630
		Brine CE 3	1,900	240.8	93	10.0666	15,330
	Mushroom Compost	Brine MC 1	1,900	225.1	93	9.9503	15,650
		Brine MC 2	1,900	227.7	93	9.9259	15,670
		Brine MC 3	1,900	227.6	93	9.9389	15,650
	Control - DI Water	Brine Control 1	1,900	226.6	93	9.9871	15,580
		Brine Control 2	1,900	242.2	93	9.9899	15,430
		Brine Control 3	1,900	237.0	93	9.9380	15,560

Abiotic Degradation Protocol

Chemical reduction of perchlorate bound to spent SMM using Pd/nZVI was evaluated. The test consisted of adding 1.5mg of Pd/nZVI and 100mL of deionized water to each of 3 vials. The reactors each contained 1.5g of spent SMM containing an average of 21,300mg ClO_4^-/kg. The vials were shaken by hand for a few seconds and allowed to incubate at room temperature for 24 hours, prior to analysis of the solution. A

control sample was prepared by adding deionized water without Pd/nZVI to a vial containing 1.5g of spent SMM (Table 4.1).

Biodegradation Protocol

To begin the freshwater biodegradation test, 97mL of a perchlorate biodegradation solution composed of 100% column effluent was added to 6 bioreactors, each containing 10g of the spent SMM (20,600mg ClO_4^-/kg). A 1:1 mixture of mushroom compost tea and deionized water (97mL total) was added to the 5 bioreactors, each containing 10g of the spent SMM. Additionally, control vials were prepared by adding 97mL of deionized water to the two remaining reactors containing 10g of spent SMM. All of the reactors were shaken vigorously by hand, sealed and incubated at room temperature with loosely fitting lids. After 4 days, 1mL samples of the liquid phase was withdrawn and analyzed for perchlorate. Aqueous samples continued to be collected once or twice a week for 120 days and 62 days for column effluent bioreactors and mushroom compost tea reactors, respectively.

Biodegradation studies also included treatment of SMM which was used to filter perchlorate from brine, which was created during regeneration of ion exchange resin. Nine bioreactors were prepared, each containing 10g of spent SMM (15,600mg ClO_4^-/kg) (Table 4.1). Three vials were prepared for each treatment by adding 85mL of column effluent, mushroom compost tea, or deionized water. Solution samples (1mL) were taken from each vial once or twice per week for 70 days.

Perchlorate Analysis

Immediately after sampling, the aliquots were passed through a 0.2µm filter to remove most all of the SMM. Both the treated and control samples were passed through carbon filters to reduce the amount of interference caused by dissolved organic material.

The samples generated during the biological treatment studies were analyzed in-house. Perchlorate was quantified using EPA test method 314.0, which utilized a Dionex DX500 Ion Chromatography System (IC) with a 500µL sample loop. Samples were diluted to between 0.002 to 1.5 mg/L and placed in 5mL Dionex auto-sampling vials. The IC setup utilized an IONPAC AS16 analytical column (4x250mm), an AG16 guard column (4x50mm), an ASRS-Ultra II Self Regenerating Suppressor (4mm) set at 300mA, and an AI-450 Chromatography Automation System with the Advanced Computer Interface Module. The 100mM sodium hydroxide eluent was degassed using a VWR Scientific Aquasonic Solicitor, model 150D. Blanks of deionized water, along with check standards, were analyzed every 10 samples to test for carry-over and instrumental drifting, respectively. If the blanks detected perchlorate or if the percent difference of a check standard was greater than 5%, the IC was recalibrated and the samples were reanalyzed.

After treatment with Pd/nZVI, Columbia Analytical Services, which is accredited under the National Environmental Laboratory Accreditation Program (NELAP), analyzed aqueous samples for perchlorate. Samples were shipped in coolers overnight to Columbia Analytical, located in Kelso, Washington. Columbia Analytical used EPA method 314.0 to quantify perchlorate using ion chromatography (IC).

RESULTS AND DISCUSSION

Abiotic Reduction of Perchlorate Bound to Spent SMM

Chemical reduction of perchlorate using Pd/nZVI was not effective at room temperature. There was no appreciable decrease in the aqueous perchlorate concentration after treatment using Pd/nZVI over a period of 24 hours (Figure 4.2). While this treatment was ineffective at room temperature, increasing the temperatures to 95-110°C would likely have increased perchlorate reduction (Xiong, 2007). However, the

increased expense of heating aqueous-clay suspensions to these high temperatures would likely cause this technology to be cost prohibitive. Therefore, investigations into the use of Pd/nZVI to abiotically treat spent SMM were not continued because the goal of this research was to develop a cost-effective method to treat perchlorate-contaminated SMM.

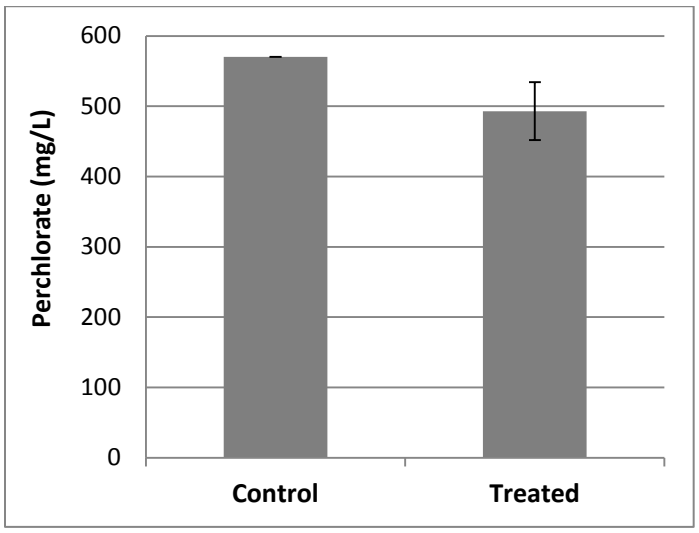

Figure 4.2. Chemical reduction of perchlorate using stabilized zero-valent iron nanoparticles.

Biodegradation of Perchlorate Bound to Spent SMM

Bioaugmentation with Bioactive Column Effluent

Biodegradation tests revealed that perchlorate bound to spent SMM could be degraded following bioaugmentation with biologically active column effluent (Figure 4.3 and Appendix K). The spent SMM with perchlorate loading of 20,600mg ClO_4^-/kg produced a maximum solution concentration of 12.6mg ClO_4^-/L. As the perchlorate in solution was degraded, more perchlorate anions were continuously desorbed from SMM

and entered the solution. Leaching of perchlorate from the solid phase was the rate limiting step in perchlorate biodegradation. After an incubation period of 25 days, biodegradation was stimulated, and the aqueous perchlorate concentrations in the reactors began to decrease. After 40 days, the perchlorate concentration in solution began to increase due to a combination of the biodegradation being limited due to consumption of most of the acetate and the continued desorption of perchlorate from the spent SMM. Acetate was added to the bioreactors on day 60, which lowered the perchlorate concentration due to increased biodegradation. After 68 days, the perchlorate concentration in solution began to increase again due to both perchlorate desorption and reduced biodegradation caused by depletion of acetate. On day 81, more acetate was added, which resulted in an increase in biodegradation that decreased the amount of perchlorate in solution. After 120 days, a 94% reduction of the perchlorate in solution was achieved. The solution perchlorate concentration in all 6 bioreactors was reduced to less than 1.1mg ClO_4^-/L and the average concentration was 0.76mg ClO_4^-/L.

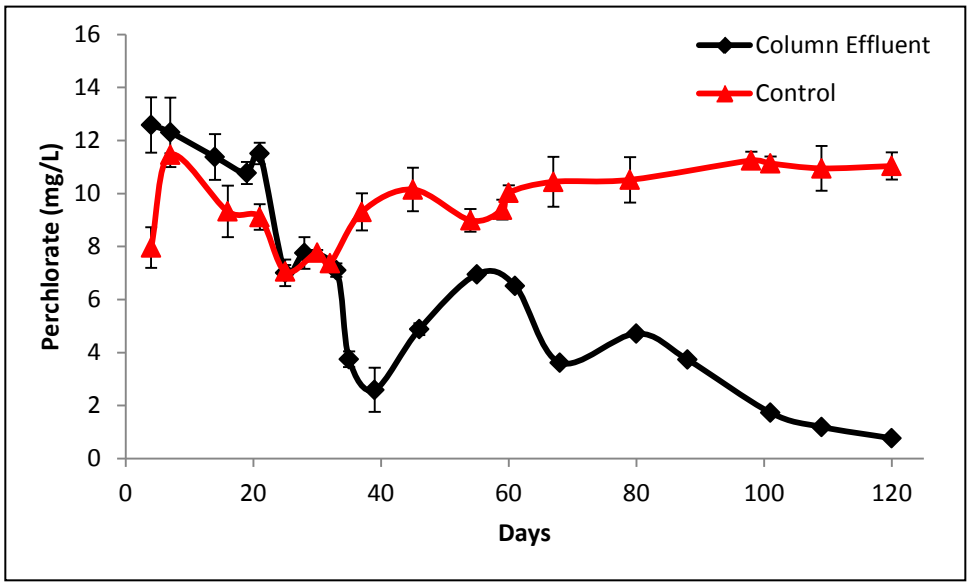

Figure 4.3. Treatment of spent SMM using biologically active column effluent. The data points are averages of the concentrations measured in 6 vials. Control points are the averages of duplicate vials containing the same mass of spent SMM and deionized water only. Error bars represent the standard deviations.

The results of degradation of perchlorate bound to SMM in this study differed from those found in a study of biodegradation of perchlorate in vadose zone soils conducted by Nozawa-Inoue *et al*. (2005). In the vadose soil study, perchlorate biodegradation was observed after 14 days and complete degradation occurred after 40-80 days. Unlike the soil bioremediation study, the biostiumlation of perchlorate degradation in SMM treatments was observed after 25 days and the solution concentrations decreased to <1.1mg/L after 120 days. There are key differences between these two studies, which include:

1. Perhaps the most significant distinction is the type of solid media utilized. In the study by Nozawa-Inoue *et al.,* biodegradation of perchlorate in vadose soil was evaluated as opposed to biodegradation of perchlorate bound to SMM, a filtration media developed for selective adsorption of perchlorate. Perchlorate has a high aqueous solubility and has little affinity for most natural soils (Urbansky, 2002). Rather than sorbing to soils, perchlorate salts precipitate in vadose zone soil as contaminated water evaporates. To account for this type of contamination, the soil used in the study by Nozawa-Inoue *et al*. was created by physically mixing soil and perchlorate salt. Immediately upon aqueous saturation, the perchlorate in the soil mixture would have desorbed completely into the aqueous phase, approaching its aqueous solubility (>200g/100mL for sodium perchlorate). This causes perchlorate to be instantly bioavailable for perchlorate-reducing bacteria (PRB). Comparatively, SMM is strongly selective for perchlorate. In the study using SMM, the perchlorate was adsorbed to the solid particles, causing desorption to limit the amount of perchlorate available for microbial degradation. As the perchlorate in solution was degraded, slow desorption from the spent SMM replenished the dissolved perchlorate. Thus, the spent SMM was a constant source of perchlorate that replenished the perchlorate in the aqueous solution. Therefore, the main difference between the two studies is that perchlorate adsorption

onto the soil was insignificant and desorption was rapid and lead to faster biodegradation of perchlorate in the vadose soil study.

2. The SMM contained approximately 200% more perchlorate (20,600 mg ClO_4^-/kg) than the soil utilized by Nozawa-Inoue *et al.* (100mg ClO_4^-/kg). The stimulation of biodegradation of such a high concentration of perchlorate adsorbed by SMM would be longer.

3. Anaerobic conditions were created in the soil studies by Nozawa-Inoue *et al.* by purging the headspace with nitrogen gas. The replacement of air with nitrogen gas reduces the lag time for perchlorate biodegradation because of the absence of oxygen, which is preferentially utilized as a terminal electron acceptor (Coates *et al*. 1999; Bardiya and Bae, 2011). Comparatively, biostimulation of perchlorate degradation in SMM was delayed by the presence of oxygen in the vial headspace.

4. Conversely, the higher concentration of nitrate in the study by Nozawa-Inoue *et al*. would have delayed perchlorate biodegradation in the vadose soil. PRB tend to prefer nitrate over perchlorate as the terminal electron acceptor. The vadose soil used contained 62mg NO_3^-/L, which is significantly higher than the <2mg NO_3^-/L measured in the SMM biodegradation study. Meanwhile, the HDTMA surfactant tends to inhibit microbial activity and would be expected to prolong the biostimulation of perchlorate in spent SMM treatments.

Bioactive Mushroom Compost Tea

In the biodegradation batch test that utilized mushroom compost tea, the perchlorate concentrations were not significantly reduced after 62 days (Figure 4.4 and Appendix L). In order to ensure that the bioreactors contained adequate electron donors, acetate was added after 21 days to increase the acetate concentration in solution to ~30mg/L. Nitrate concentrations in the mushroom compost tea were very low

(<0.2mg/L), suggesting that the presence of nitrate did not inhibit perchlorate degradation. The pH of the mushroom compost treatment (9.8) was much more basic than the pH values determined by both Wu *et al.* (pH = 8) *and* Want *et al*. (pH = 7) for optimum perchlorate degradation. The pH of the solution in the bioreactor was barely within the 6-10 range that Wu *et al.* (2008) found to be optimal for perchlorate degradation. Additionally, the mushroom compost treated bioreactors were much more basic than the column effluent treated reactors (pH = 7.2) that were capable of biodegrading perchlorate (Figure 4.3). Perhaps the addition of a buffer to maintain a more moderate pH would increase perchlorate biodegradation in the mushroom compost tea treatments.

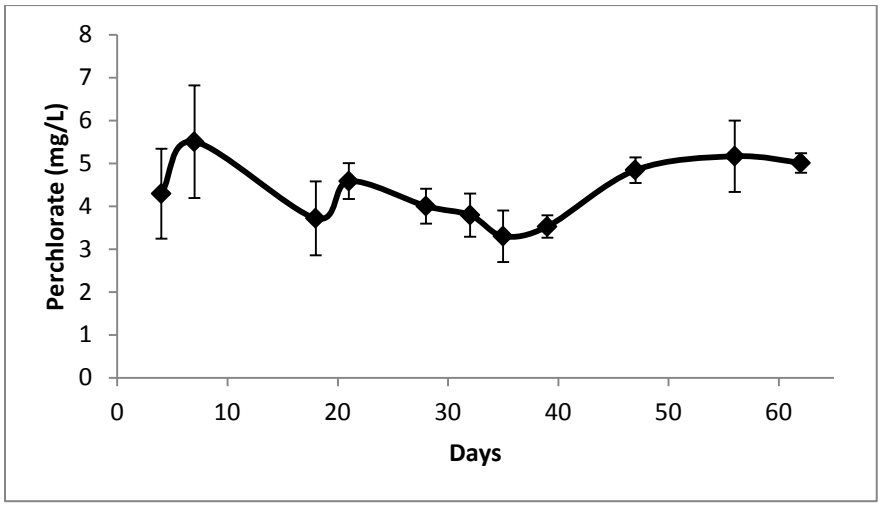

Figure 4.4. Treatment of spent SMM using biologically active mushroom compost. Data points are averages of the solution perchlorate concentrations in 5 vials and the standard deviations are represented with error bars.

Biodegradation of Perchlorate Adsorbed to SMM Regenerant Brine

The biodegradation batch tests of spent SMM used to treat brine produced during the regeneration of ion-exchange resin did not show significant reductions in the

aqueous perchlorate concentrations after 70 days (Figure 4.5 and Appendix N). The nitrate concentration in brine was almost 5000mg/L (Table 2.5), suggesting that PRB were likely to selectively reduce nitrate before perchlorate. Additionally, the elevated salt concentrations in these solutions may have been toxic to the perchlorate-reducing bacteria. Perhaps the use of salt-tolerant PRB that have been acclimated to high salt concentrations (as identified by Logan *et al*., 2001; Cang *et al*., 2004; Park and Marchand, 2006; Lehman *et al*., 2008; van Ginkel, 2008; Ryu *et al*., 2012) would be capable of reducing perchlorate bound to SMM after filtration of brines. Furthermore, the pH of the mushroom compost tea was 10, which is not optimal for perchlorate reduction (Wu *et al.*, 2008; Wang *et al*., 2008). Perhaps the application of a suitable buffer to maintain a near neutral pH will be more favorable for degradation of perchlorate that is adsorbed by SMM.

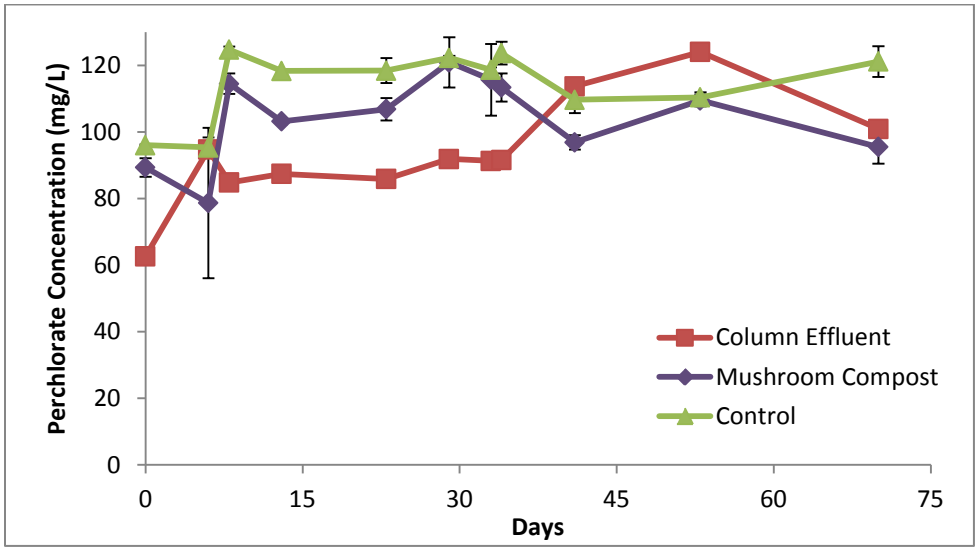

Figure 4.5. Bioremediation of spent SMM from filtration of perchlorate from brine. Significant reduction of perchlorate in solution did not occur during the 70 days of biological treatment.

CONCLUSION

While SMM is cable of removing perchlorate from water, this process is non-destructive. A second stage of treatment was used to evaluate the effectiveness of bioremediation of perchlorate bound to the spent SMM to innocuous byproducts. Batch biodegradation tests showed that perchlorate bound to spent SMM can be biologically degraded using amendments of acetate and biologically active column effluent from a perchlorate treatment column amended with acetate. Perchlorate degradation was biostimulated within 25 days after application of bioactive column effluent. The concentration of perchlorate in solution that was in equilibrium with the spent SMM was reduced from 12.6mg/L to less than 1.1mg/L in all 6 reactors (average final concentration was 0.76mg/L) within 120 days. The rate of perchlorate biodegradation was limited by the rate of desorption of perchlorate from SMM. Biodegradation of perchlorate bound to spent SMM from the treatment of regenerant brine was ineffective in a 70 day biodegradation test. Future studies should include bioaugmentation with salt-tolerant bacteria and the application of a buffer to maintain the biodegradation medium at near neutral pH.

Chemical reduction of perchlorate with zero-valent iron nanoparticles was ineffective at ambient temperatures within 24 hours. Future research should evaluate the effectiveness of chemical reduction of perchlorate bound to SMM at higher temperatures (90°C). However, the cost effectiveness of heating large quantities of aqueous-SMM solutions will likely decrease the cost effectiveness of this method.

CHAPTER 5

CONCLUSIONS

Perchlorate (ClO_4^-) has been detected in the food and drinking water supplies of millions of people worldwide and has been shown to competitively inhibit iodide uptake by the thyroid gland symporter. Although many technologies are currently applied to remove perchlorate from contaminated waters, many issues remain that limit their cost-effectiveness. For example, filtration technologies are widely accepted by the public, but these methods merely transfer the perchlorate from one phase to another, rather than destroy it. Therefore, the spent filtration media itself requires either treatment or disposal. Biodegradation can be used to breakdown perchlorate into chloride and oxygen; however, the public generally has a negative perception of biological treatment of drinking water due to potential contamination by reaction byproducts and biological materials. Chemical remediation of perchlorate is a destructive technology, but requires heating large quantities of water to high temperatures in order to degrade perchlorate, which significantly increases the remediation cost.

One possible method to optimally remove perchlorate from contaminated water is the application of a dual-phase technology, in which the filtration of perchlorate from water is followed by treatment of the sorbent so that the perchlorate is destroyed. The research presented here focused on the filtration of perchlorate from water with surfactant modified natural clays followed by biodegradation of the perchlorate bound to the spent organoclay. Bioremediation of spent clay is relatively cost-efficient and produces innocuous end products, thus, avoiding landfill disposal of the spent organoclay as a hazardous waste.

Adsorptive (TMA- and TMPA-modified) and organophilic (BDTDA- and HDTMA-modified) clays were evaluated for their effectiveness to remove perchlorate from water. The surfactant-modified montmorillonite (SMM) was produced by exchanging the natural inorganic cations in natural montmorillonite with the surfactant cations. The HDTMA-montmorillonite was relatively the most effective for the removal of perchlorate from water.

HDTMA is a quaternary ammonium cation which consists of a positively charged monovalent head group linked to a 16-chain carbon tail. The exchange of weakly hydrated inorganic cations in the montmorillonite interlayer with HDTMA caused the montmorillonite to change from hydrophilic to hydrophobic and from negatively to positively charged. Parallel tests were performed using pellet-sized surfactant-modified zeolite (SMZ).

Perchlorate anions are attracted to the positively charged head group of the HDTMA molecule that is bound to the SMM and SMZ. The kinetics of perchlorate sorption by SMM and SMZ were both very fast. SMM sorption of perchlorate approached equilibrium in <1hr. Due to its lower surface area and relatively larger particle size, the approach to sorption equilibrium for SMZ was approximately 3hrs.

Overall, both SMM and SMZ have high perchlorate sorption capacities. This study showed that SMM is a relatively more efficient sorbent for perchlorate compared to SMZ. At initial concentrations ranging from 0-24mg/L, the isotherm for perchlorate adsorption by SMZ was best described by the Langmuir model and had a maximum sorption capacity of 8,800mg ClO_4^-/kg. Over this same concentration range, adsorption by SMM was described by the linear partition model, suggesting that the available sorption sites were not saturated. The isotherms generated by additional batch tests of SMM with initial perchlorate concentrations ranging from 0-470mg/L were best described

by the Freundlich model, which indicates that the sorption capacity was approached at higher perchlorate loading.

In batch tests conducted in both groundwater and brine produced during the regeneration of ion exchange resin, evidence was obtained that SMM was selective for perchlorate in the presence of other inorganic anions. The high selectivity of perchlorate by SMM is likely the result of the differences in anion hydration energies. Perchlorate is a weakly hydrated anion that readily partitions into the weakly hydrated interlayers of the hydrophobic SMM.

After treatment with SMM, the reduction of anion concentrations in both full and half-strength (50% dilution) brine followed the order of the Hofmeister series, ClO_4^- > NO_3^- > Cl^-. The Hofmeister series is a classification of ions (usually anions) in order of their ability to interact with proteins, and is generally theorized to be closely related to hydration energies. Chaotropic anions, such as perchlorate, have a lower charge density, are less hydrated, and have a greater affinity for hydrophobic surfactant layers. More strongly hydrated anions increase the stability of water and are less likely to pass into surfactant layers. The relative sorption of anions from groundwater did not follow the Hofmeister series as was seen in batch tests conducted using brine. This difference was likely due to a reduction in the significance of hydration energies at lower salt concentrations found in the groundwater compared to the brine. The Hofmeister effect is much stronger at moderate to high salt content.

Future research should evaluate in greater detail the effects of pH, the presence of other anions, and the concentration of hydrophobic organic contaminants on perchlorate uptake by SMM and SMZ. Particular emphasis needs to be placed on anion selectivity, so that the role of the Hofmeister series and the importance of hydration energies can be further evaluated. Additional batch tests should be conducted that examine anion selectivity by SMM and SMZ when an organic solvent is used rather than

water. Theoretically, if solvation energies are significant in perchlorate sorption by SMM, the order of anion selectivity should reverse when an organic solvent is used in place of water.

The advection-dispersion equation was used to model solute transport through SMM and SMZ packed columns. The high perchlorate sorption of both sorbents allowed for the use of linear partition coefficients to calculate the retardation factors for perchlorate within concentration ranges likely to occur in most contaminated groundwater. The retardation factors for SMM and SMZ were calculated using the linear partition coefficient and were 30,480 and 16,380, respectively. Due to both its high perchlorate sorption capacity and low hydraulic conductivity, perchlorate transport through SMM consistently had the longest breakthrough times. For instance, in the case of water flowing at a velocity of 1cm/d with a dispersion of 84cm^2/d through a 1m long column with an inner diameter of 0.5m that is packed with SMM, 1% breakthrough of perchlorate would occur after ~700 years. Prior to perchlorate breakthrough, 5,700 pore volumes, or 515m^3, of solution would be treated. Under the same conditions, breakthrough of a perfect (non-reactive) tracer would occur after eight days.

The structure of SMZ consists of cage-like spheres with the layer of surfactant (HDTMA) molecules on the outer surface providing the sorption sites for perchlorate. Steric restrictions prohibit surfactants from entering into the zeolite intrastructure; therefore, the only perchlorate sorption sites tend to be on the outer surface of the SMZ. Due to the high hydraulic conductivity of SMZ, larger values of velocity and dispersivity were used to model mass transport compared to the parameters utilized to model SMM. Mass transport modeling of solution flowing at a velocity of 10cm/hr with a dispersion of 5000cm^2/hr predicted that 1% perchlorate breakthrough would occur after 2.5 years. During this time, 4,390 pore volumes (430m^3) of solution would be treated. Under the same conditions, a perfect tracer would achieve breakthrough at approximately 0.8hr.

The physical properties of the sorbents played a significant role in their possible applications. SMM has a much smaller particle size than SMZ. The small size of SMM grains (~57µm) results in a very low hydraulic conductivity (10^{-8}m/sec), which was prohibitively slow for use in a packed-bed reactor. A potential application of SMM is to use it as a filtration media in a fluidized-bed reactor to remove perchlorate from water. Furthermore, the low hydraulic conductivity of SMM makes it ideal for use as an impermeable barrier, such as a landfill liner. SMZ has a high hydraulic conductivity (10^{-3} m/sec), making it suitable as a filtration media in a packed-bed reactor or as a permeable reactive barrier to treat contaminated groundwater plumes *in situ*.

Although filtration systems are effective at removing large quantities of perchlorate from water, this process is non-destructive and the filtration media requires either treatment or disposal as a hazardous waste. This issue can be addressed by using a second phase of treatment to destroy perchlorate bound to spent filtration media. Both chemical reduction and biodegradation were evaluated as potential options to treat perchlorate bound to spent SMM. Chemical reduction of perchlorate using stabilized zero valent iron nanoparticles were ineffective at ambient temperatures. While its application could potentially be effective at high temperatures (95°C), the expense of heating large quantities of SMM and water would likely cause this treatment to be cost prohibitive.

The use of perchlorate-reducing bacteria (PRB) was effective in degrading perchlorate bound to spent SMM. The spent material was placed in a bioreactor with freshwater, biologically active solution, and acetate. The perchlorate was degraded as it desorbed from the SMM and became biologically available in solution. Perchlorate was continuously desorbed into solution, causing SMM to serve as a constant source. Spent SMM containing 20,500mg ClO_4^-/kg produced an initial aqueous solution concentration of 12mg/L. After 120 days, the perchlorate solution concentration was reduced by 94%

to <1.1mg/L in all 6 bioreactors (average concentration of 0.76mg/L). Biodegradation of perchlorate bound to spent clays required only a few months, indicating that this technique is a viable option to quickly treat spent organoclays so that only non-hazardous wastes remain.

Future studies should optimize the use of PRB to degrade perchlorate bound to spent SMM by using a buffer to maintain a neutral pH and by sustaining enough of the electron donor (e.g. acetate) so that biodegradation is not limited. The effects of Cl^- accumulation in solution on biodegradation of perchlorate bound to spent SMM should also be examined. Additional evaluations should include the quantification of the total amount of perchlorate destroyed by measuring the accumulation of Cl^-, which is a byproduct of perchlorate degradation. A comparison of the total amount of perchlorate degraded to the quantity initially adsorbed to the SMM should reveal the amount of perchlorate irreversibly bound to the SMM. The impact of nitrate on biological treatment of spent SMM should be evaluated through biodegradation of spent SMM used to treat perchlorate contamination in waters containing a range of nitrate concentrations.

Additional research should also include an evaluation of the effectiveness of using biodegradation to remediate perchlorate bound to spent SMZ. After undergoing biodegradation, the possibility of reusing SMM and SMZ as perchlorate filtration media should also be examined, including the possibility of enhancement of its efficiency by exchanging additional surfactant (HDTMA) onto SMM and SMZ after biological treatment has concluded.

Biodegradation of perchlorate bound to SMM used to treat brine was insignificant after 70 days of treatment. Future studies should include the use of salt-tolerant bacteria that would likely be better suited to the conditions produced during treatment of SMM used to filter brine. In particular, the effect of using buffers to maintain a neutral pH

should be evaluated. Such a study should also examine the effects of pH, the accumulation of Cl^-, the effect of nitrate, and the types and amounts of electron donors.

The decision of the EPA to regulate perchlorate in drinking water has raised the importance of developing more effective methods to remove perchlorate from solution. This research has shown that SMM is an effective sorbent of perchlorate from both freshwater and brines and could be used as a filtration media, for pre-treatment prior to the application of a more expensive method, or as an *in situ* impermeable reactive barrier (e.g. landfill liner). Furthermore, spent SMM could be biologically treated so that perchlorate is degraded and only non-hazardous materials remain.

REFERENCES

Achenbach, Laurie A., Urania Michaelidou, Royce A. Bruce, Johanna Fryman, and John D. Coates. 2001. *Dechloromonas agitate* gen. nov., sp. Nov. and *Dechlorosoma suillum* gen. nov., sp. Nov., tow environmentally dominant (per)chlorate-reducing bacteria and their phylogenetic position. International *Journal of Systematic and Evolutionary Microbiology* **51**(2): 527-533.

Alther, George. 2004. Some practical observations on the use of bentonite. *Environmental & Engineering Geoscience* **10**(4): 347-359.

Azejjel, H., J.M. Ordax, K. Draoui, M.S. Rodríguez-Cruz, and M.J. Sánches-Martín. 2010. Effect of cosolvents on the adsorption of ethofumesate by modified Moroccan bentonite and common clay. *Applied Clay Science* **49**(3): 120-126.

Aziz, Carol, Robert Borch, Paul Nicholson, and Evan Cox. 2006. Alternative causes of wide-spread, low concentration perchlorate impacts to groundwater. In *Perchlorate: Environmental Occurrence, Interactions and Treatment,* edited by Baohua Gu and John D. Coates. Springer-Science Business Media, New York. pp. 71-91.

Bao, Huiming, and Baohua Gu. 2004. Natural perchlorate has a unique oxygen isotope signature. *Environmental Science &Technology* **38**(19): 5073-5077.

Bardiya, Nirmala, and Jae-Ho Bae. 2011. Dissimilatory perchlorate reduction: a review. *Microbiological Research* **166**(4): 237-254.

Bender, Kelly S., Susan M. Oconnor, Romy Chakraborty, John D. Coates, and Laurie A. Achenbach. 2002. Sequencing and transcriptional analysis of chlorite dismutase gene of *Dechloromonas agitata* and its use as a metabolic probe. *Applied and Environmental Microbiology* **68**(10): 4820-4826.

Bilgili, M. Sinan. 2006. Adsorption of 4-chlorophenol from aqueous solutions by xad-4 resin: Isotherm, kinetic, and thermodynamic analysis. *Journal of Hazardous Materials* **137**(1): 157-164.

Blount, Benjamin C., Liza Valentin-Blasini, John D. Osterloh, Joshua P. Mauldin, and James L. Pirkle. 2007. Perchlorate exposure of the US population, 2001-2002. *Journal of the Exposure Science and Environmental Epidemiology* **17**: 400-407.

Bonczek, James L., W.G. Harris and Peter Nkedi-Kizza. 2002. Monolayer to bilayer transitional arrangements of hexadecyltrimethylammonium cations on Na-montmorillonite. *Clays and Clay Minerals* **50**(1): 11-17.

Borden, Robert C. 2007. Concurrent bioremediation of perchlorate and 1,1,1-trichloroethane in an emulsified oil barrier. *Journal of Contaminant Hydrology* **94**: 13-33.

Borden, Robert C., and M. Tony Lieberman. 2009. Passive bioremediation of perchlorate using emulsified edible oils. In *In Situ Bioremediation of Perchlorate in Groundwater,* edited by H.F. Stroo and C.H. Ward. Springer. New York. pp. 29-52.

Boyd, Stephen A., Max M. Mortland, and Cary T. Chiou. 1988a. Sorption characteristics of organic compounds on hexadecyltrimethylammonium-smectite. *Soil Science Society of America Journal* **52**: 652-657.

Boyd, Stephen A., Sun Shaobai, Juinn-Fwu Lee, and Max M. Mortland. 1988b. Pentachlorophenol sorption by organo-clays. *Clays and Clay Minerals* **36**(2): 125-130.

Brixie, J.M., and S.A. Boy. 1994. Treatment of contaminated soils with organoclays to reduce leachable pentachlorophenol. *Journal of Environmental Quality* **23**(6): 1283-1290.

Brown, Gilbert M., and Baohua Gu. 2006. The chemistry of perchlorate in the environment. In *Perchlorate Environmental Occurrence, Interactions and Treatment*, edited by Baohua Gu and John D. Coates. Springer, New York. pp. 17-47.

Brown, Jess C., Vernon L. Snoeyink, Lutgarde Raskin, and Richard Lin. 2003. The sensitivity of fixed-bed biological perchlorate removal to changes in operating conditions and water quality characteristics. *Water Research* **37**: 206-214.

Brown, Michael J., and David R. Burris. 1996. Enhanced organic contaminant sorption on soil treated with cationic surfactants. *Ground Water* **34**(4): 734-744.

Bruce, Royce A., Laurie A. Achenbach, and John D. Coates. 1999. Reduction of (per)chlorate by a novel organism isolated from paper mill waste. *Environmental Microbiology* **1**(4): 319-329.

Cang, Y., D.J. Roberts, and D.A. Clifford. 2004. Development of cultures capable of reducing perchlorate and nitrate in high salt solutions. *Water Research* **38**: 3322-3330.

Cao, Jiasheng, Daniel Elliott, and Wei-xian Zhang. 2005. Perchlorate reduction by Nanoscale iron particles. *Journal of Nanoparticle Research* **7**: 499-506.

Capen, Charles C., and Sharron L. Martin. 1989. The effects of xenobiotics on the structure and function of thyroid follicular and C-cells. *Toxicologic Pathology* **17**(2): 266-293.

Celis, R., W.C. Koskinen, A.M. Cecchi, G.A. Bresnahan, M.J. Carrisoza, M.A. Ulibarri, I. Pavlovic, and M.C. Hermosin.1999. Sorption of the ionizable pesticide imazamox by organo-clays and organohydrotalcites. *Journal of Environmental Science and Health* **B34**(6): 929-941.

Chang, Chia M., Ming K. Wang, Ta W. Wang, C. Lin, and Yih R. Chen. 2001. Transport modeling of copper and cadmium with linear and nonlinear retardation factors. *Chemosphere* **43**(8): 1133-1139.

Chaudhuri, Swades K., Joseph G. Lack, and John D. Coates. 2001. Biogenic magnetite formation through anaerobic biooxidation of Fe(II). *Applied and Environmental Microbiology* **67**(6): 2844-2848.

Chaudhuri, Swades K., Susan M. O'Connor, Ruth L. Gustavson; Laurie A. Achenbach, and John D. Coates. 2002. Environmental Factors that Control Microbial Perchlorate Reduction. *Applied and Environmental Microbiology* **68**(9): 4425-4430.

Chen, Zhen, Wei Ma, and Mei Han. 2008. Biosorption of nickel and copper onto treated alga (*Undaria pinnatifida*): Application of isotherm and kinetic models. *Journal of Hazardous Materials* **155**(1-2): 327-333.

Chitrakar, Ramesh, Yoji Makita, Takahiro Hirotsu, and Akinari Sonoda. 2012. Montmorillonite modified with hexadecylpyridinium chloride as a highly efficient anion exchanger for perchlorate ion. *Chemical Engineering Journal* **191**: 141-146.

Chowdhury, T., and M. Das. 2010. Moisture sorption isotherm and isoteric heat of sorption characteristics of starch based edible films containing antimicrobial preservative. *International Food Research Journal* **17**: 601-614.

Coates, John D., and Laurie A. Achenbach. 2004. Microbial perchlorate reduction: Rocket-fueled metabolism. Nature Reviews *Microbiology* **2**(7): 569-580.

Coates, John D., Laurie A. Achenbach. 2006. In-situ bioreduction and removal of ammonium perchlorate. Strategic Environmental Research and Development Program (SERDP) Project Number CU 1162. 138p.

Coates, John D., and W. Andrew Jackson. 2009. Principles of perchlorate treatment. In *In Situ Bioremediation of Perchlorate in Groundwater,* edited by H.F. Stroo and C.H. Ward. Springer, New York. pp. 29-52.

Coates, John D., Urania Michaelidou, Royce A. Bruce, Susan M. O'Connor, Jill N. Crespi, and Laurie A. Achenbach. 1999. Ubiquity and diversity of dissimilatory (per)chlorate-reducing bacteria. *Applied and Environmental Microbiology* **65**(12): 5234-5241.

Coates, John D., Kimberly A. Cole, Romy Chakraborty, Susan M. O'Connor, and Laurie A. Achenbach. 2002. Diversity and ubiquity of bacteria capable of utilizing humic substances as electron donors for anaerobic respiration. *Applied and Environmental Microbiology* **68**(5): 2445.

Collins, Kim D., and Michael W. Washabaugh. 1985. The Hofmeister effect and the behavior of water at interfaces. *Quarterly Reviews of Biophysics* **18**(4): 323-422.

Cox, Evan E. 2009. Development of *in situ* bioremediation technologies for perchlorate. In *In Situ Bioremediation of Perchlorate in Groundwater,* edited by H.F. Stroo and C.H. Ward. Springer, New York. pp. 15-27.

Cramer, Randall J., Carey Yates, Paul Hatzinger, and Jay Diebold. 2004. Field demonstration of *in situ* perchlorate bioremediation at building 1419. Naval Sea Systems Command Report NOSSA-TR-2004-001. Accessed on April 25, 2012 http://www.dtic.mil/cgi-bin/ GetTRDoc?AD=ADA421555.

Cunniff, S.E., R.J. Cramer, and H.E. Maupin. 2006. Perchlorate: challenges and lessons. In *Perchlorate: Environmental Occurrence, Interactions and Treatment,* edited by Baohua Gu and John D. Coates. Springer-Science Business Media, New York. pp. 1-15.

Custelcean, Radu, and Bruce A. Moyer. 2007. Anion separation with metal-organic frameworks. *European Journal of Inorganic Chemistry* **2007**(10): 1321-1340.

Dasgupta, Purnendu K., P. Kalyani Martinelango, W. Andrew Jackson, Todd A. Anderson, Kang Tian, Richard W. Tock, and Srinath Rajagopalan. 2005. The origin of naturally occurring perchlorate: the role of atmospheric processes. *Environmental Science and Technology* **39**(6): 1569-1575.

Dugan, Nicholas R., Daniel J. Williams, Maria Meyer, Ross R. Schneider, Thomas F. Speth, and Deborah H. Metz. 2009. The impact of temperature on the performance of anaerobic biological treatment of perchlorate in drinking water. *Water Research* **43**: 1867-1878.

Duke, Frederick R., and Paul R. Quinney. 1954. The kinetics of the reduction of perchlorate ion by Ti(III) in dilute solution. *Journal of the American Chemical Society* **76**(14): 3800-3803.

El Aribi, Houssain, Yves J.C. Le Blanc, Stephen Antonsen, and Takeo Sakuma. 2006. Analysis of perchlorate in foods and beverages by ion chromatography coupled with tandem mass spectrometry (IC-ESI-MS/MS). *Analytica Chimica Acta* **567**(1): 39-47.

Erdem, Bilge, A. Safa Özcan, and Adnan Özcan. 2010. Preparation of HDTMA-bentonite: characterization studies and its adsorption behavior toward dibenzofuran. *Surface and Interface Analysis* **42**: 1351-1356.

Evans, Patrick J., and Mary M. Trute. 2006. *In situ* bioremediation of nitrate and perchlorate in vadose zone soil for groundwater protection using gaseous electron donor injection technology. *Water Environment Research* **78**(13): 2436-2446.

Evans, Patrick J., Rodney A. Fricke, Karl Hopfensperger, and Tom Titus. 2011. *In situ* destruction of perchlorate and nitrate using gaseous electron donor injection technology. *Ground Water Monitoring & Remediation* **31**(4): 103-112.

Federal Registry. 2011. Drinking water: regulatory determination on perchlorate (Drinking). U.S. Environmental Protection Agency. 2011. Federal Register 76

(February 11, 2011): 7762-7767. Accessed on April 25, 2012 at http://www.regulations.gov/#!docketDetail;dct=FR+PR+N+O+SR;rpp=10;so=DESC;sb=postedDate;po=0;D=EPA-HQ-OW-2009-0297.

Fetter, C.W. 2001. *Applied Hydrogeology Fourth Edition*. Prentice-Hall. New Jersey.

Freeze, R. Allan, and John A. Freeze. 1979*. Groundwater.* Prentice-Hall, New Jersey.

Frost, Ray L., Quin Zhou, Hongping He, Wei Shen, Peng Yuan, and Jian Xi Zhu. 2008. Mechanism of p-nitrophenol adsorption from aqueous solution by HDTMA+-pillared montmorillonite: implications for water purification. *Journal of Hazardous Materials* **154**(1-3): 1025-1032.

Fuller, Mark E., Paul B. Hatzinger, Charles W. Condee, and A. Paul Togna. 2007. Combined treatment of perchlorate and RDX in ground water using a fluidized bed reactor. *Ground Water Monitoring & Remediation* **27**(3): 59-64.

Fusi, P., P. Arfaioli, L. Calamai, and M. Bosetto. 1993. Interactions of two acetanilide herbicides with clay surfaces modified with Fe(III) oxyhydroxides and hexadecyltrimethyl ammonium. *Chemosphere* **27**(5): 765-771.

Galforé, Juan Carlos, Amelia Marí, Rosa Maria Príncipe, and Javier Salvador. 2009. Markers of thyroid function. Pp. 27-48 in: *Thyroid Hormones: Functions, Related Diseases and Uses,* edited byFrancis S. Kuehn and Mauris P. Lozada. Nova Biomedical Books, New York.

Groisman, Ludmila, Chaim Rav-Acha, Zev Gerstl, and Uri Minglegrin. 2004. Sorption of organic compounds of varying hydrophobicities from water and industrial wastewater by long- and short-chain organoclays. *Applied Clay Science* **24**(3-4): 159-166.

Gu, Baohua, Gilbert M. Brown, Leon Maya, Michael J. Lance, and Bruce A. Moyer. 2001. Regeneration of perchlorate (ClO_4^-)-loaded anion exchange resins by a novel tetrachloroferrate ($FeCl_4^-$) displacement technique. *Environmental Science and Technology* **35**: 3363-3368.

Gu, Baohua, Bilbert M. Brown, and Chen-Chou Chiang. 2007. Treatment of perchlorate-contaminated groundwater using highly selective, regenerable ion-exchange technologies. *Environmental Science and Technology* **41**: 6277-6282.

Gurol, Mirat D., and Kyehee Kim. 2000. Investigation of perchlorate removal in drinking water sources by chemical methods. In *Perchlorate in the Environment,* edited by Edward Todd Urbansky. Pp.99-108.

Hackenthal, E. 1965. Die reduction von perchlorate durch bacterien. II. Die identitat der nitratreduktase und des perchlorate reduzierenden enzyms aus *B. cereus*. *Biochemical Pharmacology* **14**: 1313-1324.

Hackenthal, E., W. Mannheim, R. Hackenthal, and R. Becher. 1964. Die reduction von perchlorate durch bakterien. I.* Untersuchungen an intakten zellen (The

reduction of perchlorate by bacteria – I. Studies with whole cells). *Biochemical Pharmacology* **13**: 195-206.

Haggerty, Grace M., and Robert S. Bowman. 1994. Sorption of chromate and other inorganic anions by organo-zeolite. *Environmental Science and Technology* **28**(3): 452-458.

Hatzinger, Paul B. 2005. Perchlorate biodegradation for water treatment. *Environmental Science and Technology* **39**: 239A-247A.

Hatzinger, Paul B., Charles E. Schaefer, and Evan E. Cox. 2009. Active Bioremediation. In *In Situ Bioremediation of Perchlorate in Groundwater,* edited by H.F. Stroo and C.H. Ward. Springer, New York. pp. 91-133.

Hatzinger, Paul B., M. Casey Whittier, Martha D. Arkins, Chris W. Bryan, and William J. Guarini. 2002. In-situ and ex-situ bioremediation options for treating perchlorate in groundwater. *Remediation* **12**(2): 69-86.

He, Hongping, Ray L. Frost, Thor Bostrom, Peng Yuan, Loc Duong, Dan Yang, Yunfei Xi, and J. Theo Kloprogge. 2006a. Changes in the morphology of organoclays with HDTMA (super +) surfactant loading. *Applied Clay Science* **31**(3-4): 262-271.

He, Hongping, Qin Zhou, Wayde N. Martens, Theo J. Kloprogge, Peng Yuan, Yunfei Xi, Jianxi Zhu, and Ray L. Frost. 2006b. Microstructure of HDTMA+-modified montmorillonite and its influence on sorption characteristics. *Clays and Clay Minerals* **54**(6): 689-696.

Hendricks, S.C., R.A. Nelson, and L.T. Alexander. 1940. Hydration mechanism of the clay mineral montmorillonite saturated with various cations. *Journal of the American Chemical Society* **62**(6): 1457-1464.

Henry, Bruce M., Michael W. Perlmutter, and Douglas C. Downey. 2009. Permeable organic biowalls for remediation of perchlorate in groundwater. In *In Situ Bioremediation of Perchlorate in Groundwater,* edited by H.F. Stroo and C.H. Ward. Springer. New York. pp. 177-198.

Hinz, C. and H.M. Selim. 1993. Transport of zinc and cadmium in soils: experimental evidence and modeling approaches. *Soil Science Society of America Journal* **58**(5): 1316-1327.

Hofmeister, Franz. 1888. Zur lehre von der wirkung der salze dritte mittheilung. *Naunyn-Schmiedeberg's Archives of Pharmacology* **25**(1): 1-30.

Hsu, Y.H., M.K. Wang, C.W. Pai, and Y.S. Wang. 2000. Sorption of 2,4-dichlorophenoxy propionic acid by organo-clay complexes. *Applied Clay Science* **16**: 147-159.

Huq, Hasina Parvin, Jung-Seok Yang, and Ji-Won Yang. 2007. Removal of perchlorate from groundwater by the polyelectrolyte-enhanced ultrafiltration process. *Desalinization* **204**(1-3): 335-343.

Interstate Technology and Regulatory Council (ITRC). 2002. Technical/regulatory guidelines: a systematic approach to *in situ* bioremediation in groundwater including decision trees on *in situ* bioremediation for nitrates, carbontetrachloride, and perchlorate. Accessed on August 18, 2010 from http://www.itrcweb.org /Documents/ISB-8.pdf.

Interstate Technology and Regulatory Council (ITRC). 2008. Technical/regulatory guidance: remediation technologies for perchlorate contamination in water and soil. Accessed on May 4, 2011 from http://www.itrcweb.org/documents/perc-2. pdf.

Jackson, W. Andrew, Preethi Joseph, Patil Laxman, Kui Tan, Philip N. Smith, Lu Yu, and Todd A. Anderson. 2005. Perchlorate accumulation in forage and edible vegetation. *Journal of Agricultural and Food Chemistry* **53**(2): 369-373.

Jackson, W. Andrew, Todd Anderson, Greg Harvey, Greta Orris, Srinath Rajagopalan, and Namgoo Kang. 2006. Occurrence and formation of non-anthropogenic perchlorate. In *Perchlorate: Environmental Occurrence, Interactions and Treatment,* edited by Baohua Gu and John D. Coates. Springer-Science Business Media, New York. pp. 49-69.

Jarraya, Ikram, Sophie Fourmentin, Mourad Benzina, and Samir Bouaziz. 2010. VOC adsorption on raw and modified clay materials. *Chemical Geology* **275**: 1-8.

Jaynes, W.F., and S.A. Boyd. 1991a. Clay mineral type and organic compound sorption by hexadecyltrimethylammonium-exchanged clays. *Soil Science Society of America Journal* **55**(5): 43-48.

Jaynes, W.J., and Boyd S.A. 1991b. Hydrophobicity of siloxane surfaces in smectites as revealed by aromatic hydrocarbon adsorption from water. *Clays and Clay Minerals* **39**: 428-436.

Jaynes, W.F., and G.F. Vance. 1996. BTEX sorption by organo-clays: cosorptive enhancement and equivalence of interlayer complexes. *Soil Science Society of America Journal* **60**: 1742-1749.

Ju, Xiumin, Reyes Sierra-Alvarez, Jim A. Field, David J. Byrnes, Harold Bentley, and Richard Bentley. 2008. Microbial perchlorate reduction with elemental sulfur and other inorganic electron donors*. Chemisphere* **71**:114-122.

Kang, Namgoo, W. Andrew Jackson, Purnendu K. Dasgupta, and Todd A. Anderson. 2008. Perchlorate production by ozone oxidation of chloride in aqueous and dry systems. *Science of the Total Environment* **405**(1-3): 301-309.

Kenegen, Servé W.M., Geoffrey B. Rikken, Wilfred R. Hagen, Cees G. van Ginkel, and Alfons J.M. Stams. 1999. Purification and characterization of per(chlorate) reductase from the chlorate-respiring strain GR-1. *Journal of Bacteriology* **181**(21): 6706-6711.

Kim, Joo Young, Sridhar Komarneni, Robert Parette, Fred Cannon, and Hiroaki Katsuki. 2011. Perchlorate uptake by synthetic layered double hydroxides and organo-clay minerals. *Applied Clay Science* **51**: 158-164.

Kim, Kijung, and Bruce E. Logan. 2001. Microbial reduction of perchlorate in pure and mixed culture packed-bed bioreactors. *Water Research* **35** (13): 3071-3076.

Kinnlburgh, David G. 1986. General purpose adsorption isotherms. *Environmental Science and Technology* **20**(9): 895-904.

Kirk, Andrea B., Ernest E. Smith, Kang Tian, Todd A. Anderson, and Purnendu K. Dasgupta. 2003. Perchlorate in milk. *Environmental Science and Technology* **37**(21): 4979-4981.

Kirk, Andrea B., P. Kalyani Martinelango, Kang Tian, Aniruddha Dutta, Ernest E. Smith, and Purnendu K. Dasgupta. 2005. Perchlorate and iodide in dairy and breast milk. *Environmental Science and Technology* **39**(7):2011-2017.

King, William R., Jr., and Clifford S. Garner. 1954. Kinetics of the oxidation of vanadium(II) and vanadium(III) ions by perchlorate ion. *Journal of Physical Chemistry* **58**(1): 29-33.

Krauter, Palua W., 2001. Using a wetland bioreactor to remediate ground water contaminated with nitrate (mg/L) and perchlorate (µg/L). *International Journal of Phytoremediation* **3**: 415-433.

Krauter, Paula, Bill Dailey Jr., and Valerie Dibley, Holly Pinkart, and Tina Legler. 2005. Perchlorate and nitrate remediation efficiency and microbial diversity in a containerized wetland bioreactor. *International Journal of Phytoremediation* **7**: 113-128.

Krishna, B.S., D.S.R. Murty, and B.S. Jai Prakash. 2001. Surfactant-modified clay as adsorbent for chromate. *Applied Clay Science* **20**: 65-71.

Krishnamoorthy, C., and R. Overstreet. 1950. An experimental evaluation of ion-exchange relationships. *Soil Science* **69**: 41-53.

Krug, Thomas A., and Evan E. Cox. 2009. Semi-passive *in situ* bioremediation. In *In Situ Bioremediation of Perchlorate in Groundwater,* edited by H.F. Stroo and C.H. Ward. Springer, New York. pp. 135-154.

Kunz, W., J. Henle, and B.W. Niham. 2004. 'Zur lehre von der wirkung der salze' (about the science of the effect of salts): Franz Hofmeister's historical papers. *Current Opinion in Colloid and Interface Science* **9**(1-2): 19-37.

Lee, Seung Yeop, and Soo Jin Kim. 2002a. Expansion of smectite by hexadecyltrimethylammonium. *Clays and Clay Minerals* **50**(4): 435-445.

Lee, Seung Yeop, and Soo Jin Kim. 2002b. Expansion characteristics of organoclay as a precursor to nanocomposites. Colloids *and Surfaces A: Physicochemical and Engineering Aspects* **211**(1): 19-26.

Lee, Jung-Ju, Jaeyoung Choi, and Jae-Woo Park. 2002c. Simultaneous sorption of lead and chlorobenzene by organobentonite. *Chemosphere* **49**(10): 1309-1315.

Lee, Seung Yeop, and Soo Jin Kim. 2003a. Study on the exchange reaction of HDTMA with the inorganic cations in reference montmorillonites. *Geosciences Journal* **7**(3): 203-208.

Lee, Seung Yeop, and Soo Jin Kim. 2003b. Dehydration behavior of hexadecyltrimethylammonium-exchanged smectite. *Clay Minerals* **38**(2): 225-232.

Lee, Seung Y., Won J. Cho, Phil S. Hahn, Minhee Lee, Young B. Lee, and Kang L. Kim. 2005. Microstructural changes of reference montmorillonites by cationic surfactants. *Applied Clay Science* **30**: 174-180.

Lee, Sungyun, N. Quyet, Eunkyung Lee, Suhan Kim, Sangyoup Lee, Young D. Jung, Seok Ho Choi, and Jaeweon Cho. 2008. Efficient removals of tris (2-chloroethyl) phosphate (TCEP) and perchlorate using NF membrane filtrations. *Desalination* **221**: 234-237.

Lehman, S. Geno, Mohammad Badruzzaman, Samer Adham, Deborah J. Roberts, and Dennis A. Clifford. 2008. Perchlorate and nitrate treatment by ion exchange integrated with biological brine treatment. *Water Research* **42**: 969-976.

Lemke, Shawna L., Patrick G. Grant, and Timothy D. Phillips. 1998. Adsorption of zearalenone by organophilic montmorillonite clay. *Journal of Agricultural and Food Chemistry* **46**(9): 3789-3796.

Leyva-Ramos, R., A. Jacobo-Azuara, P.E. Diaz-Flores, R.M. Guerrero-Coronado, J. Mendoza-Barron, and M.S. Berber-Mendoza. 2008. Adsorption of chromium(VI) from an aqueous solution on a surfactant-modified zeolite. *Colloids and Surfaces A: Physicochemical and Engineering Aspects* **330**(1): 35-41.

Li, Xu. 2008. Biological treatment of perchlorate and nitrate contaminated drinking water – Optimization of system performance using microbial community characterization. Dissertation. University of Michigan.

Li, Zhaohui. 1999. Oxyanion sorption and surface anion exchange by surfactant-modified clay minerals. *Journal of Environmental Quality* **28**(5): 1457-63.

Li, Zhaohui, Stephen J. Roy, Yiqiao Zou, and Robert S. Bowman. 1998. Long-term chemical and biological stability of surfactant-modified zeolite. *Environmental Science and Technology* **32**(17): 2628-2632.

Logan, B.E. 2001. Assessing the outlook for perchlorate remediation. *Environmental Science & Technology* **35**(23): 482A- 487A.

Logan, B.E., and D. LaPoint, 2002. Treatment of perchlorate- and nitrate-contaminated groundwater in an autotrophic gas phase, packed-bed bioreactor. *Water Research* **36**: 3647-3653.

Logan, Bruce E., Jun Wu, and Richard F. Unz. 2001. Biological perchlorate reduction in high-salinity solutions. *Water Resources Research* **35** (12): 3034-3038.

Lorenzetti, R. Jason, Shannon L. Bartlet-Hunt, Susan E. Burns, and James A. Smith. 2005. Hydraulic conductivities and effective diffusion coefficients of geosynthetic clay liners with organobentonite amendments. *Geotextiles and Geomembranes* **23**: 385-400.

Luthy, Richard G., George R. Aiken, Mark L. Brusseau, Scott D. Cunningham, Philip M. Gschwend, Joseph J. Pignatello, Martin Reinhard, Samuel J. Traina, Walter J. Weber, Jr, and John C. Westall. 1997. Sequestration of hydrophobic organic contaminants by geosorbents. *Environmental Science and Technology* **31**(12): 3341-3347.

Maes, Andre, Leo van Leemput, Adrien Cremers, and Jan Uytterhoeven. 1980. Electron-density distribution as a parameter in understanding organic cation-exchange in montmorillonite. *Journal of Colloid and Interface Science* **77**(1): 14-20.

Majdan, Marek, Oskana Maryuk, Stanislaw Pikus, Elizbieta Olszewska, Ryszard Kwiatkowski, and Henryk Skrzypek. 2005. Equilibrium, FTIR, scanning electron microscopy and small wide angle X-ray scattering studies of chromates adsorption on modified bentonite. *Journal of Molecular Structure* **740**: 203-211.

Marshall, C.E., and G. Garcia. 1963. Exchange equilibria in a carboxylic resin and in attapulgite clay. *Journal of Physical Chemistry* **63**: 1663-1666.

Mattie, David R., Joan Strawson, and Jay Zhao. 2006. Perchlorate toxicity and risk assessment. In *Perchlorate: Environmental Occurrence, Interactions and Treatment,* edited by Baohua Gu and John D. Coates. Springer-Science Business Media, New York. pp. 169-196.

McCarty, Perry L., and Travis E. Meyer. 2005. Numerical model for biological fluidized-bed reactor treatment of perchlorate-contaminated groundwater. *Environmental Science and Technology* **39**(3): 850-858.

Michalski, Greg, J.K. Bölke, and Mark Thiemens. 2004. Long term atmospheric deposition as the source of nitrate and other salts in the Atacama Desert, Chile: new evidence from mass-independent oxygen isotopic compositions. *Geochimica et Cosmochimica Act* **68**(20): 4023-4038.

Miller, J.P., and B.E. Logan. 2000. Sustained perchlorate degradation in an autotrophic, gas-phase, packed-bed bioreactor. *Environmental Science and Technology* **34**: 3018-3022.

Min, Booki, Patrick J. Evans, Allyson K. Chu, and Bruce E. Logan. 2004. Perchlorate removal in sand and plastic media bioreactors. *Water Research* **38**: 47-60.

Mishael, Yael Golda, Tomas Undabeyta, Giora Rytwo, Brigitte Papahadjopoulos-Sternberg, Baruch Rubin, and Shlomo Nir. 2002. Sulfometuron incorporation in cationic micelles adsorbed on montmorillonite. *Journal of Agricultural and Food Chemistry* **50**(10): 2856-2863.

Mizutani, Tadashi, Tetsuo Takano, and Hisanobu Ogoshi. 1995. Selectivity of adsorption of organic ammonium ions onto smectite clays. *Langmuir* **11**(3): 880-884.

Moore, Angela M., Corinne H. de Leon, and Thomas M. Young. 2003. Rate and extent of aqueous perchlorate removal by iron surfaces. *Environmental Science and Technology* **37**: 3189-3198.

Moore, Duane M., and Robert C. Reynolds, Jr. 1997. *X-Ray Diffraction and the Identification and Analysis of Clay Minerals, Second Edition*. Oxford University Press, Oxford, New York.

Moore, Angela M., and Thomas M. Young. 2005. Chloride interactions with iron surfaces: Implications for perchlorate and nitrate remediation using permeable reactive barriers. *Journal of Environmental Engineering* **131**(6): 924-933.

Mortland, Max M., Sun Shaobai, and Stephen A. Boyd. 1986. Clay-organic complexes as adsorbents for phenol and chlorophenols. *Clays and Clay Minerals* **34**(5): 581-585.

Motzer, William E. 2001. Perchlorate: problems, detection, and solutions. *Environmental Forensics* **2**(4): 301-311.

Na, Chongzheng, Fred S. Cannon, and Ben Hagerup. 2002. Perchlorate removal via iron-preloaded GAC and borohydride regeneration. *Journal of the American Water Works Association* **94**(11): 90-102.

Nerenberg, R., and B.E. Rittmann. 2004. Hydrogen-based, hollow-fiber membrane biofilm reactor for reduction of perchlorate and other oxidized contaminants. *Water Science and Technology* **49**(11-12): 223-230.

Nerenberg, Robert, Yasunori Kawagoshi, and Bruce E. Rittmann. 2008. Microbial ecology of a perchlorate-reducing, hydrogen-based membrane biofilm reactor. *Water Research* **42**: 1151-1159.

Nozawa-Inoue, Mamie, Kate M. Scow, and Dennis E. Rolston. 2005. Reduction of perchlorate and nitrate by microbial communities in vadose soil. *Applied and Environmental Microbiology* **7**1(7): 3928-3934.

Nzengung, Valentine A. 1993. Organoclays as sorbents for organic contaminants in aqueous and mixed-solvent systems. Ph.D thesis, Georgia Institute of Technology, Atlanta, Georgia.

Nzengung, Valentine A., Chuhua Wang, and Greg Harvey. 1999. Plant-mediated transformation of perchlorate into chloride. *Environmental Science and Technology* **33**: 1470-1478.

Nzengung, Valentine A., K.C. Das, and James R. Kastner. 2001. Pilot scale in-situ bioremediation of perchlorate-contaminated soils at the Longhorn Army Ammunition Plant. Final report for contract DAA09-00-C-0060. Retrieved February 26, 2009 from http://www.clu-in.net/download/contaminantfocus/perchlorate/LHAAPbio.pdf.

Nzengung, Valentine A., Holger Penning, and Walter O'Niell. 2004. Mechanistic changes during phytoremediation of perchlorate under different root-zone conditions. *International Journal of Phytoremediation* **6**(1): 63-83.

Nzengung, Valentine A., Evangelos A. Voudrias, Peter Nkedi-Kizza, J.M. Wampler, and Charles E. Weaver. 1996. Organic Cosolvent Effects on Sorption Equilibrium of Hydrophobic Organic Chemicals by Organoclays. *Environmental Science and Technology* **30**(1):89-96.

O'Connor, Susan M., and John D. Coates. 2002. Universal immunoprobe for (per)chlorate-reducing bacteria. *Applied and Environmental Microbiology* **68**(6): 3108-3113.

Ogata, Akio, and R.B. Banks. 1961. A solution of the differential equation of longitudinal dispersion in porous media. *U.S. Geological Survey Professional Paper 411-A.*

Ogawa, Makoto, Hidenori Shirai, Kazuyuki, and Chuzo Kato. 1992. Solid-state intercalation of naphthalene and anthracene into alkylammonium-montmorillonites. *Clays and Clay Minerals* **40**(5): 485-490.

Oh, Seok-Young, Pei C. Chiu, Byung J. Kim, and Daniel K. Cha. 2006. Enhanced reduction of perchlorate by elemental iron at elevated temperatures. *Journal of Hazardous Materials* **129**: 304-307.

Orris, G.J, G.J. Harvey, D.T. Tsui, and J.E. Eldridge. 2003. Preliminary analyses for perchlorate in selected natural materials and their derivative products. U.S. Geological Survey. USGS Open-File Report 03-314.

Özkaya, Bestamin. 2006. Adsorption and desorption of phenol on activated carbon and a comparison of isotherm models. *Journal of Hazardous Materials* **129**(1-3): 158-163.

Padmesh, T.V.N., K. Vijayaraghavan, G. Sekaran, and M. Velan. 2006. Application of two- and three- parameter isotherm models: Biosorption of acid red 88 onto Azolla microphylla. *Bioremediation Journal* **10**(1-2): 37-44.

Parette, Robert, and Fred S. Cannon. 2005. The removal of perchlorate from groundwater by activated carbon tailored with cationic surfactants. *Water Research* **39**: 4020-4028.

Park, C., and E.A. Marchand. 2006. Modelling salinity inhibition effects during biodegradation of perchlorate. *Journal of Applied Microbiology* **101**: 222-233.

Parker, David R., Angelia L. Seyfferth, and Brandi Kiel Reese. 2008. Perchlorate in groundwater: a synoptic survey of "pristine" sites in the coterminous United States. *Environmental Science and Technology* **42**(5): 1465-1571.

Patel, Hasmuk A., Hari C. Bajaj, and Raksh V. Jasra. 2009. Sorption of nitrobenzene from aqueous solution on organoclays in batch and fixed-bed systems. *Industrial and Engineering Chemistry Researc*h **48**(2): 1051-1058.

Patterson, Judodine, Robert Parette, Fred S. Cannon, Chris Lutes, and Trent Henderson. 2011. Competition of anions with perchlorate for exchange sites on cationic surfactant-tailored GAC. *Environmental Engineering Science* **28**(4): 249-256.

Pearce, Elizabeth N., Angela M. Leung, Benjamin C. Blount, Hamid R. Bazrafshan, Xuemei He, Sam Pino, Liza Valentin-Blasini, and Lewis E. Braverman. 2007. Breast milk iodide and perchlorate concentrations in lactating Boston-area women. *The Journal of Clinical Endocrinology & Metabolism* **92**(2): 1673-1677.

Polubesova, Tamara, Shlomo Nir, Onn Rabinovitz, Mikhail Borisover, and Baruch Rubin. 2003. Sulfentrazone adsorbed on micelle-montmorillonite complexes for slow release in soil. *Journal of Agricultural and Food Chemistry* **51**(11): 3410-3414.

Pontius, Frederick W., Paul Damian, and Andrew D. Eaton. 2000. Regulating perchlorate in drinking water. Pp. 31-36 in: *Perchlorate in the Environment,* edited by E.T. Urbansky. Environmental Science Research Series **57**, Kulwer Academic/Plenum Publishers, New York.

Rajagopalan, Srinath, Todd A. Anderson, Lynne Fahlquist, Ken A. Rainwater, Moira Ridley, and W. Andrew Jackson. 2006. Widespread presence of naturally occurring perchlorate in High Plains of Texas and New Mexico. *Environmental Science and Technology* **40**(10): 3156-3162.

Rao, Balaji, Todd A. Anderson, Aaron Redder, and W. Andrew Jackson. 2010. Perchlorate formation by ozone oxidation of aqueous chlorine/oxy-chlorine species: role of Cl_XO_Y radicals." *Environmental Science and Technology* **44**(8): 2961-2967.

Rikken, G.B., A.G.M. Kroon, and C.G. van Ginkel. 1996. Transformation of (per)chlorate into chloride by a newly isolated bacterium: reduction and dismutation. *Applied Microbiology and Biotechnology* **45**(3): 420-426.

Roberts, Michael G., Hui Li, Brian J. Teppen, and Stephen A. Boyd. 2006. Sorption of nitroaromatics by ammonium- and organic ammonium-exchanged smectite: shifts from adsorption/complexation to a partition-dominated process. *Clays and Clay Minerals* **54**(4): 426-434.

Robertson, W.D., C.J. Ptacek, and S.J. Brown. 2009. Rates of nitrate and perchlorate removal in a 5-year-old wood particle reactor treating agricultural drainage. *Ground Water Monitoring & Remediation*. **29**(2): 87-94.

Rodríguez-Sarmiento, David Christian, and Jorge Alejo Pinzón-Bello. 2001. Adsorption of sodium dodecylbenzene sulfonate on organophilic bentonites*. Applied Clay Science* **18**: 173-181.

Ryu, Hee Wook, Seong Jin Nor, Kyung Eun Moon, Kyung-Suk Cho, Daniel K Cha, and Kang In Rhee. 2012. Reduction of perchlorate by salt tolerant bacteria consortia. *Bioresource Technology* **103**: 279-285.

Sahu, Ashish K., Teresa Conneely, Klaus R. Nüsslein, and Sarina J. Ergas. 2009. *Environmental Science and Technology* **43**: 4466-4471.

Sanchez, C.A., B.C. Blount, L. Valentin-Blasini, S.M. Lesch, and R.I. Krieger. 2008. Perchlorate in the Feed-Dairy Continuum of the Southwestern United States. *Journal of Agricultural and Food Chemistry* **56**(13): 5443-5450.

Sanchez, C.A., K.S. Crump, R.I. Krieger, N.R. Khandaker, and J.P. Gibbs. 2005a. Perchlorate and nitrate in leafy vegetables of North America. *Environmental Science and Technology* **39**(24): 9391-9397.

Sanchez, C.A., R.I. Krieger, N. Khandaker, R.C. Moore, K.C. Holts, and L.L. Neidel. 2005b. Accumulation and perchlorate exposure potential of lettuce produced in the Lower Colorado River Region. *Journal of Agricultural and Food Chemistry* **53**(13): 5479-5486.

Sawhney, B.L. 1970. Potassium and cesium ion selectivity in relation to clay mineral structure. *Clays and Clay Minerals* **18**: 47-52.

Seliem, Moaaz K., S. Komarneni, R. Parette, H. Katsuki, F.S. Cannon, M.G. Shahien, A.A. Khalil, and I.M. Abd El-Gaid. 2011. Perchlorate uptake by organosilicas, organo-clay minerals and composites of rice husk with HCM-48. *Applied Clay Science* **53**: 621-626.

Sessler, Jonathan L., Philip A. Gale, and Won-Seob Cho. 2006. *Anion Receptor Chemistry.* The Royal Society of Chemistry, Cambridge.

Seyfferth, Angelia L., and David R. Parker. 2007. Effects of genotype and transpiration rate on the uptake and accumulation of perchlorate (ClO_4^-) in lettuce. *Environmental Science &Technology* **41**(9): 3361-3367.

Sharmasarkar, Shankar, William F. Jaynes, and George F. Vance. 2000. BTEX sorption by montmorillonite organo-clays: TMPA, ADAM, HDTMA. *Water, Air, and Soil Pollution* **119**: 257-273.

Sheng, Guangyao, and Stephen A. Boyd. 2000. Polarity effect on dichlorobenzene sorption by hexadecyltrimethylammonium-exchanged clays. *Clays and Clay Minerals* **48**(1): 43-50.

Sheng, Guangyao, Shihe Xu, and Stephen A. Boyd. 1996. Cosorption of organic contaminants from water by hexadecyltrimethylammonium-exchanged clays. *Water Resources Research* **30**(6): 1483-1489.

Shrout, Joshua D., Garrett C. Struckhoff, Gene F. Parkin, and Jerald L. Schnoor. 2006. Stimulation and molecular characterization of bacterial perchlorate degradation by plant-produced electron donors. *Environmental Science and Technology* **40**(1): 310-317.

Smith, James A., Peter R. Jaffé, and Cary T. Chlou. Effect of ten quaternary ammonium cations on tetrachloromethane sorption to clay from water. *Environmental Science and Technology* **24**(8): 1167-1172.

Snyder, Shane A., Richard C. Pleus, Brett J. Vanderford, and Janie C. Holady. 2006. Perchlorate and chlorate in dietary supplements and flavor enhancing ingredients. *Analytica Chimica Acta* **567**(1): 26-32.

Son, Ahjeong, Carl J. Schmidt, Hyejin Shin, and Daniel K. Cha. 2011. Microbial community analysis of perchlorate-reducing cultures growing on zero-valent iron. *Journal of Hazardous Materials* **185**(2-3): 669-676.

Sposito, Garrison, R. Prost, and Jean-Pierre Gaultier. 1983. Infrared spectroscopic study of adsorbed water on reduced-charge Na/Li-montmorillonites. *Clays and Clay Minerals* **31**(1): 9-16.

Srinivasan, Rangesh, and George A. Sorial. 2009. Treatment of perchlorate in drinking water: a critical review. *Separation and Purification Technology* **69**(1): 7-21.

Stroo, Hans F., and Robert D. Norris. 2009. Alternatives for *in situ* bioremediation of perchlorate. *In Situ Bioremediation of Perchlorate in Groundwater,* edited by Paul B. Hatzinger, Charles E. Schaefer, and Evan E. Cox. pp. 79-90.

Struckhoff, Garrett Cletus. 2009. Plant-assisted bioremediation of perchlorate and the effect of plants on redox conditions and biodiversity in low and high organic carbon soil. Dissertation, University of Iowa. Retrieved on May 4, 2012 at http://ir.uiowa.edu/etd/441/.

Sturchio, Neil C., J.K. Böhlke, Baohua Gu, Juske Horita, Gilbert M. Brown, Abelardo D. Beloso, Leslie J. Patterson, Paul B. Hatzinger, W. Andrew Jackson, and Jacimaria Batista. 2006. Stable isotopic composition of chlorine and oxygen in synthetic natural perchlorate. In: *Perchlorate: Environmental Occurrence, Interactions and Treatment,* edited by Baohua Gu, and John D. Coates. Springer-Science Business Media, New York. pp. 93-109.

Susarla, S., S.T. Bacchus, G. Harvey, and S.C. McCutcheon. 2000. Phytotransformations of perchlorate contaminated waters. *Environmental Technology* **21**: 1055-1065.

Susarla, Sridhar, Sydney T. Bacchus, Steven C. McCutcheon, and N. Lee Wolfe. 1999. Potential species for phytoremediation of perchlorate. U.S. Environmental Protection Agency Report EPA/600/R-99/069. 58 pp. Accessed on April 25 2012 at http://cluin.org/download/contaminantfocus/perchlorate/EPA600R99069.pdf.

Teppen, Brian J., and Vaneet Aggarwal. 2007. Thermodynamics of organic cation exchange selectivity in smectites. *Clays and Clay minerals* **55**(2): 119-130.

van Aken, Benoit, and Jerald L. Schnoor. 2002. Evidence of perchlorate (ClO_4-) reduction in plant tissues (poplar tree) using radio-labeled $^{36}ClO_4$-. *Environmental Science and Technology* **36**: 2783-2788.

van Ginkel, Steven W., Chang Hoon Ahn, Moohammad Badruzzaman, Deborah J. Roberts, S. Geno Lehman, Samer S. Adham, and Bruce E. Rittmann. 2008. Kinetics of nitrate and perchlorate reduction in ion-exchange brine using the membrane biofilm reactor (MBfR). *Water Research* **42**: 4197-4205.

Tsai, Shih-Chin, and Kai-Wei Juang. 2000. Comparison of linear and nonlinear forms of isotherm models for strontium sorption on a sodium bentonite. *Journal of Radioanalytical and Nuclear Chemistry* **243**(3): 741-746.

Tsai, Shih-Chin, Kai-Wei Juang, and Yi-Lin Jan. 2005. Sorption of cesium on rocks using heterogeneity-based isotherm models. *Journal of Radioanalytical and Nuclear Chemistry* **266**(1): 101-105.

Urbansky, Edward T. 1998. Perchlorate chemistry: implications for analysis and remediation. *Bioremediation Journal* **2**(2): 81-95.

Urbansky, Edward Todd. 2002. Perchlorate as an environmental contaminant. *Environmental Science and Pollution Research* **9**(3): 187-192.

Urbanksy, E.T., and M.B. Schock. 1999. Issues in managing the risks associated with perchlorate in drinking water. *Journal of Environmental Management* **56**(2): 79-95.

Urbansky, E.T., S.K. Brown, M.L. Magnuson, and C.A. Kelty. 2001. Perchlorate levels in samples of sodium nitrate fertilizer derived from Chilean Caliche. *Environmental Pollution* **112**(3): 299-302.

U.S. Environmental Protection Agency (USEPA). 2005a. EPA sets reference dose for perchlorate. Retrieved July 26, 2010 from http://yosemite.epa.gov/opa/admpress.nsf/a4a961970f783d3a85257359003d480d/c1a57d2077c4bfda85256fac005b8b32!OpenDocument.

U.S. Environmental Protection Agency (USEPA). 2005b. Integrated risk information system: perchlorate and perchlorate salts. Retrieved on September 8, 2010 from http://www.epa.gov /iris/subst/1007.htm#oralrfd.

U.S. Environmental Protection Agency (USEPA). 2009. Drinking water contaminant candidate list 3—final. Pp. 51850-51862 in: *Federal Register* 74:194 (October 8, 2009.). Accessed on July 26, 2010 at http://www.epa.gov/fedrgstr/EPA-WATER/2009/October/Day-08/w24287.pdf.

U.S. Environmental Protection Agency (USEPA). 2010 CLU-IN: perchlorate. Accessed on September 13, 2010 from http://www.clu-in.org/contaminantfocus/default.focus/ sec/perchlorate/cat/Overview/.

U.S. Environmental Protection Agency (USEPA). 2011. Perchlorate. Accessed on September 13, 2011 from: http://water.epa.gov/drink/contaminants/unregulated/perchlorate.cfm.

U.S. Food and Drug Administration (USFDA). 2009. 2004-2005 Exploratory data on perchlorate in food. Washington, DC. Retrieved on July 21, 2010 from http://www.fda.gov/Food/FoodSafety/FoodContaminantsAdulteration/Chemical Contaminants/Perchlorate/ucm077685.htm.

U.S. Government Accountability Office (USGAO). 2010. Perchlorate occurrence is widespread but at varying levels; federal agencies have taken some actions to

respond to and lessen releases. Report to the Ranking Member, Committee on Environment and Public Works, U.S. Senate. GAO-10-769. Retrieved on September 13, 2011 from: http://www.gao.gov/ new.items/d10769.pdf.

van Ginkel, Steven W., Chang Hoon Ahn, Mohammad Badruzzaman, Deborah J. Roberts, S. Geno Lehman, Samer S. Adham, and Bruce E. Rittmann. 2008. Kinetics of nitrate and perchlorate reduction in ion-exchange brine using the membrane biofilm reactor (MBfR). *Water Research* **42**: 4197-4205.

Vazquez, A., M. López, G. Kortaberria, L. Martín, and I. Mondragon. 2008. Modification of montmorillonite with cationic surfactants. Thermal and chemical analysis including CEC determination. *Applied Clay Science* **41**: 24-36.

Videla, Luis A., and Virginia Fernandez. 2009. Redox signaling in thyroid hormone action: a novel strategy for liver preconditioning. Pp. 49-74 in: *Thyroid Hormones: Functions, Related Diseases and Uses,* edited by Francis S. Kuehn and Mauris P. Lozada. Nova Biomedical Books, New York.

Vijayaraghavan, K., T.V.N. Padmesh, K. Palanivelu, and M. Velan. 2006. Biosorption of nickel(II) ions onto *Sargassum wighitir*: Application of two-parameter and three-parameter isotherm models. *Journal of Hazardous Materials* **133**(1-3): 304-308.

Volzone, C., J.O. Rinaldi, and J. Ortiga. 2006. Retention of gases by hexadecyltrimethyl-ammonium-montmorillonite clays. *Journal of Environmental Management* **79**: 247-252.

Waller, Alison S., Evan E. Cox, and Elizabeth A. Edwards. 2004. Perchlorate-reducing microorganisms isolated from contaminated sites. *Environmental Microbiology* **6**(5): 517-527.

Wang, Chao, Zhengdao Huang, Lee Lippincott, and Xiaoguang Meng. 2010. Rapid Ti(III) reduction of perchlorate in the presence of β-alanine: kinetics, pH effect, complex formation, and β-alanine effect. *Journal of Hazardous Materials* **175**(1-3): 159-164.

Wang, D.M., and C.P. Huang. 2008. Electrodialytically assisted catalytic reduction (EDACR) of perchlorate in dilute aqueous solutions. *Separation and Purification Technology* **59**: 333-341.

Wang, D.M., S. Ismat Shah, J.G. Chen, and C.P. Huang. 2008. Catalytic reduction of perchlorate by H_2 gas in dilute aqueous solutions. *Separation and Purification Technology* **60**(1): 14-21.

Water Research Foundation (WRF). 2011. Perchlorate in drinking water regulatory update and treatment options. Accessed on April 25, 2012 at http://www.waterrf.org/resources/StateOfTheScienceReports/Perchlorate_StateOfTheScience.pdf.

Webster's Online Dictionary. 2008. Perchlorate. Retrieved on September 12, 2012 from: http://www.websters-online-dictionary.org/definitions/perchlorate.

Wibulswas, R. 2004. Batch and fixed bed sorption of methylene blue on precursor and QACs modified montmorillonite. *Separation and Purification Technology* **39**(1-2): 3-12.

Wu, Donglei, Ping He, Xinhua Xu, Mi Zhou, Zhen Zhang, and Zaidi Houda. 2008. The effect of various reaction parameters on bioremediation of perchlorate-contaminated water. *Journal of Hazardous Materials* **150**: 419-423.

Wu, Jun, Richard F. Unz, Husen Zhang, and Bruce E. Logan. 2001. Persistence of perchlorate and the relative numbers of perchlorate- and chlorate-respiring microorganisms in natural waters, soils, and wastewater. *Bioremediation Journal* **5**(2): 119-130.

Urbansky, Edward T. 1998. Perchlorate chemistry: implications for analysis and remediation. *Bioremediation Journal* **2**(2): 81-95.

U.S. Environmental Protection Agency (USEPA). 2005. Integrated risk information system: perchlorate and perchlorate salts. Retrieved on September 8, 2010 from http://www.epa.gov/iris/subst/1007.htm#oralrfd.

U.S. Environmental Protection Agency (USEPA). 2011. Perchlorate. Accessed on September 13, 2011 from: http://water.epa.gov/drink/contaminants/unregulated/perchlorate.cfm.

U.S. Government Accountability Office (USGAO). 2010. Perchlorate occurrence is widespread but at varying levels; federal agencies have taken some actions to respond to and lessen releases. Report to the Ranking Member, Committee on Environment and Public Works, U.S. Senate. GAO-10-769. Retrieved on September 13, 2011 from: http://www.gao.gov/new.items/d10769.pdf.

Wallace, W., S. Beshear, D. Williams, S. Hospadar, and M. Owens. 1998. Perchlroate reduction by a mixed culture in an up-flow anaerobic fixed bed reactor. *Journal of Industrial Microbiology and Biotechnology* **20**(2): 126-131.

Waller, Alison S., Evan E. Cox, Elizabeth A. Edwards. 2004. Perchlorate-reducing microorganisms isolated from contaminated sites. *Environmental Microbiology* **6**(5): 517-527.

Wang, D.M. and C.P. Huang. 2008. Electrodialytically assisted catalytic reduction (EDACR) of perchlorate in dilute aqueous solutions. *Separation and Purification Technology* **59**(3): 333-341.

Wang, Chao, Zhengdao Huang, Lee Lippincott, and Xiaoguang Meng. 2010. Rapid Ti(III) reduction of perchlorate in the presence of β-alanine: Kinetics, pH effect, complex formation, and β-alanine effect. *Journal of Hazardous Materials* **175**: 159-164.

Xi, Yunfei, Zhe Ding, Hongping He, and Ray L. Frost. 2004. Structure of organoclays—an X-ray diffraction and thermogravimetric analysis study. *Journal of Colloid and Interface Science* **277**: 116-120.

Xin, Xiao-Dong, Jin Wang, Hai-Qin Yu, Bin Du, Qin Wei, and Liang-Guo Yan. 2011. Removal of o-nitrobenzoic acid by adsorption on to a new organoclay: montmorillonite modified with HDTMA microemulsion. *Environmental Technology* **32**(4): 447-454.

Xiong, Zhong. 2007. Destruction of perchlorate and nitrate by stabilized zero-valent iron nanoparticles and immobilization of mercury by a new class of iron sulfide nanoparticles. Dissertation. Auburn University, Auburn, Alabama.

Xiong, Zhong, Dongye Zhao, and Gang Pan. 2007. Rapid and complete destruction of perchlorate in water and ion-exchange brine using stabilized zero-valent iron nanoparticles. *Water Research* **41**:3497-3505.

Xu, Jian-hong, Nai-yun Gao, Yang Deng, Ming-hao Sui, and Yu-lin Tang. 2011. Perchlorate removal by granular activated carbon coated with cetyltrimethylammonium chloride. *Desalination* **275**: 87-92.

Yang, Liuyan, Lijuan Jiang, Zhi Zhou, Yuangao Chen, and Xiaorong Wang. 2002. The sedimentation capabilities of hexadecyltrimethylammonium-modified montmorillonites. *Chemosphere* **48**: 461-466.

Yang, Liuyan, Zhi Zhou, Lin Xiao, and Xiaorong Wang. 2003. Chemical and biological regeneration of HDTMA-modified montmorillonite after sorption with phenol. *Environmental Science and Technology* **37**: 5057-5061.

Yariv, Shmuel, Mikhail Borisover, and Isaac Lapides. 2011. Few introducing comments on the thermal analysis of organoclays. *Journal of Thermal Analysis and Calorimetry* **105**(3): 897-906.

Yifru, Dawit D., and Valentine A. Nzengung. 2008. Organic carbon biostimulates rapid rhizodegradation of perchlorate. *Environmental Toxicology and Chemistry* **27** (12): 2419-2426.

Yoon, Yeomin, Gary Amy, Jaeweon Cho, Namguk Her, and John Pellegrino. 2000. Transport of perchlorate (ClO_4^-) through NF and UF membranes. *Desalination* **142**: 11-17.

Yoon, Yeomin, Gary Amy, Jaeweon Cho, and John Pellegrino. 2004. Systematic bench-scale assessment of perchlorate (ClO_4^-) rejection mechanisms by nanofiltration and ultfrafiltration membranes. *Separation Science and Technology* **39**(9): 2105-2135.

Yoon, Jaekyung, Gary Amy, Jinwook Chung, Jinsik Sohn, and Yeomin Yoon. 2009. Removal of toxic ions (chromate, arsenate, and perchlorate) using reverse osmosis, nanofiltration, and ultrafiltration membranes. *Chemosphere* **77**: 228-235.

Yoon, Jaekyung, Yeomin Yoon, Gary Amy, Jaeweon Cho, David Foss, and Tae-Hyung Kim. 2003. Use of surfactant modified ultrafiltration for perchlorate (ClO_4^-) removal. *Water Research* **37**: 2001-2012.

Yu, Xueyuan, Christopher Amrhein, Marc A. Deshusses, and Mark R. Matsumoto. 2007. *Environmental Science and Technology* **41**: 990-997.

Zeng, Q.H., A.B. Yu, G.Q. Lu, and R.K. Standish. 2003. Molecular dynamics simulation of organic-inorganic nanocomposites: layer behavior and interlayer structure of organoclays. *Chemistry of Materials* **15**(25):4732-4738.

Zhang, Pengfei, David M. Avudzega, and Robert S. Bowman. 2007. Removal of perchlorate from contaminated waters using surfactant-modified zeolite. *Journal of Environmental Quality* **36**: 1069-1075.

Zhang, Yanjie, and Paul S. Cremer. 2006. Interactions between macromolecules and ions: the Hofmeister series. *Current Opinion in Chemical Biology* **10**(6): 658-663.

Zhang, Yanjie, Steven Furky, David E. Bergbreiter, and Paul S. Cremer. 2005. Specific ion effects on the water solubility of macromolecules: PNIPAM and the Hofmeister Series. *Journal of the American Chemical Society* **127**(41): 14505-14510.

Zhang, Z. Zhong, Donald L.Sparks, and Noel C. Scrivner. 1993. Sorption and desorption of quaternary amine cations on clays. *Environmental Science and Technology* **27**: 1625-1631.

Zhao, Donge, and Yinhui Xu. 2009. *In situ* remediation of inorganic contaminants using stabilized zero-valent iron nanoparticles. United States Patent US 7,635,236 B2, filed March 30, 2007, and issued December 22, 2009.

Zhao, Hongting, William F. Jaynes, and George F. Vance. 1996. Sorption of the ionizable oroganic compound, dicamba (3,6-dichloro-2-methoxy benzoic acid), by organo-clays. *Chemosphere* **33**(10): 2089-2100.

Zhao, Hongting, and George F. Vance. 1998. Sorption of trichloroethylene by organoclays in the presence of humic substances. *Water Research* **32**(12): 3710-3716.

Ziv-El, Michal C., and Bruce E. Rittmann. 2009. Systematic evaluation of nitrate and perchlorate bioreduction kinetics in groundwater using a hydrogen-based membrane biofilm reactor. *Water Research* **43**(1): 173-181.

APPENDICES

APPENDIX A. DATA FROM KINETIC STUDIES OF PERCHLORATE SORPTION BY SMM AND SMZ.

Sorbent	Time (hrs)	C_0 (mg/L)	C (mg/L)	C/C_0
SMM	0.0	1168	1168	1.000
	0.4	1168	55.9	0.048
	1.0	1168	48	0.041
	2.0	1168	41.8	0.036
	3.1	1168	35.4	0.030
	4.0	1168	30.56	0.026
	8.0	1168	22.843	0.020
	12.0	1168	22.8	0.020
	0.0	395.5	395.5	1.000
	0.4	395.5	25.68	0.065
	1.1	395.5	12.31	0.031
	2.0	395.5	13.49	0.034
	3.0	395.5	16.64	0.042
	4.0	395.5	12.33	0.031
	8.2	395.5	12.62	0.032
	12.0	395.5	14.88	0.038
SMZ	0.0	705	705	1.000
	0.4	705	660	0.936
	1.0	705	469	0.665
	1.9	705	281	0.399
	3.0	705	218	0.309
	3.9	705	193	0.274
	8.1	705	172	0.244
	13.5	705	192.7	0.273

APPENDIX B. DATA OF LOW PERCHLORATE CONCENTRATION SORPTION BATCH TESTS.

C_0 (mg/L)	SMM				SMZ			
	C_{aq} (mg/L)	Vol (mL)	Mass (g)	C_{ads} (mg/kg)	C_{aq} (mg/L)	Vol (mL)	Mass (g)	C_{ads} (mg/kg)
0.014	0.00	100	0.1999	7.12	0.00	100	0.2062	6.90
0.014	0.00	100	0.2016	7.06	0.00	100	0.2032	7.00
0.014	0.00	100	0.2059	6.91	0.00	100	0.2058	6.92
0.077	0.00	100	0.2070	37.2	0.00	100	0.2034	37.8
0.077	0.00	100	0.2028	37.9	0.00	100	0.2010	38.3
0.077	0.00	100	0.2016	38.1	0.00	100	0.2029	37.9
1.104	0.00	100	0.2033	543	0.036	100	0.2068	517
1.104	0.00	100	0.2055	537	0.029	100	0.2012	535
1.104	0.00	100	0.2024	545	0.030	100	0.2029	529
11.406	0.284	100	0.2004	5,550	0.649	100	0.2030	5,299
11.406	0.207	100	0.2078	5,389	0.719	100	0.2001	5,341
11.406	0.278	100	0.2053	5,420	0.477	100	0.2064	5,295
23.831	0.606	100	0.2021	11,492	6.713	100	0.2022	8,466
23.831	0.694	100	0.2010	11,511	7.088	100	0.2068	8,096
23.831	0.686	100	0.2006	11,538	6.786	100	0.2003	8,509

APPENDIX C. PERCHLORATE SORPTION ONTO SMM AT HIGH INITIAL CONCENTRATIONS.

C_0 (mg/L)	C_{aq} (mg/L)	Vol (mL)	Mass (g)	C_{ads} (mg/kg)
49.42	0.293	50	0.5000	4,913
49.42	0.0318	50	0.5008	4,931
150.0	53.123	50	0.4995	9,697
150.0	56.521	50	0.5008	9,333
352.1	228.6	50	0.4996	12,367
352.1	239.8	50	0.5003	11,224
472.2	359.6	50	0.4998	11,258
472.2	340.0	50	0.5001	13,209

APPENDIX D. DATA FOR PERCHLORATE SORPTION BY SMM IN DEIONIZED WATER SPIKED WITH NITRATE.

Mass SMM (g)	Volume Solution (L)	Perchlorate			Nitrate		
		C_0 (mg/L)	C_{aq} (mg/L)	C_{ads} (mg/kg)	C_0 (mg/L)	C_{aq} (mg/L)	C_{ads} (mg/g)
0.1997	0.1	33.16	9.875	11,658	0.00	0.00	0.00
0.1975	0.1	33.16	10.107	11,670	0.00	0.00	0.00
0.198	0.1	33.16	10.041	11,674	0.00	0.00	0.00
0.199	0.1	32.95	10.053	11,508	1.742	1.696	0.023
0.198	0.1	32.95	10.089	11,548	1.742	1.643	0.050
0.1974	0.1	32.95	10.338	11,457	1.742	1.700	0.021
0.2015	0.1	33.34	10.695	11,240	8.144	8.018	0.063
0.1991	0.1	33.34	10.892	11,276	8.144	8.006	0.069
0.2048	0.1	33.34	10.258	11,272	8.144	7.992	0.074
0.2006	0.1	32.98	10.895	11,011	12.65	12.327	0.161
0.1966	0.1	32.98	11.219	11,070	12.65	12.376	0.139
0.1992	0.1	32.98	10.965	11,053	12.65	12.326	0.162
0.1985	0.1	33.37	11.289	11,125	17.49	16.528	0.486
0.2033	0.1	33.37	11.021	10,994	17.49	16.465	0.505
0.2022	0.1	33.37	11.481	10,827	17.49	16.639	0.422
0.199	0.1	33.16	12.13	10,566	20.82	20.418	0.202
0.2014	0.1	33.16	11.396	10,805	20.82	20.382	0.217
0.1998	0.1	33.16	11.564	10,807	20.82	20.962	-0.072

APPENDIX E. DATA FOR PERCHLORATE SORPTION BY SMM IN GROUNDWATER SPIKED WITH NITRATE.

Mass SMM (g)	Volume Solution (L)	Perchlorate			Nitrate		
		C_0 (mg/L)	C_{aq} (mg/L)	C_{ads} (mg/kg)	C_0 (mg/L)	C_{aq} (mg/L)	C_{ads} (mg/g)
0.1958	0.1	32.13	11.10	10,739	0.09	0.10	-0.001
0.2017	0.1	32.13	9.84	11,049	0.09	0.08	0.005
0.1972	0.1	32.13	10.69	10,874	0.09	0.09	0.004
0.2011	0.1	32.37	11.29	10,483	1.8	1.8	-0.019
0.2018	0.1	32.37	10.44	10,872	1.8	1.8	-0.009
0.2018	0.1	32.37	10.57	10,803	1.8	1.8	-0.009
0.1989	0.1	32.37	11.15	10,672	8.8	8.2	0.307
0.1992	0.1	32.37	11.05	10,706	8.8	8.4	0.219
0.1984	0.1	32.37	11.37	10,588	8.8	8.2	0.312
0.1984	0.1	32.22	11.61	10,387	12.6	12.6	0.041
0.1964	0.1	32.22	11.64	10,478	12.6	12.4	0.145
0.2012	0.1	32.22	11.44	10,326	12.6	12.7	-0.021
0.2067	0.1	32.49	11.39	10,212	16.5	16.1	0.207
0.2028	0.1	32.49	11.40	10,400	16.5	16.2	0.174
0.2029	0.1	32.49	11.28	10,456	16.5	16.2	0.154
0.1951	0.1	32.76	11.84	10,725	20.0	23.3	-1.679
0.2056	0.1	32.76	11.53	10,326	20.0	20.5	-0.213
0.2018	0.1	32.76	11.69	10,444	20.0	20.0	0.035

APPENDIX F. PERCHLORATE ADSORPTION BY SMM FROM BRINE.

	C_0 (mg/L)	C_{aq} (mg/L)	Vol (mL)	Mass (g)	C_{ads} (mg/kg)
Full-Strength Brine	5.607	1.912	100	0.5003	739
	5.607	2.069	100	0.5016	705
	5.607	1.876	100	0.4994	747
	9.039	5.021	100	0.5002	803
	9.039	4.913	100	0.5001	825
	9.039	3.928	100	0.5020	1,018
	13.572	6.564	100	0.5009	1,399
	13.572	6.062	100	0.5048	1,488
	13.572	6.886	100	0.5023	1,331
	22.117	11.094	100	0.5048	2,184
	22.117	11.464	100	0.5007	2,128
	22.117	9.252	100	0.5030	2,558
	26.362	11.097	100	0.5003	3,051
	26.362	10.607	100	0.5004	3,148
Half-Strength Brine	2.347	1.272	100	0.5040	213
	2.347	0.994	100	0.5034	269
	2.347	1.337	100	0.5003	202
	10.177	2.896	100	0.5033	1,447
	10.177	2.995	100	0.5010	1,434
	9.039	2.749	100	0.5015	1,254
	16.876	6.569	100	0.5020	2,053
	16.876	6.877	100	0.5037	1,985
	16.876	3.593	100	0.5022	2,645
	28.501	9.301	100	0.5006	3,835
	28.501	9.389	100	0.5030	3,800
	28.501	5.885	100	0.5017	4,508
	36.06	12.342	100	0.4999	4,745
	36.06	11.225	100	0.5033	4,934
	36.06	7.062	100	0.5014	5,783

APPENDIX G. PARAMETERS USED TO MODEL MASS TRANSPORT THROUGH SMM.

Hydraulic Gradient	Velocity (cm/d)	Mechanical Dispersion (cm)	Dispersivity (cm^2/d)	Flow Rate (cm^3/d)	EBCT (days)
1	0.336	50	16.8	659	298
1	0.336	75	25.2	659	298
1	0.336	100	33.6	659	298
1	0.336	125	42	659	298
1	0.336	150	50.4	659	298
2	0.672	50	33.6	1319	149
2	0.672	75	50.4	1319	149
2	0.672	100	67.2	1319	149
2	0.672	125	84	1319	149
2	0.672	150	100.8	1319	149
3	1.008	50	50.4	1978	99
3	1.008	75	75.6	1978	99
3	1.008	100	100.8	1978	99
3	1.008	125	126	1978	99
3	1.008	150	151.2	1978	99
4	1.368	50	68.4	2685	73
4	1.368	75	102.6	2685	73
4	1.368	100	136.8	2685	73
4	1.368	125	171	2685	73
4	1.368	150	205.2	2685	73
5	1.704	50	85.2	3344	59
5	1.704	75	127.8	3344	59
5	1.704	100	170.4	3344	59
5	1.704	125	213	3344	59
5	1.704	150	255.6	3344	59

APPENDIX H. PARAMETERS USED TO MODEL MASS TRANSPORT THROUGH SMZ.

Velocity (cm/hr)	**Mechanical Dispersion (cm)**	**Dispersivity (cm^2/hr)**	**Flow Rate (cm3/hr)**	**EBCT (hr)**
1	50	50	1962.5	100
1	75	75	1962.5	100
1	100	100	1962.5	100
1	125	125	1962.5	100
1	150	150	1962.5	100
5	50	250	9812.5	20
5	75	375	9812.5	20
5	100	500	9812.5	20
5	125	625	9812.5	20
5	150	750	9812.5	20
10	50	500	19625	10
10	75	750	19625	10
10	100	1000	19625	10
10	125	1250	19625	10
10	150	1500	19625	10
12	50	600	23550	8.3
12	75	900	23550	8.3
12	100	1200	23550	8.3
12	125	1500	23550	8.3
12	150	1800	23550	8.3
15	50	750	29437.5	6.7
15	75	1125	29437.5	6.7
15	100	1500	29437.5	6.7
15	125	1875	29437.5	6.7
15	150	2250	29437.5	6.7

APPENDIX I. MODELED MASS TRANSPORT THROUGH SMM.

V_x (cm/d)	D (cm^2/d)	Breakthrough (days)		Volume treated before 1% perchlorate breakthrough	
		Perfect Tracer	Perchlorate	m^3	Pore Volumes
0.336	16.8	39.9	1,215,000	801	8875
0.336	25.2	28.2	857,700	566	6265
0.336	33.6	21.7	658,900	434	4813
0.336	42	17.6	533,500	352	3897
0.336	50.4	14.7	447,600	295	3269
0.336	67.2	11.1	338,100	223	2470
0.336	68.4	10.9	332,300	219	2427
0.336	75.6	9.88	301,100	199	2199
0.336	84	8.91	271,400	179	1982
0.336	85.2	8.78	267,600	176	1955
0.336	100.8	7.44	226,500	149	1654
0.336	102.6	7.31	222,700	147	1627
0.336	126	5.96	181,600	120	1326
0.336	127.8	5.88	179,000	118	1307
0.336	136.8	5.49	167,300	110	1222
0.336	151.2	4.97	151,400	100	1106
0.336	170.4	4.41	134,400	89	982
0.336	171	4.4	134,000	88	979
0.336	205.2	3.67	111,700	74	816
0.336	213	3.53	107,600	71	786
0.336	255.6	2.95	89,700	59	655
0.672	16.8	33.1	1,009,000	1331	14740
0.672	25.2	25	760,200	1003	11106
0.672	33.6	20	607,200	801	8870
0.672	42	16.6	503,500	664	7355
0.672	50.4	14.1	428,900	566	6266
0.672	67.2	10.9	329,500	435	4814
0.672	68.4	10.7	324,100	427	4735
0.672	75.6	9.68	294,900	389	4308
0.672	84	8.76	266,800	352	3898
0.672	85.2	8.64	263,200	347	3845

V_x (cm/d)	D (cm^2/d)	Breakthrough (days)		Volume treated before 1% perchlorate breakthrough	
		Perfect Tracer	Perchlorate	m^3	Pore Volumes
0.672	100.8	7.35	223,800	295	3269
0.672	102.6	7.22	220,000	290	3214
0.672	126	5.91	180,100	238	2631
0.672	127.8	5.83	177,600	234	2595
0.672	136.8	5.45	166,200	219	2428
0.672	151.2	4.94	150,600	199	2200
0.672	170.4	4.39	133,800	176	1955
0.672	171	4.38	133,400	176	1949
0.672	205.2	3.66	111,400	147	1627
0.672	213	3.52	107,300	142	1568
0.672	255.6	2.94	89,500	118	1307
1.008	16.8	28.2	858,100	1697	18804
1.008	25.2	22.1	672,100	1330	14728
1.008	33.6	18.2	552,400	1093	12105
1.008	42	15.4	467,900	926	10253
1.008	50.4	13.3	404,800	801	8870
1.008	67.2	10.5	317,400	628	6955
1.008	68.4	10.3	312,500	618	6848
1.008	75.6	9.38	285,900	566	6265
1.008	84	8.53	260,000	514	5697
1.008	85.2	8.42	256,600	508	5623
1.008	100.8	7.21	219,700	435	4814
1.008	102.6	7.09	216,100	427	4735
1.008	126	5.84	177,900	352	3898
1.008	127.8	5.76	175,500	347	3846
1.008	136.8	5.4	164,400	325	3603
1.008	151.2	4.9	149,200	295	3269
1.008	170.4	4.36	132,900	263	2912
1.008	171	4.35	132,400	262	2901
1.008	205.2	3.64	110,800	219	2428
1.008	213	3.51	106,800	211	2340
1.008	255.6	2.93	89,200	176	1955
1.368	16.8	24.4	743,300	1996	22105
1.368	25.2	19.6	597,200	1603	17760
1.368	33.6	16.5	500,900	1345	14896
1.368	42	14.2	431,400	1158	12829

V_x (cm/d)	D (cm^2/d)	Breakthrough (days)		Volume treated before 1% perchlorate breakthrough	
		Perfect Tracer	Perchlorate	m^3	Pore Volumes
1.368	50.4	12.5	378,400	1016	11253
1.368	67.2	9.93	302,600	812	8999
1.368	68.4	9.79	298,300	801	8871
1.368	75.6	9.01	274,600	737	8166
1.368	84	8.24	251,100	674	7467
1.368	85.2	8.14	248,000	666	7375
1.368	100.8	7.03	214,100	575	6367
1.368	102.6	6.92	210,700	566	6266
1.368	126	5.74	174,700	469	5195
1.368	127.8	5.66	172,500	463	5130
1.368	136.8	5.31	161,900	435	4815
1.368	151.2	4.84	147,300	395	4381
1.368	170.4	4.32	131,500	353	3911
1.368	171	4.32	131,100	352	3899
1.368	205.2	3.61	110,000	295	3271
1.368	213	3.48	106,100	285	3155
1.368	255.6	2.92	88,760	238	2640
1.704	16.8	21.8	663,000	2217	24560
1.704	25.2	17.8	542,000	1813	20078
1.704	33.6	15.2	460,700	1541	17066
1.704	42	13.2	401,300	1342	14866
1.704	50.4	11.7	355,400	1188	13165
1.704	67.2	9.47	288,700	965	10694
1.704	68.4	9.35	284,800	952	10550
1.704	75.6	8.65	263,600	882	9765
1.704	84	7.95	242,300	810	8976
1.704	85.2	7.86	239,500	801	8872
1.704	100.8	6.83	208,200	696	7712
1.704	102.6	6.73	205,000	686	7594
1.704	126	5.61	171,300	573	6346
1.704	127.8	5.55	169,200	566	6268
1.704	136.8	5.22	159,100	532	5894
1.704	151.2	4.77	145,200	486	5379
1.704	170.4	4.27	130,000	435	4816
1.704	171	4.25	129,500	433	4797
1.704	205.2	3.58	109,000	365	4038

V_x (cm/d)	D (cm^2/d)	Breakthrough (days)		Volume treated before 1% perchlorate breakthrough	
		Perfect Tracer	Perchlorate	m^3	Pore Volumes
1.704	213	3.46	105,200	352	3897
1.704	255.6	2.9	88,260	295	3269

APPENDIX J. MODELED MASS TRANSPORT THROUGH SMZ.

V_x cm/hr	D cm^2/hr	Breakthrough (hr)		Volume treated before perchlorate breakthrough	
		Perfect Tracer	Perchlorate	m^3	Pore Volumes
1	50	13.4	219,400	430.6	4,388
1	75	9.46	154,900	303.9	3,097
1	100	7.27	119,000	233.5	2,380
1	125	5.89	96,340	189.1	1,927
1	150	4.94	80,820	158.6	1,616
1	250	3	49,000	96.2	980
1	375	2.01	32,780	64.3	655
1	500	1.51	24,620	48.3	492
1	625	1.21	19,720	38.7	394
1	750	1.01	16,424	32.2	328
1	1000	0.76	12,322	24.2	246
1	1125	0.67	10,954	21.5	219
1	1250	0.61	9,860	19.4	197
1	1500	0.51	8,218	16.1	164
1	1875	0.41	6,574	12.9	131
1	2250	0.34	5,480	10.8	109
5	50	7.37	120,640	1183.8	12,060
5	75	6.02	98,500	966.5	9,850
5	100	5.11	83,660	820.9	8,366
5	125	4.45	72,820	714.5	7,282
5	150	3.94	64,460	632.5	6,446
5	250	2.68	43,860	430.4	4,386
5	375	1.9	30,980	304.0	3,098
5	500	1.46	23,800	233.5	2,380
5	625	1.18	19,270	189.0	1,927
5	750	0.99	16,160	158.6	1,616
5	1000	0.75	12,210	119.8	1,221
5	1125	0.67	10,880	106.7	1,087
5	1250	0.6	9,800	96.2	980
5	1500	0.5	8,182	80.3	818
5	1875	0.41	6,556	64.3	656
5	2250	0.34	5,468	53.7	547
10	50	4.87	79,700	1564.1	15,940

V_x cm/hr	D cm^2/hr	Breakthrough (hr)		Volume treated before perchlorate breakthrough	
		Perfect Tracer	Perchlorate	m^3	Pore Volumes
10	75	4.18	68,380	1342.0	13,680
10	100	3.69	60,320	1183.8	12,060
10	125	3.31	54,160	1062.9	10,830
10	150	3.01	49,240	966.3	9,848
10	250	2.23	36,420	714.7	7,284
10	375	1.68	27,460	538.9	5,492
10	500	1.34	21,940	430.6	4,388
10	625	1.11	18,180	356.8	3,636
10	750	0.95	15,484	303.9	3,097
10	1000	0.73	11,900	233.5	2,380
10	1125	0.65	10,650	209.0	2,130
10	1250	0.59	9,634	189.1	1,927
10	1500	0.5	8,082	158.6	1,616
10	1875	0.4	6,504	127.6	1,301
10	2250	0.33	5,438	106.7	1,088
12	50	4.31	70,560	1661.7	16,934
12	75	3.74	61,240	1442.2	14,698
12	100	3.33	54,520	1283.9	13,085
12	125	3.02	49,320	1161.5	11,837
12	150	2.76	45,140	1063.0	10,834
12	250	2.08	34,020	801.2	8,165
12	375	1.6	26,120	615.1	6,269
12	500	1.29	21,120	497.4	5,069
12	625	1.08	17,670	416.2	4,241
12	750	0.93	15,150	356.8	3,636
12	1000	0.72	11,730	276.3	2,816
12	1125	0.65	10,530	247.9	2,527
12	1250	0.59	9,542	224.7	2,290
12	1500	0.5	8,028	189.1	1,927
12	1875	0.4	6,474	152.5	1,554
12	2250	0.34	5,420	127.6	1,301
15	50	3.69	60,400	1778.0	18,120
15	75	3.25	53,140	1564.3	15,940
15	100	2.92	47,800	1407.1	14,340
15	125	2.67	43,620	1284.1	13,090
15	150	2.46	40,220	1184.0	12,070
15	250	1.9	31,000	912.6	9,300

V_x cm/hr	D cm^2/hr	Breakthrough (hr)		Volume treated before perchlorate breakthrough	
		Perfect Tracer	Perchlorate	m^3	Pore Volumes
15	375	1.49	24,280	714.7	7,284
15	500	1.22	19,950	587.3	5,985
15	625	1.04	16,896	497.4	5,069
15	750	0.9	14,620	430.4	4,386
15	1000	0.7	11,460	337.4	3,438
15	1125	0.64	10,320	303.9	3,097
15	1250	0.58	9,386	276.3	2,816
15	1500	0.49	7,934	233.6	2,380
15	1875	0.4	6,422	189.0	1,927
15	2250	0.33	5,388	158.6	1,616

APPENDIX K. BIOLOGICAL TREATMENT OF SPENT CLAY USING COLUMN EFFLUENT.

Time (days)	Perchlorate (mg/L)						
	CE-1	CE-2	CE-3	CE-4	CE-5	CE-6	Average
4	11.2	10.7	14.4	11.2	15.7	12.2	12.6
7	11.0	10.3	13.6	12.4	15.7	10.8	12.3
14	10.4	9.50	11.6	11.1	15.6	10.1	11.4
19	9.91	8.23	10.8	10.5	15.3	9.93	10.8
21	10.7	10.3	10.8	10.1	16.8	10.5	11.5
25	6.81	7.24	5.82	5.23	11.0	5.93	7.01
28	7.125	6.63	7.28	7.47	10.8	7.25	7.76
33	6.74	5.73	6.56	7.17	9.76	6.70	7.11
35	3.90	2.21	3.66	3.55	5.18	3.97	3.75
39	2.96	1.67	2.83	3.38	3.20	1.54	2.59
46	4.93	3.96	4.74	5.00	5.95	4.69	4.88
55	5.92	5.20	6.10	10.8	7.70	5.96	6.95
61	5.69	5.49	6.47	6.75	8.84	5.84	6.51
68	1.30	4.41	3.38	3.45	5.71	3.45	3.62
80	3.37	5.63	3.50	4.64	6.35	4.81	4.72
88	3.16	3.46	2.70	3.49	5.04	4.56	3.73
101	1.09	1.99	1.60	0.79	2.98	1.95	1.73
109	0.68	1.43	1.10	0.54	1.98	1.42	1.19
120	0.75	0.41	0.78	0.75	1.05	0.85	0.77

APPENDIX L. BIOLOGICAL TREATMENT OF SPENT CLAY USING MUSHROOM COMPOST TEA.

Time (days)	Perchlorate (mg/L)					
	MC-1	MC-2	MC-3	MC-4	MC-5	Average
4	5.55	3.33	3.03	3.41	3.15	4.29
7	3.34	5.56	5.87	6.91	5.83	5.50
18	3.54	2.45	4.20	4.77	3.64	3.72
21	4.01	4.94	4.38	5.04	4.57	4.59
28	3.83	4.49	4.00	4.27	3.43	4.00
32	3.10	4.39	3.49	4.05	3.94	3.79
35	3.41	4.21	2.62	3.35	2.91	3.30
39	3.28	3.67	3.27	3.87	3.55	3.53
47	4.53	5.02	5.11	5.05	4.50	4.84
56	6.64	4.66	4.83	4.98	4.73	5.17
62	5.35	4.77	4.94	4.87	5.11	5.01

APPENDIX M. CONTROL BIODEGRADATION DATA FROM TREATMENT OF SMM USED TO ADSORB PERCHLORATE FROM DEIONIZED WATER.

Time (days)	Perchlorate (mg/L)		
	Control-1	Control-2	Average
4	7.42	8.51	7.96
7	11.50	11.42	11.46
16	8.63	10.01	9.32
21	8.77	9.45	9.11
25	7.23	6.88	7.05
30	7.70	7.84	7.77
32	7.41	7.33	7.37
37	9.80	8.81	9.30
45	9.57	10.73	10.15
54	8.68	9.29	8.99
59	9.12	9.66	9.39
60	10.22	9.83	10.02
67	11.10	9.78	10.44
79	11.12	9.91	10.52
98	11.48	11.01	11.25
101	11.32	10.94	11.13
109	11.54	10.35	10.95
120	11.40	10.67	11.03

APPENDIX N. BIOLOGICAL TREATMENT OF SMM USED TO FILTER BRINE.

Treatment	Time (days)	Perchlorate (mg/L)		
		Reactor-1	Reactor-2	Average
Column Effluent	0	92	96	94
	6	155	124	139
	8	124	122	123
	13	124	125	125
	23	120	115	117
	29	125	121	123
	33	122	119	120
	34	122	119	120
	41	116	112	114
	53	126	122	124
	70	114	102	108
Mushroom Compost	0	87	91	89
	6	95	63	79
	8	112	117	115
	13	104	103	103
	23	109	104	107
	29	126	116	121
	33	108	123	116
	34	116	110	113
	41	95	98	97
	53	111	108	109
	70	99	92	96
Control - Deionized Water	0	96	96	96
	6	97	93	95
	8	125	124	125
	13	119	118	118
	23	116	121	118
	29	123	121	122
	33	119	118	119
	34	121	126	124
	41	113	107	110
	53	111	109	110
	70	124	118	121